Center for Geo-Information

Thesis Report GIRS-2006-09

ESTIMATION OF LEAF AREA INDEX USING OPTICAL FIELD INSTRUMENTS AND IMAGING SPECTROSCOPY

Alemu Gonsamo Gosa



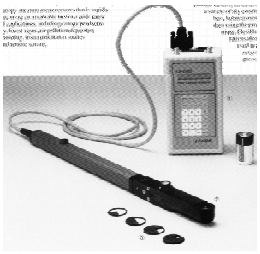

February 2006

WAGENINGEN UNIVERSITY
WAGENINGEN UR

ESTIMATION OF LEAF AREA INDEX USING OPTICAL FIELD INSTRUMENTS AND IMAGING SPECTROSCOPY

Alemu Gonsamo Gosa

Registration number: 800204269020

Supervisors:

Dr. Lammert Kooistra
Dr. sc. nat. Gabriela Schaepman
Prof. Dr. sc. nat. Michael E. Schaepman

A thesis submitted in partial fulfillment of the degree of Master of Science at Wageningen University and Research Centre, The Netherlands.

February, 2006
Wageningen, the Netherlands

Thesis code number: GRS-80436
Wageningen University and Research Centre
Laboratory of Geo-Information Science and Remote Sensing
Thesis Report: GIRS-2006-09

Acknowledgements

First of all, I am deeply indebted to my supervisors Dr. Lammert Kooistra, Dr. Gabriela Schaepman and Prof. Dr. Michael E. Schaepman for their advice and help related to the estimation of leaf area index using optical field instruments and imaging spectroscopy. I would particularly like to thank Dr. Lammert Kooistra, and Dr. Gabriela Schaepman for their critical, continuous and valuable guidance through all the thesis work.

This study is a result of a contribution from different organizations and individuals. The research would have not been done without the ground measurements of leaf area index and airborne data. I would like to express my thanks to the MGI staff and students who participated in the field campaign in the Millingerwaard. Many thanks to VITO for the AHS image acquisition and provision. Raul Zurita is due a special note of thanks for his idea during the initiation of the thesis.

I am grateful to Prof. Jing M. Chen, Dr. Sylvain G. Leblanc, Dr. Ir. Inge Jonckheere and Dr. Marie Weiss for being free to be consulted via e-mail. Their comments and suggestions were very valuable as the thesis progressed. I am grateful to my study advisor Willy ten Haaf for his advice and arrangement of conditions during my study.

I would like to thank all my friends of MGI students for making our time so enjoyable at Alterra. I would also like to take this opportunity to express my gratitude to my family in Ethiopia for their contribution in my study since the beginning.

Last but not least my special heart felt thanks goes to my beloved Petrita, for her encouragement, support, inspiration and splendid love.

Abstract

Leaf area index (LAI) is an important vegetation structural variable for the quantitative analysis of biophysical processes in the terrestrial ecosystem. In particular, it can be a crucial parameter related to hydrological modeling, carbon cycle and climate study at different spatial scales. The main objective of the study was to evaluate and compare performances of LAI estimation using three selected optical field instruments namely: LAI-2000 plant canopy analyzer (PCA), TRAC and hemispherical photography. These results shall subsequently be used to calibrate and validate the estimation of LAI based on imaging spectrometer data. The study involves diverse plant functional types, namely grass, shrub and forest canopies, of a river floodplain along the river Rhine in the Netherlands.

Ground-based LAI measurements were acquired from June 19 to 30, 2005 after acquiring the Airborne Hyperspectral System (AHS) image on June 19, 2005 of the Millingerwaard, a managed natural ecosystem which consists of a wide range of plant species and plant functional types. Ground measurements were collected following the VALERI sampling scheme. The Reduced Simple Ratio (RSR) was used to derive LAI from the AHS imaging spectrometer data and was calibrated based on the ground measurements. This study compares the individual LAI estimates, and the potential advantages and disadvantages of each method are discussed in relation to its use in different plant functional types and to field data collection supporting remote sensing data calibration and validation.

The comparison of LAI from optical field instruments indicates that TRAC and LAI-2000 PCA underestimate the LAI for grass plots when compared to hemispherical photography. This demonstrates that the LAI from TRAC and LAI-2000 PCA does not encompass the contribution of the vegetation below the sensor height for short canopies. The comparison of LAI from hemispherical photography alone and the combined method of hemispherical photography and TRAC demonstrates a good agreement (R^2 = 0.74), which indicates their comparable performance. Hemispherical photography proves to be the most appropriate method to estimate LAI of short canopy vegetation, and improved classification techniques in applied software (CAN_EYE) give a good discrimination possibility for the classification of foliage elements and gaps, whereas the clumping index as derived from the TRAC instrument is more reliable in determining the effect of spatial distribution of foliage elements. The clumping index from TRAC instrument can then be used in combination with hemispherical photography or LAI-2000 for a more accurate estimation of the LAI. A key benefit, however, of all of these estimation methods is that observations can be collected in a short period of time. A poor correlation of RSR and the LAI from all three methods of ground measurements were obtained in this study for all plant functional types. A possible reason for this can be found in the low dynamics of the reflectance in the wavelength bands which are used to compute the RSR.

Keywords: Leaf Area Index, LAI-2000 PCA, TRAC, Hemispherical Photography, Imaging Spectroscopy.

Table of Contents

List of Tables

List of Figures

Abbreviations and Acronyms

AGL	Above Ground Level
AHS	Airborne Hyperspectral System
ALA	Average Leaf Inclination Angle
APAR	Absorbed Photosynthetically Active Radiation [Wm^{-2}]
CCD	Couple Charge Device
CEOS-WGCV	Committee Earth Observing Satellites' Working Group on Calibration and Validation
CNES	Centre National D'etudes Spatiales (France)
DHP	Digital Hemispherical Photography
ESU	Elementary Sampling Unit
fAPAR	Fraction of Absorbed Photosynthetically Active Radiation
fCover	Fractional Cover
FR	Forest
FWHM	Full Width at Half the Maximum
GB	Giga Byte
GH	Grasses and Herbs
HP	Hemispherical Photography
IFOV	Instantaneous Field of View
INRA	Institut National de la Recherche Agronomique(France)
IR	Infra Red
Kme	Effective Mean contact number
LAI	Leaf Area Index
LAIe	Effective Leaf Area Index
LAIt	True Leaf Area Index
LPV	Land Product Validation
LUT	Look Up Table
MIR	Middle Infrared
µm	Micrometer
mrad	Milliradian
NDVI	Normalized Difference Vegetation Index
NIR	Near Infrared
NL	Netherlands
nm	Nanometer
PAI	Plant Area Index
PAIe	Effective Plant Area Index
PAR	Photosynthetically Active Radiation
PCA	Plant Canopy Analyzer
PLAI	Projected Leaf Area Index
PPFD	Photosynthetic Photon Flux Density
RMSE	Root Mean Square Error
RSR	Reduced Simple Ratio
SH	Shrub
SLAI	Silhouette Leaf Area Index

SR	Simple Ratio
SVI	Spectral Vegetation Index
SWIR	Shortwave Infrared
TLAI	Total Leaf Area Index
TRAC	Tracing Radiation and Architecture Canopies
UTC	Coordinated Universal Time
UTM	Universal Transverse Mercator
VALERI	Validation of Land European Remote sensing Instruments
VI	Vegetation Index
WAI	Wood Area Index
WDVI	Weighted Difference Vegetation Index
WGS84	World Grid System 84
WL	Wavelength

1. Introduction

1.1. Background

The majority of world vegetation which is complex and widely distributed ecosystem on the Earth, affecting the life of most humans daily, either as an economic good or an environmental regulator is naturally occurring in remote and inaccessible area in wide variety and extent of range. To study the characteristics of vegetation, remote sensing techniques are useful because they provide spatially explicit information and access to remote locations. Remote sensing uses radiance data obtained from air- or space-borne sensors to indirectly estimate key characteristics of the biosphere (Gower *et al.*, 1999). These techniques allow scientists to examine properties and processes of ecosystems and their interannual variability at multiple scales because remote sensing observations can be obtained over large areas of interest with high revisitation frequencies.

Leaf area index (LAI) is one of the vegetation parameters that has importance in climate, weather, and ecological studies, and has been routinely estimated from remote sensing measurements (Knyazikhin *et al.*, 1998; Chen *et al.*, 2002; Myneni *et al.*, 2002; Hu *et al.*, 2003; Wang *et al.*, 2004). The leaf area index, or LAI, defined most recently by Chen and Black (1992) and Fassnacht *et al.* (1997) as half the total leaf area per unit ground surface area is a vegetation structural parameter of fundamental importance for quantitative analysis of many physical and biological processes related to vegetation dynamics and its effects on the global carbon cycle and climate. Leaf area index drives both the within- and the below-canopy microclimate, determines and controls canopy water interception, radiation extinction, water and carbon gas exchange and is, therefore, a key component of biogeochemical cycles in ecosystems (Breda, 2003). Process-based ecosystem simulations are then often required to produce quantitative analyses of productivity and LAI is a key input parameter to such models. Ecophysiologists, but also managers (farmers and foresters), ecologists, site and global modelers of ecosystem productivity, climate, hydrology and biogeochemistry, request information about canopy leaf area index.

However, calibration of remotely sensed data requires often extensive ground truth data. In addition, validation of remotely sensed vegetation products is important to determine the accuracy of the products from different sensors and variety of methods. Vegetation is a challenging target as a consequence of its architectural heterogeneity, clumping of optically active surfaces at multiple scales and spatial–temporal foliage dynamics. Remote sensing of vegetation biophysical variables such as LAI is further complicated by the contribution of understory vegetation, litter, soil, bark as well as plant and relief shadow, all of which influence the radiometric signal (Tian *et al.*, 2002; Schlerf *et al.*, 2005). Additionally, the canopy reflectance depends on sun and viewing geometry that impacts the estimation of the LAI based on empirical methods (Strub *et al.*, 2002).

Extensive research has been done on the estimation of forest LAI from remote sensing data within the last one and half decades (Brown *et al.*, 2000; Chen *et al.*, 2002; Hall *et*

al., 2003; Stenberg *et al.*, 2004; Wang *et al.*, 2004; Manninen *et al.*, 2005). Most of the studies on forest are based on the relation of LAI with vegetation indices (VIs), such as the simple ratio (SR) or the normalized difference vegetation index (NDVI), computed from broadband remote sensing data (Schlerf *et al.*, 2005). However, the application of such relationships to large areas or at different seasons is limited by being site and sensor specific. Apart from this, the sensitivity of VIs to changes in LAI is often not dynamic enough to allow accurate estimation of LAI. This problem has been encountered for example in boreal coniferous forests, where NDVI typically has a very narrow range due to the presence of a green understory (Manninen *et al.*, 2005).

Above and beyond, the broadband indices, usually constructed with near-infrared (NIR) and red (R) bands, use average spectral information over broad bandwidths, resulting in loss of critical information available in specific narrow bands Also, VI-based relations and are known to be heavily affected by soil background at low vegetation cover (Eriksson *et al.*, 2005). Now a days, the advent of airborne imaging spectrometers has made it possible to construct more refined VIs through the use of distinct narrow bands. Recent studies on LAI estimation (Brown *et al.*, 2000; Chen *et al.*, 2002); suggest that inclusion of shortwave infrared (SWIR) reflectance in VIs may be useful to suppress the background influence. For example the reduced simple ratio (RSR) has been found to perform well in coniferous forests (Stenberg *et al.*, 2004; Wang *et al.*, 2004).

The validation of the derived LAI products can be achieved using a bottom-up approach, i.e. from local field level measurements to global comparison with satellite derived LAI products (for example LAI products of MODIS, AVHRR, VEGETATION, Landsat TM, POLDER, and MERIS) (Morisette *et al.*, 2005). International initiatives for LAI databases and validation become increasingly important for users to determine the most appropriate product, or combination of products, to use for their applications (for instance global leaf area index data from field measurements can be found through the period of 1932-2000 **(**http://www-eosdis.ornl.gov/VEGETATION/lai_des.html**)**. Field validation of global or regional satellite-derived products generally relies on point measurements from the field that need to be scaled up to compare to the corresponding moderate-resolution global products. This question is generally addressed by associating the field measurements with high-resolution imagery to make a high-resolution map of the same variable derived from field measurements. Then, the quality of the large scale global LAI products can be assessed by comparing it with the high-resolution product.

There are several techniques of in-situ LAI determination, generally categorized as direct and indirect methods (Gower *et al.*, 1999; Breda, 2003; Jonckheere *et al.*, 2004a). LAI can be assessed directly by using harvesting methods such as destructive sampling and the model tree method or by non-harvesting litter traps during autumn leaf-fall period in deciduous forests (Jonckheere *et al.*, 2004a; Jonckheere *et al.*, 2004b). Direct methods of LAI estimation are the most accurate, but they have the disadvantage of being extremely time-consuming and as a consequence making large-scale implementation only marginally feasible. Because of its time-consuming and labor-intensive character and operational constraints, it can be said that direct LAI determination is not really compatible with long-term monitoring of spatial and temporal dynamics of leaf area

development. LAI can also be estimated indirectly from the incident radiation transmitted through the canopy at a given sun or view zenith angle. Commercial canopy analyzers are a tool to locally characterize canopy structure for calibration and validation of satellite or airborne remote sensing products. This method is known as the gap fraction method and is used with a number of instruments (LAI-2000, TRAC, DEMON, Ceptometer, hemispherical photography; (Chen *et al.*, 1997; Weiss *et al.*, 2004)).

1.2. Problem Definition

As many regional and global air- or space-borne LAI maps are being produced regularly (e.g., Mercury Search Tool, http://mercury.ornl.gov/ornldaac/), accuracy assessment and validation of these products are of central concern to the potential users. There are several in-situ techniques to determine LAI for up-scaling purpose from plot to pixel level in order to calibrate and validate spectrally retrieved LAI products from high or medium resolution hyperspectral data. LAI can be measured directly by destructive methods, or through allometric relationships (Chen *et al.*, 1997). However, these are quite time consuming, and cannot be applied routinely to multiple locations. This is the reason why various studies are mainly using indirect methods to estimate LAI from gap faction measurements. Accordingly, LAI for grass, shrub and forest canopy was estimated in this study using indirect optical field instruments.

However, the use of gap fraction to estimate LAI poses a number of problems. Among these (Morisette *et al.*, 2005): (1) the footprint corresponding to these measurements depends mainly on the device used and the canopy sampled, (2) unequal illumination of the canopy violates the assumption of the LAI-2000 and TRAC calculations or creates thresholding problems (sky or soil vs. vegetation) in DHP software, (3) clumping occurs at several scales, from the landscape to the shoot, and influences greatly the LAI-gap fraction relationship, (4) the optical field measurement techniques are less apt at distinguishing green leaves (green LAI) from non-green leaves and woody material (Barclay *et al.*, 2000) and (5) understory LAI can significantly impact vegetation indices commonly used to generate fine resolution LAI maps. In addition to these, the LAI depends on the vegetation type and age and the moment of the growing season at which measurements are carried out (Mussche *et al.*, 2001); of course the LAI of each vegetation type is strongly dependent of the biotic and climatic conditions at which the vegetation grows. The sum of these factors, together with the different methods used, results in widely different LAI-values.

Even though, significant amount of studies have been conducted to estimate LAI using either of most widely used ground measurement techniques and/or using retrieval techniques from imaging spectrometer data (Gong *et al.*, 2003; Lee *et al.*, 2003; Berterretche *et al.*, 2005; Schlerf *et al.*, 2005), there has nor been conducted ample comprehensive study to combine in-situ LAI estimation techniques. Additionally, optical field instruments have different assumptions for the spatial distribution of canopy which mainly depends on the plant-functional type. This suggests that inter-comparison of clumping corrections for optically-based in-situ LAI estimates should be investigated

further. It is recommended (Chen *et al.*, 1997) that TRAC be used to investigate the foliage spatial distribution pattern while LAI-2000/hemispherical photography is useful to study foliage angular distribution pattern. The TRAC clumping index can be applied to correct LAI-2000 or hemispherical photography estimates of LAI for deviations from the assumption of randomly distributed foliage used in the LAI-2000 processing algorithms. Hemispherical photography-based LAI estimates were corrected for clumping by applying the TRAC clumping index algorithm for successive zenithal rings in the field of view (Leblanc, 2002; Leblanc *et al.*, 2005). These have been shown to be well correlated with allometric LAI over a number of boreal sites in Canada (Gower *et al.*, 1999). However, most of the studies solely focus on estimation of forest and agricultural crops LAI and only minor work has been done for other plant-functional types such as shrub- and grass-lands. Therefore, studies must be carried out for comparison and integration of different methods and techniques to estimate LAI of varying plant-functional types. Furthermore, sampling strategy has to be developed for short canopy vegetation such as grass-lands in order to minimize the error of LAI value which results from the footprint of the instruments being used. This study assess the feasibility of the selected three optical field instruments for LAI determination per plant functional type and evaluate the potential of combination of these methods to enhance the accuracy of LAI estimation.

As most of the above mentioned processes are examined on a limited sample leaf area basis, the LAI is necessary for scaling up the results to the level of the forest stand, vegetation type or ecosystem. Remote sensing provides the only feasible alternative for the estimation or monitoring of LAI at regional scales. Models developed for application to remotely sensed optical data rely on physically based relationships between LAI and canopy spectral reflectance, typically expressed in the form of spectral vegetation indices (SVIs). Numerous ratio-based SVIs have been statistically related to LAI, with the most common being the simple ratio (SR) and the normalized difference vegetation index (NDVI) which uses red and infrared bands (Gower *et al.*, 1999; Manninen *et al.*, 2005; Schlerf *et al.*, 2005). In the near-infrared region the spectral reflectance and transmittance of the leaves is high and absorptance is low. In this situation leaves from lower canopy layers contribute considerably to total measured reflectance (Clevers, 1989). This multiple reflectance reveals that measured near infrared reflectance may be suitable estimator of LAI. However, background reflectance e.g., soil reflectance influence the relationship between measured near infrared reflectance and LAI. To compensate for differences in canopy closure and background reflectance, studies have used shortwave infrared (SWIR) reflectance to quantify canopy closure (Brown *et al.*, 2000) and modification have been made for other vegetation indices such as NDVI (Nemani *et al.*, 1993) and SR (Brown *et al.*, 2000; Chen *et al.*, 2002).

Results from Brown *et al.* (2000) and from a later study by Chen *et al.* (2002) and Stenberg *et al.* (2004), comprising data from the major boreal tree species in Canada and Finnish pine and spruce stands, showed that for both coniferous and deciduous stands RSR correlated better with LAI than did NDVI and SR. This study focus on evaluating and quantifying the suitability of the Reduced Simple Ratio (RSR) to estimate LAI of forest, shrub and grass from Airborne Hyperspectral System (AHS) data.

Generally, in this study, regional LAI of grass, shrub and broad leaf soft-wood forest was estimated using three ground-based measurement techniques and subsequent analysis for calibration and validation purposes of airborne imaging spectrometer data of a river floodplain vegetation in the Netherlands. The integration of three in-situ LAI estimation techniques namely: TRAC, LAI-2000 and hemispherical photography was used for calibration and comparison of retrieved LAI value from imaging spectroscopy data. Furthermore, in-situ optical LAI determination techniques were evaluated for shrub- and grass-land LAI estimation in addition to the forest plant-functional type which was the major study target for the validation of different LAI estimation methods (Chen and Black, 1992; Roxburgh and Kelly, 1995; Gower *et al.*, 1999; Leblanc *et al.*, 2002a; Breda, 2003; Coops *et al.*, 2004).

1.3. Research Objectives

General objective

- Estimation of forest, shrub and grass leaf area index using three indirect ground measurement techniques and imaging spectroscopy.

Specific objective

- Quantify leaf area index of grass, shrub and forest canopy using hemispherical photography, TRAC and LAI-2000,
- Combine ground-based LAI determination methods for more accurate estimation of LAI,
- Assess plant-functional type specific relations of RSR-LAI,
- Develop a strategy for reproducible and accurate in-situ measurement of LAI per plant-functional type as a base for validation of remote sensing derived LAI and
- Documentation of sampling strategy, measurements, input variables, processing techniques and computed outputs for further use.

Research questions

- Is it possible to integrate different ground-based leaf area index estimation methods and techniques to achieve more accurate result?
- How significant is the difference of the leaf area index values using different methods?
- How can we build a spatially distributed LAI map from different ground measurement techniques for calibration of imaging spectrometer data at the stand scale?
- What is plant-functional type relation of RSR-LAI?
- How feasible are various optical field LAI determination methods for different plant-functional types?

1.4 Structure of the Report

Chapter one of this report comprises an introduction about the general background, overview of the context, definition of the topic and the importance of leaf area index as a key biophysical parameter. Description and definition of the problem is also main part of this chapter. The objectives of this study and research questions are covered in this chapter, as well. Chapter two deals with review of the relevant literature and discusses similar studies conducted in the field of the study area. The third chapter describes the methodologies followed in order to achieve the research objectives. The results of this study are presented and discussed in chapter four. Conclusion and recommendations are given in the fifth chapter.

2. Literature Review

2.1. Definition of Leaf Area Index (LAI)

Leaf area index (LAI) is a dimensionless variable and was first defined by Watson (1947) as the total one-sided area of photosynthetic tissue per unit ground surface area (Jonckheere *et al.*, 2004a). For broad-leaved trees with flat leaves, this definition is applicable because both sides of a leaf have the same surface area. However, if foliage elements are not flat, but wrinkled, bent or rolled, the one-sided area is not clearly defined. The same problem exists for coniferous trees, as needles may be cylindrical or hemi-cylindrical (Chen and Black, 1992).

Leaf area index (usually abbreviated to LAI or simply L) is broadly defined as the amount of leaf area in a vegetation canopy per unit land area:

$$LAI = S/G \quad (1)$$

where S is the functional (green) leaf area of the canopy standing on ground area G (Scurlock *et al.*, 2001). Because both S and G are normally measured as areas (m2), LAI is dimensionless, although it is sometimes presented in units of m2/m2. Most commonly S is measured as the projected area (e.g., after placing a sampled leaf on a horizontal surface). However, LAI may be more precisely defined in a number of different ways (Chen and Black, 1992; Barclay, 1998; Scurlock *et al.*, 2001; Eriksson *et al.*, 2005). For example, leaf area may be measured as the total surface area of leaves in a canopy. This will be equal to 2s for flat leaves and greater than 2S for needle-shaped and succulent leaves and photosynthetic stems. Care should be taken when making comparisons between LAI determinations that may not necessarily use the same methodology or even the same definition of LAI (Chen and Black, 1992).

According to Barclay (1998), there are at least five common measures of LAI, which partly reflect the different purposes for which LAI is determined :
(1) total leaf area per unit area of horizontal land below, TLAI, is based on the total outside area of the leaves, taking leaf shape into account;
(2) total one-sided leaf area per unit area of horizontal land below is usually defined as half of the total leaf area, even if the two sides of the leaves are not symmetrical; it is a commonly used parameter because it represents the gas exchange potential;
(3) projected area of horizontal leaves per unit of horizontal land below, PLAI, is defined as the area of horizontal shadow that would be cast beneath a horizontal leaf from a light at infinite distance directly above it; this measurement is common in remote sensing applications, because it represents the maximum leaf area that could be seen by sensors from overhead;
(4) projected area of leaves inclined to the horizontal, called silhouette leaf area index (SLAI) by Weiss *et al.* (2004), is a useful measure for modeling the effects of light penetration through a canopy (Chen and Black, 1991; Chen and Black, 1992) and for

remote sensing, because it is equivalent to the area for intercepting light and represents what would be observed by a nadir view from above, ignoring leaf overlaps; and
(5) projected area of inclined leaves, but counting overlapping areas only once; this measure is common in remote sensing applications, because it represents the proportion of ground obscured by foliage in a remotely acquired image.

Definition (1) is relatively rarely used depending upon the details of the calibration of the allometric equations (Scurlock *et al.*, 2001). Definition (2) suffers from the problem that the meaning of "one-sided" is unclear for coniferous needles, highly clumped foliage, or rolled leaves (Chen and Black, 1992). Chen and Black (1992) suggest that the LAI of non-flat leaves should be defined as half the total intercepting area per unit ground area, and that definition (3) should be abandoned. LAI according to definition (2) may exceed LAI according to definition (3) by a factor ranging from 1.28 (hemi-circular cylinders representing conifer needles), through 1.57 (representing cylindrical green branches) to 2.0 (spheres or square bars representing highly clumped shoots and some spruce needles) (Chen and Cihlar, 1996). Regrettably, many individual reports of LAI in the literature fail to provide any details of the LAI definition assumed, and a significant fraction do not even describe the methodology used (Scurlock *et al.*, 2001).

So, in current literature and next to Watson (1947) definition, LAI defined as one half the total leaf area per unit ground surface area is being used (Chen and Black, 1991; Chen and Black, 1992; Fassnacht *et al.*, 1997; Stenberg *et al.*, 2004). It is important to note that these different definitions can result in significant differences between calculated LAI values (Jonckheere *et al.*, 2004a). Consequently, for all plant functional types considered in this study, LAI is defined as one half the total leaf area per ground surface area as being used for flat leaves in current studies (Chen and Black, 1991; Chen, 1996a; Liu *et al.*, 1997; Brown *et al.*, 2000; Leblanc *et al.*, 2002b).

2.2. Methods for LAI Determination

There are two main categories of in-situ LAI determination: direct and indirect methods (Gower *et al.*, 1999; Jonckheere *et al.*, 2004a). Direct measurement approaches include area harvest, application of allometric equations to stand diameter data, and leaf litterfall collection. Numerous commercially available instruments (e.g., Decagon ceptometer, Li-Cor LAI-2000, DEMON, TRAC and hemispherical photography) are used to indirectly estimate LAI (Chen *et al.*, 1997). All of the instruments measure light transmittance and assume foliage is randomly distributed in the canopy.

Direct methods are the most accurate, but they have the disadvantage of being extremely time-consuming and as a consequence making large-scale implementation only marginally feasible. Accuracy problems may in this case result from the definition of LAI, the up-scaling method, or from the error accumulation due to frequently repeated measurements (Jonckheere *et al.*, 2004a). Because of its time-consuming and labor-intensive character and apart from other operational constraints, it can be said that direct LAI determination is not really compatible with the long-term monitoring of spatial and

temporal dynamics of leaf area development (Chason *et al.*, 1991). However, the need for validation of indirect methods remains, so the direct techniques can be considered important as calibration methods.

Scurlock *et al.* (2001) summarized common direct measurement techniques of LAI: (1) destructive harvesting and direct determination of one-sided leaf area, using squared grid paper, weighing of paper replicates, or an optically based automatic area measurement system; (2) collection and weighing of total leaf litterfall, converted to leaf area by determining specific leaf area (leaf area/leaf mass) for sub-samples; and (3) allometry (based on simple physical dimensions, such as stem diameter at breast height), using species-specific or stand-specific relationships based on detailed destructive measurement of a sub-sample of leaves, branches, or whole individuals.

Indirect methods, in which leaf area is inferred from observations of another variable, are generally faster, amendable to automation, and thereby allow for a larger number of spatial samples to be obtained. For reasons of convenience when compared to the direct methods, they are becoming more and more important. Indirect methods of estimating LAI in situ can be divided in two categories: (1) indirect contact LAI measurements such as plumb lines and inclined point quadrates (Gower *et al.*, 1999; Scurlock *et al.*, 2001; Jonckheere *et al.*, 2004a); and (2) indirect non-contact measurements.

Recently, much emphasis has been placed on using indirect optical measurement techniques, particularly suited to measuring the canopy gap fraction, to estimate LAI of vegetation canopies (Morisette *et al.*, 2005). Several optical instruments that measure the canopy gap fraction from beneath, or within, plant canopies, over a range of zenith angles are now commercially available (Welles, 1990; Welles and Cohen, 1996). Air- and space-borne methods on the other hand are applied for LAI determination on forest or landscape level. These methods are based on differences in spectral reflection between vegetation and other coverage (Jonckheere *et al.*, 2004a).

However, a number of correcting factors need to be applied to such indirect estimates to improve their accuracy and their comparability to direct measurement of LAI (Chen *et al.*, 1997; Kucharik *et al.*, 1998). The optimum strategy for collecting extensive “ground truth” LAI in the future may be to use a combination of several indirect optical methods, corrected and calibrated against a more limited number of direct estimates of LAI (Chen and Cihlar, 1996).

2.3. In-situ Optical LAI Assessment Techniques and Instruments

Indirect optical methods measure canopy gap fraction to estimate leaf area index from measurements of the transmission of radiation through the canopy, making use of the radiative transfer theory (Breda, 2003). These methods are non-destructive and are based on a statistical and probabilistic approach to foliar element (or its complement, gap fraction) distribution and arrangement in the canopy. Three optical instruments are commonly used and investigated in this study:

- the LAI-2000 Plant Canopy Analyzer (Li-Cor Inc., Lincoln, NB, USA), (Campbell and Norman, 1990),
- digital hemispherical photographs (DHP) (Weiss, 2004; Weiss *et al.*, 2004), and
- the Tracing Radiation and Architecture of Canopies (TRAC) instrument (3rd Wave Engineering, ON, Canada) (Leblanc *et al.*, 2002a).

The use of gap fraction to estimate LAI and the principle of the aforementioned instruments are discussed in the following section.

2.3.1. LAI Estimation Based on Gap Fraction Measurement

Many optical instruments measure canopy gap fraction based on radiation transmission through the canopy. The gap fraction can be expressed mathematically as (Norman and Campbell, 1989):

$$P(\theta) = e^{-G(\theta,\varphi)LAI/\cos(\theta)} \quad (2)$$

where $P(\theta)$ is the gap fraction, θ is the zenith angle of view, φ is the leaf angle, $G(\theta, \varphi)$ is the projection coefficient of the foliage on a plane (normal) perpendicular to incoming radiation (Norman and Campbell, 1989), $\cos(\theta)$ is the zenith angle of view, and LAI is the Leaf Area Index of the canopy including all above ground structural components (branches, stems, cones, and epiphytes). The projection coefficient $G(\theta,\varphi)$ depends greatly on the angular distribution of the foliage φ and determines the light interception by the canopy. Several foliage angle distributions (e.g., planophile, spheric or elliptical) are used to simulate real leaf angle (Norman and Campbell, 1989). The foliage angle φ, is generally not known, and the LAI calculation requires gap fraction measurements for a range of θ angles of view (Breda, 2003).

The gap fraction-based methods are dependent on leaf-angle distribution (Campbell, 1986). By inverting Eq. (2), the expression for LAI is:

$$LAI = \ln(P(\theta))\cos(\theta)/G(\theta) \quad (3)$$

as the G-function here is independent of the leaf-angle distribution, φ. The `gap fraction'-based methods (canopy analyzer systems and hemispherical images) use several ways to solve this equation as described in theory papers (Miller, 1967; Nilson, 1971; Norman and Campbell, 1989; Breda, 2003).

An important consideration implicitly expressed in Eq. (3) is that LAI can be calculated without knowledge of foliage angle distribution if the gap fraction is measured at several zenith angles covering the full range from 0 to 90^o (Chen *et al.*, 1997), because most of optical instruments assume foliage is azimuthally randomly oriented. The LI-COR LAI-2000 is well suited for this purpose because of its ability to measure $P(\theta)$ at five zenith angles simultaneously from diffuse blue light transmission through the canopy. Hemispherical photography can also provide gap fractions in the full zenith angle range and hence can be used to measure LAI (Chen *et al.*, 1997)

Although Eq. (2) was originally developed for the calculation of LAI, Chen et al. (1991) regard the result from Eq. (2) as the effective LAI (LAIe) because leaves in plant canopies are often not randomly distributed in space. Effective LAI (LAIe), is leaf area index (including branches, stems and cones) which is not corrected for non random distribution of foliage elements. The meaning of this term is perhaps better understood with the following expression (Nilson, 1971):

$$P_o(\theta) = e^{-G(\theta)\,\Omega LAIt/\cos(\theta)} \quad (4)$$

LAIt, is the plant area index including leaf and woody areas, and Ω is a parameter determined by the spatial distribution pattern of leaves. When the foliage spatial distribution is random, Ω is unity. If leaves are regularly distributed (extreme case: leaves are all laid side by side), Ω is larger than unity. When leaves are clumped (extreme case: leaves are stacked on top of each other), Ω is less than unity. Foliage in plant canopies is generally clumped, and hence Ω is often referred to as the clumping index (Chen *et al.*, 1997). Eq. (4) is derived based on the Markov chain theory to estimate the probability of beam penetration through multiple independent canopy layers. It can be considered as a modified Poisson model to account for the variation in foliage spatial distribution patterns. When $\Omega = 1$, the canopy is random, and Eq. (4) returns to the Poisson model (Chen, 1996a; Chen, 1996b). Since ΩLAIt, is an important quantity determining the canopy gap fraction and hence the radiation environment in the canopy, it deserves the separate term "effective LAI," denoted by LAIe (Chen *et al.*, 1997).

When LAIe is measured, LAIt can be obtained from:

$$LAIt = LAIe/\Omega \quad (5)$$

By treating shoots as the basic foliage units, (Chen and Cihlar, 1996) derived that

$$\Omega = \Omega_E/\gamma_E \quad (6)$$

where γ_E is the needle-to-shoot area ratio quantifying the effect of foliage clumping within a shoot (it increases with increasing clumping) and Ω_E includes the effect of foliage clumping at scales larger than the shoot (it decreases with increasing clumping). For deciduous forests, individual leaves are considered as the foliage elements, and $\gamma_E = 1$.

By combining Eq. (5) and (6) we have

$$LAIt = LAIe * \gamma_E / \Omega_E \quad (7)$$

The plant area index LAIt, is the sum of leaf area index, denoted by LAI, and the woody area index, denoted by WAI, and therefore

$$LAI = LAIt - WAI = LAIt\,(1-\alpha) \quad (8)$$

where α is the woody-to-total area ratio, = WAI/LAI. By using the factor (1 - α), the contributions of non-leaf materials are removed.

From Eq. (7) and (8), the final equation for LAI then becomes

$$LAI = (1- \alpha)\ LAIe * \gamma_{E\ /}\ \Omega_{E} \quad (9)$$

The above equation shows that to obtain the leaf area index (LAI), three corrections must be made (Eq. (6), (7) and (8)) to the effective leaf area index (LAIe) obtained from multi-angle gap fraction measurements (Chen, 1996a)

2.3.2. Optical Field Instruments to Measure LAI

LAI-2000 Plant Canopy Analyzer

The LAI-2000 plant canopy analyzer calculates leaf area index (LAI) and other canopy structure attributes from radiation measurements made with a "fish-eye" optical sensor (148^{o} field-of-view) (LAI-2000, 2005). The LAI-2000 plant canopy analyzer is a portable instrument that does not require additional data acquisition and processing, but it is able to provide immediate LAI estimates, measuring simultaneously diffuse radiation by means of a fisheye light sensor in five distinct angular bands, with central zenith angle of 7^{o}, 23^{o}, 38^{o}, 53^{o} and 68^{o} (Jonckheere *et al.*, 2004b). LAI-2000 measures the transmitted blue sky light (400-490 nm) under the canopy in five concentric rings from 0^{o} to 75^{o}, from which to calculate the gap fraction for five zenith angle ranges (Chen *et al.*, 1997). The light level is measured in clearings without trees and below the canopy. Moreover, there is an in-built optical filter that rejects incoming radiation with wavelengths above 490 nm in order to minimize the radiation scattered by the canopy. Thereby, a maximum contrast between leaf and sky is achieved. The ratio of the two values gives the transmittance simultaneously for each sky sector. LAI is then estimated by inversion of the Poisson model comparing the transmittances (Eq. (3)).

In use, gap fractions at five zenith angles can be measured by making a reference reading above the canopy (sensor aimed up at the sky), and one or more readings beneath the canopy (sensor again looking up). The below readings are divided by above readings to obtain an estimate of the gap fraction at the five angles. Snap-on view restrictors can be used to limit the sensor's azimuthal field of view. This is necessary in small plots, or very clumped canopies, or when the sun is shining (Welles, 1990).

The calculations, which are automatically derived by the internal software, are based on four assumptions (LAI-2000, 2005): (1) the foliage is black, it is assumed that the below-canopy readings do not include radiation that has been reflected or transmitted by foliage; (2) the foliage elements are small compared to the area of view of each ring; (3) the foliage is randomly distributed within certain foliage containing envelopes, these envelopes might be parallel tubes (a row crop), a single ellipsoid (an isolated bush), an infinite box (turf grass), or a finite box with holes (deciduous forest with gaps); and (4)

foliage is azimuthally randomly oriented. That is, it does not matter how the foliage is inclined, but the leaves should be facing all compass directions.

The LAI-2000 performs all computations on-board, and stores measurements and results. It has been used with success to estimate LAI in continuous and homogeneous canopies, such as millet and grasslands, validated by direct estimates of LAI based on harvesting (Levy and Jarvis, 1999). In discontinuous and heterogeneous canopies, the potential of this instrument is restricted by a general tendency towards underestimating LAI (Chason *et al.*, 1991). Until now, the underestimation errors caused by clumping could not be satisfactorily addressed including correction factors or adapting radiation models. Adapted models such as the Markov model or the negative binomial model are not compatible with the data measured by the LAI-2000 and are not in an operational form (Chason *et al.*, 1991). Impact of external factors (illumination conditions and boundary effects) can be minimized by means of a 270° view cap (Nackaerts *et al.*, 2000). A disadvantage is that it captures the forest canopy with only a coarse resolution of five concentric rings using immediate integration procedures, so making a posteriori detailed spatial analyses (i.e. foliage distribution) impossible (Jonckheere *et al.*, 2004b).

A potential practical weakness of the LAI-2000 approach is the requirement for an above canopy reference reading in order to get an accurate LAI estimation (Welles, 1990). There exists the potential for sky conditions to change between the reference and below canopy readings. If two separate systems are employed, one system can be made to log readings unattended outside the canopy, while the other system is used to collect the in-canopy data. Later, the two datasets can be merged and calculations performed. This merging can be done by connecting the two control boxes together, or else by using an external computer with software supplied with the instrument (Welles, 1990).

Different software codes exist to analyze LAI-2000 measurement such as: FV2000, C2000.EXE, and the 1000-90 DOS communications program. FV2000 is a Windows™ application for downloading, viewing, and manipulating data files from the LI-COR LAI-2000 Plant Canopy Analyzer. It replaces the DOS program C2000.EXE, and the 1000-90 DOS communications program. FV2000 adds some functionality, especially in the area of visualizing and designing isolated canopy models for determining path lengths, and also for general data graphing and analysis (FV2000, 2005).

Tracing Radiation and Architecture of Canopies (TRAC)

TRAC is an optical instrument for measuring the Leaf Area Index and the Fraction of Photosynthetically Active Radiation absorbed by plant canopies (*FPAR*) (Leblanc *et al.*, 2002a). The LAI and *FPAR* absorbed by plant canopies are biophysical parameters required in many ecological and climate models. In spite of their importance, the commercially available techniques for measuring these quantities are often less than adequate. Many studies have relied on commercial instruments such as the LAI-2000 Plant Canopy Analyzer (LI-COR), AccuPAR Ceptometer (Decagon), and Demon (CSIRO) as well as hemispherical photography (Leblanc *et al.*, 2002c). However, these optical instruments have been repeatedly found to underestimate LAI of forests and

discontinuous canopies where the spatial distribution of foliage elements is not random. TRAC was developed to cope with this problem.

TRAC measures canopy "gap size" distribution in addition to canopy "gap fraction". Plant canopies, especially forests, have distinct architectural elements such as tree crowns, whorls, branches, shoots, etc. Since these structures dictate the spatial distribution of leaves, this distribution cannot be assumed to be random. Previous commercial instruments have been based on the gap fraction principle. Because of foliage clumping in structured canopies, those instruments often considerably underestimate LAI. A canopy gap size distribution contains information of canopy architecture and can be used to quantify the effect of foliage clumping on indirect (i.e., nondestructive) measurements of LAI.

TRAC (including the recording and data analysis components) is hand-carried by a person walking at a steady pace (about 0.3 meter per second). Using the solar beam as a probe, TRAC records the transmitted direct light at a high frequency (32 Hz). Such measurements are recorded and stored as spike where each spike, large or small, in the time trace represents a gap in the canopy in the sun's direction. These individual spikes are converted into gap size values to obtain a gap size distribution. A gap size distribution curve like reveals the composition of the gap fraction and contains much more information than the conventional gap fraction measurements. A gap size distribution contains many gaps that result from non-randomness of the canopy, such as the gaps between tree crowns and branches. Since we know the distribution for a random canopy, based on Welles and Norman (1991), the gaps resulting from non-randomness can be identified and excluded from the total gap fraction accumulation using a gap removal method (Chen and Cihlar, 1995a). The difference between the measured gap fraction and the gap fraction after the non-random gaps removal can then be used quantify the clumping effect (Leblanc and Fournier, 2005).

The clumping index obtained from TRAC can be used to convert effective PAI to PAI. Leblanc (2002) showed that the TRAC can accurately measure a change in PAI when trees are cut, inducing clumping in a canopy. When TRAC is used for half a clear day, or at solar zenith angle near 57.3°, an accurate LAI value for a stand can also be obtained using TRAC alone. TRAC technology has been validated in several studies (Chen and Cihlar, 1995; Chen, 1996b; Chen *et al.*, 1997; Kucharik *et al.*, 1998; Leblanc, 2002; Leblanc *et al.*, 2002a; Leblanc *et al.*, 2002c). For deciduous stands the clumping index measured from TRAC includes the clumping effect at all scales, but in conifer stands it only resolves the clumping effect at scales larger than the shoot (the basic collection of needles) because conifer needles are blow the resolution of TRAC instrument. The TRAC device is suitable for computing PAI, but (Chen *et al.*, 1997) advised correcting indirect LAI measurements (e.g. from the LAI-2000) using the clumping factor derived from TRAC estimates (Breda, 2003).

.

Hemispherical Canopy Photography

In recent years, off-the-shelf digital cameras have finally reached a quality standard that can start competing with film-based camera. Hemispherical canopy (fisheye) photography is a technique used to measure subcanopy light conditions (Roxburgh and Kelly, 1995). Jonckheere *et al.* (2004a) defined explicitly as, it is a technique for studying plant canopies via photographs acquired through a hemispherical (fisheye) lens from beneath the canopy (oriented upwards) or placed above the canopy looking downward. Digital cameras acquire photographs using a couple charge device (CCD) matrix. A CCD is a light-sensitive integrated circuit that is placed at the focal plane of an optical imaging system and is assumed to have a linear response to light. The cameras' resolution, usually quantified in mega pixel, can now allow an angular resolutions better than 0.5^{o}, which is the sun angular disc solid angle (Leblanc *et al.*, 2005).

A hemispherical photograph provides a permanent record and is therefore a valuable information source for position, size, density, and distribution of canopy gaps (Jonckheere *et al.*, 2004a). It is able to capture the species-, site- and age-related differences in canopy architecture, based on light attenuation and contrast between features within the photo (sky/soil versus canopy). Hemispherical photographs generally provide a 180^{o} field of view. In essence hemispherical photographs produce a projection of a hemisphere on a plane (Rich, 1990). The exact nature of the projection varies according to the used lens.

Hemispherical photography provides also information on the clumpiness through the gap size distribution (Chen and Cihlar, 1995). Due to this quality and use of the images for future processing, hemispherical photographs are progressively replacing LAI-2000 devices. Furthermore, hemispherical photographs are used in the case of low vegetation canopies by taking downward looking photographs. They are also used in more variable illumination conditions, particularly when looking upwards, which make the measurements more flexible as compared to LAI-2000.

Traditionally, hemispherical canopy photography relied on conventional black and white, or color films (negatives or diapositives), and charge-coupled device (CCD) scanners to produce digital images for analysis (Frazer *et al.*, 2001). Today, however, high-resolution (2–6 million pixels) consumer-grade digital cameras offer forest scientists better alternative to traditional film photography. With the advent of affordable digital technologies, standard graphic image formats, and more powerful desktop computing, digital image analysis techniques have been used increasingly to examine hemispherical canopy photographs (Rich, 1990). In that context, analysis of hemispherical photographs has been successfully used in a diverse range of studies to characterize plant canopy structure and light penetration (Jonckheere *et al.*, 2004a).

To date, few published data are available to assess the performance of digital pictures compared with classical ones from film (Frazer *et al.*, 2001; Hale and Edwards, 2002). Digital cameras are available now with a very large number of pixels that provides a spatial resolution close to that of classical photographic films (Hale and Edwards, 2002).

In comparison to analogue cameras, these digital sensors have better radiometric image quality (linear response, greater dynamic range, wider spectral sensitivity range (Jonckheere *et al.*, 2004a) and offer some practical advantages: (1) digital images make the expense and time associated with photographic film, film development, and scanning unnecessary and thereby eliminate errors that may occur during this procedure; (2) the potential of real time processing and assessment in the field; and finally (3) the unlimited image treatment possibilities.

One of the main problems cited in the literature of hemispherical photography for determination of LAI is the selection of the optimal brightness threshold in order to distinguish leaf area from sky area thus producing a binary image (Leblanc and Fournier, 2005; Zhang *et. al.*, 2005). A series of software packages for hemispherical images processing have been developed, Hemiview (Delta-T Device), SCANOPY (http://www.regentinstruments.com/products/Scanopy/Scanopy.html), GLA (Forest Renewal BC) and CAN_EYE (Weiss *et al.*, 2004; Baret *et al.*, 2005). Previous research demonstrated that with a high resolution digital camera, the choice of the threshold level would be less critical, because the frequency of mixed pixels is reduced in comparison to the aggregation of pixels in cameras with lower resolution.

Jonckheere *et al.* (2004a) described characteristics of an ideal device for measuring LAI. It should be a hemispherical sensor in order to simultaneously measure the canopy gap fraction at a range of zenith angles, enabling more efficient sampling than is possible with linear sensors (Welles and Norman, 1991). It should permit derivation of the gap fraction distribution as a function of the zenith angle to get information on leaf clumping. It should have predefined exposure, and ability to detect green and non-green elements. Further, it should permit acquisition of data over low vegetation by looking downward. It should also provide a visualization of the canopy, which can help identify possible measurement problems. In addition to the estimation of the leaf area index, such an ideal hemispherical device could also be used to characterize directly the light climate within canopies. Obviously, hemispherical cameras have these potential features. Hemispherical photography, a technique that is markedly cheaper than alternatives, has already proven to be a powerful indirect method for measuring various components of canopy structure and under story light regime. Numerous advances in hemispherical analysis, which have taken place over the last decade, are directly related to evolving computer, photographic, and digital technologies and scientific modeling methods. Hemispherical photographs can be archived, reprocessed when improved models become available and used to perform other measurements, for example, fractal dimension, architecture and light regime below the canopy.

2.3.3. Combination of Techniques

Although indirect measurements of LAI using optical instruments have the advantage of convenience and low labor costs, many researchers have been deterred by the drawbacks of the indirect methods. The difficulties arise from the complexity of radiation transfer in vegetation canopies. The problems include (Breda, 2003): (1) the unknown foliage angle distribution, (2) the error due to nonrandom foliage distribution, and (3) the contribution

of supporting woody material to the radiation interception. Each of these (2 and 3) errors is in the range of 5-l0%, making the sum of the error in the range of 15-30% (Chen *et al.*, 1997). LAI can be calculated without knowledge of foliage angle distribution if the gap fraction is measured at several zenith angles covering the full range from 0 to 90^{o} (Chen *et al.*, 1997).

Several papers have compared plant area index as measured by indirect methods with direct LAI estimates (Chason *et al.*, 1991; Nemani *et al.*, 1993; Chen *et al.*, 1997; Fassnacht *et al.*, 1997; Barclay *et al.*, 2000; Breda, 2003; Jonckheere *et al.*, 2004b). Most of these papers concluded that indirect methods underestimated LAI compared with direct measurement. The reported underestimation varies from 25% to 50% in different stands (Gower *et al.*, 1999). It is now widely accepted that a reason for the underestimation is the non-random distribution of foliar elements within the canopy.

All estimates based on indirect optical methods correspond to the Plant Area Index (PAI), because they include the contribution of stems and branches. The recent review by Gower *et al.* (1999) makes the contribution of woody parts to PAI as measured by indirect methods ranges from 5-35%. Calculation of woody area index can be found based on in situ measurements of foliage and woody area per tree, derived from destructive measurements of the branches and measured total tree height, bole length, crown dimensions and crown length, and plotted against DBH (Jonckheere *et al.*, 2004b). They found woody area index value from destructive measurement consistent with analysis of the digital hemispherical images, where the amount of woody material was estimated by means of image classification, assuming the stems and branches seen on the photographs were simple cone shapes (Barclay *et al.*, 2000).

Canopy architecture may be separated into two essential attributes: foliage angle distribution and foliage spatial distribution. The commercial instruments and hemispherical photography techniques are well suited for measuring LAI without a priori knowledge on the leaf angle distribution by acquiring multiple angle gap fraction data, but estimates of LAI, are often incorrect because foliage spatial distribution is not random, a key assumption to gap fraction models. Chen and Cihlar (1995) developed an optical instrument named TRAC (tracing radiation and architecture of canopies) and theory to measure LAI of clumped canopies. The theory utilizes canopy gap size information in addition to canopy gap fraction and provides a foliage clumping index which quantifies the effect of nonrandom spatial distribution of foliage on LAI measurements.

Clumping factors estimated by the TRAC have recently been validated (Chen and Cihlar, 1995; Chen, 1996a; Chen *et al.*, 1997; Kucharik *et al.*, 1998). The TRAC device can be used for computing LAI, but Chen *et al.* (1997) advised correcting indirect LAI measurements (e.g. from the LAI-2000 or hemispherical photography) using the clumping factor derived from TRAC estimates. It is recommended (Chen *et al.*, 1997; Leblanc and Chen, 2001; Leblanc, 2002; Leblanc *et al.*, 2002a; Leblanc *et al.*, 2002c; Leblanc and Fournier, 2005) that TRAC can be used to investigate the foliage spatial distribution pattern (clumpiness) while LAI-2000/hemispherical photography is useful to

study foliage angular distribution pattern. The combined use of TRAC and LAI-2000/hemispherical photography allows quick and accurate LAI assessment of a canopy.

The TRAC clumping index was applied to correct LAI-2000 estimates of LAI for deviations from the assumption of randomly distributed foliage used in the LAI-2000 processing algorithms. Hemispherical photography-based LAI estimates were corrected for clumping by applying the TRAC clumping index algorithm for successive zenithal rings in the field of view (Leblanc and Fournier, 2005). These have been shown to be well correlated with allometric LAI over a number of boreal sites in Canada (Gower *et al.*, 1999) up to an LAI of six.

Currently, the global validation activity (Morisette *et al.*, 2005) of leaf area index is based on either a combined use of LAI-2000/TRAC or hemispherical photography/TRAC method for in-situ LAI measurements.

However, to combine optical field instruments as suggested by Leblanc *et al.* (2002a), care must be taken when a stand is not homogeneous. The plot size and number of measurements (points or transects) has some general rules, but an understanding of the geometry of the measurements can be used to estimate if the plot design correspond to the desired area to be sampled (Leblanc and Fournier, 2005). The footprint corresponding to optical field measurements depends mainly on the device used and the canopy sampled. For devices based on multidirectional gap fraction measurements such as LAI-2000 or hemispherical photography, observations up to θ_o =60-70° are used; where θo is the angular measure of view from zenith. Therefore, the footprint will correspond to a disk with diameter D=2 * tan(θ_o).H, where H is the canopy height (Morisette *et al.*, 2005). For TRAC, to be used under clear sky conditions, the footprint depends mainly on the sun zenith angle (θs) and tree height. The TRAC instrument requires transect sampling, preferably along transects oriented perpendicular to the sun direction. The foot print will therefore be a rectangle the length of the transect, and a width defined by tan(θs) * H (Morisette *et al.*, 2005).

2.4. LAI Validation Procedure

Initiated in 1984, the Committee Earth Observing Satellites' Working Group on Calibration and Validation (CEOS WGCV) pursues activities to coordinate, standardize and advance calibration and validation of civilian satellites and their data (Baret *et al.*, 2005; Morisette *et al.*, 2005). One subgroup of CEOS WGCV, Land Product Validation (LPV), was established in 2000 to define standard validation guidelines and protocols and to foster data and information exchange relevant to the validation of land products.

Having multiple global LAI products and validation activities related to these products, presents the opportunity to realize efficiency through international collaboration. The global validation activity can be achieved using a bottom-up approach, i.e. from local field level measurements to global comparison with satellite derived LAI products. Field validation of global or large regional satellite- or air-borne-derived products generally relies on point measurements from the field that need to be scaled up to compare to the corresponding moderate-resolution global products. This question is generally addressed

by associating the field measurements with high-resolution imagery to make a high-resolution map of the same variable derived from field measurements (Morisette *et al.*, 2005). Then, the quality of the moderate-resolution product is assessed by comparing it with the high-resolution product. Fig. 1 shows the relationship between the major steps.

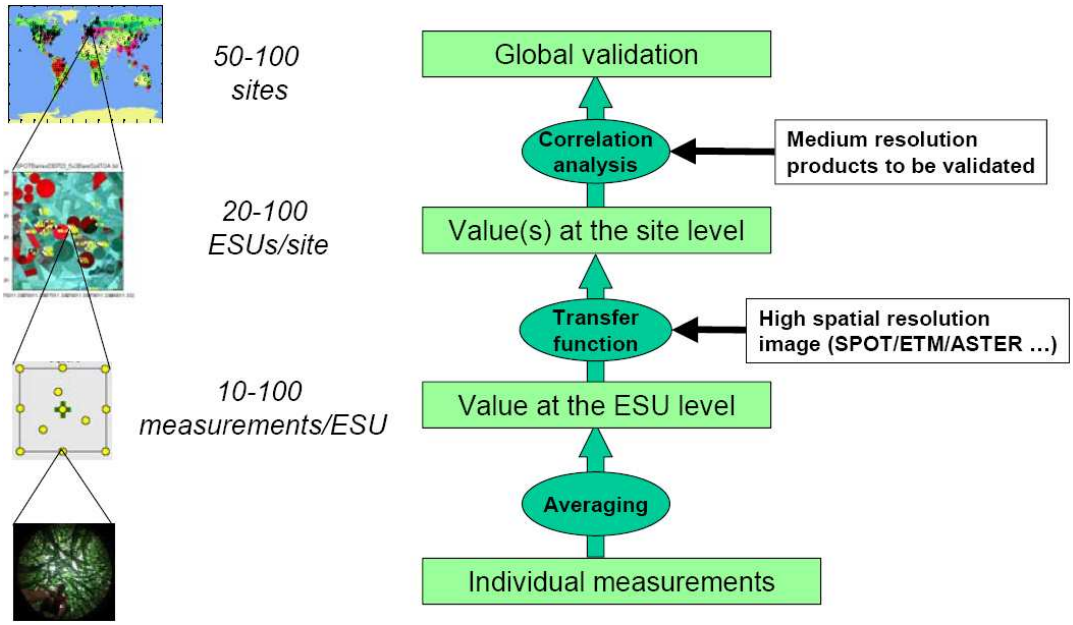

Fig. 1. General validation procedure applied to LAI according to CEOS LAI intercomparison overview submission. Source, (Morisette *et al.*, 2005).

Various optical methods have been used to acquire a large number of data points for validation of LAI values from high resolution remote sensing. The Validation of LAnd European Remote sensing Instruments (VALERI) (http://www.avignon.inra.fr/valeri/), supported mainly by CNES and INRA, has focused on the development of an effective methodology to generate high spatial resolution maps of biophysical variables from satellites and the use of those maps for the validation of moderate-resolution global products. The methodology developed by VALERI is mature enough to be applied on a routine basis.

The local measurements performed over the series of Elementary Sampling Units (ESUs) will be extended to the whole site using a dedicated process (Fig.1). The transfer function relates the high spatial resolution radiometric data to the corresponding ground measurements. It can be calibrated or evaluated over the ESUs, and subsequently applied to the high spatial resolution image to derive a first version of the high spatial resolution map of the LAI product. Several types of transfer functions were investigated that can be either derived from radiative transfer model inversion or purely empirical (Baret *et al.*, 2005).

Establishing the relationship between the field-based LAI estimates and imagery is known as up-scaling. Methodology for up-scaling has evolved over the last five years and is now starting to stabilize. The up-scaling process is mainly based on the calibration of empirical transfer functions that establish a relationship between the average LAI values from each ESU and the multispectral values from a satellite or airborne image. Selection of the optimal transfer function is site-specific and the one that reduces the difference between the observed LAI values and those predicted by the transfer function or other cross validation techniques (Morisette *et al.*, 2005).

A "bottom-up" approach is used in this study to validate the regional LAI products from local field measurements. LAI values are computed from ground data for each ESU in order to make the subsequent comparison from the corresponding pixel value of AHS data after degrading AHS LAI map to low resolution (20 x 20m) so as to correspond with VALERI plot size.

2.5. Imaging Spectroscopy for Estimation of LAI

Leaf area index (LAI) is a significant ecological attribute that controls physical and physiological processes in vegetation canopies and is widely used as input to biogeochemical process models over extensive terrestrial areas (Berterretche *et al.*, 2005). For such purposes, LAI predictions are often needed as maps, which can be derived from remotely-sensed data using empirically derived regression relationships based on spectral vegetation indices (SVIs). SVIs are calculated from reflectance data and, through regression, often related to field-based LAI measurements of the dominant canopy (Chen, 1996a; Turner *et al.*, 1999; Broge and Leblanc, 2001; Gong *et al.*, 2003; Stenberg *et al.*, 2004). Measuring LAI on the ground is difficult and requires a great amount of labor and cost. To produce an LAI map of a large area, a model relating field data with remote sensing data is typically developed, the model is inverted, and the remote sensing data are then used to extrapolate that relationship to the landscape (Lee *et al.*, 2003; Lee *et al.*, 2004).

The majority of studies for extracting biophysical variables from remotely sensed data have used empirical techniques to relate the spectral measurements to biophysical parameters (Schlerf *et al.*, 2004; Berterretche *et al.*, 2005; Schlerf *et al.*, 2005) although several have used canopy reflectance models (Nemani *et al.*, 1993; Lee *et al.*, 2004). With few exceptions, such studies used broad-band multispectral data, like Landsat TM or ETM+ rather than narrow-band, hyperspectral sensors. Above and beyond, the broadband indices, usually constructed with near-infrared (NIR) and red (R) bands, use average spectral information over broad bandwidths, resulting in loss of critical information available in specific narrow bands, and are known to be heavily affected by soil background at low vegetation cover (Eriksson *et al.*, 2005). Now a days, the advent of airborne imaging spectrometers has made it possible to construct more refined VIs through the use of distinct narrow bands.

2.5.1. Vegetation Indices for LAI Estimation

A lot of research has been done on the estimation of forest LAI from remote sensing data within the last one and half decades (Turner *et al.*, 1999; Brown *et al.*, 2000; Jacquemoud *et al.*, 2000; Chen *et al.*, 2002; Hall *et al.*, 2003; Sun-Hwa and Kyu-Sung, 2003; Lee *et al.*, 2004; Wang *et al.*, 2004; Pu *et al.*, 2005; Schaepman *et al.*, 2005). Most of the studies on forest are based on the relation of LAI with vegetation indices (VIs), such as the simple ratio (SR) or the normalized difference vegetation index (NDVI). However, the application of such relationships to large areas or at different seasons is limited by being site and sensor specific. Apart from this, the sensitivity of VIs to changes in LAI is often not dynamic enough to allow accurate estimation of LAI. This problem has been encountered for example in boreal coniferous forests, where NDVI typically has a very narrow range due to the presence of a green understory (Manninen *et al.*, 2005).

In practice, LAI prediction from remotely sensed data faces two major difficulties: (1) vegetation indices approach a saturation level asymptotically when LAI exceeds certain value, depending on the type of vegetation index; (2) there is no unique relationship between LAI and a vegetation index of choice, but rather a family of relationships, each a function of chlorophyll content and/or other canopy characteristics. To address these issues, a few studies have been carried out to assess and compare various vegetation indices in terms of their stability and their prediction power of LAI (Schlerf *et al.*, 2004; Berterretche *et al.*, 2005) while others have dealt with modifying some vegetation indices to improve their linearity with, and increase their sensitivity to, LAI (Nemani *et al.*, 1993; Chen, 1996a; Chen and Cihlar, 1996; Brown *et al.*, 2000). Consequently, some indices have been identified as best estimators of LAI because they are less sensitive to the variation of external parameters affecting the spectral reflectance of the canopy, namely soil optical properties, illumination geometry, and atmospheric conditions. There are extensive literature for most widely used VIs for LAI estimation (Schlerf et al., 2004; Schlerf *et al.*, 2005).

Recent studies on LAI estimation (Brown *et al.*, 2000; Chen *et al.*, 2002), suggest that inclusion of shortwave infrared (SWIR) reflectance in VIs may be useful to suppress the background influence. For example the reduced simple ratio (RSR) has been found to perform well in coniferous forests (Stenberg *et al.*, 2004; Wang *et al.*, 2004), and is discussed in the following section.

2.5.2. Reduced Simple Ratio

Three bands (RED, NIR, and SWIR) were used to form a new vegetation index named reduced simple ratio (RSR). It is defined as follows Eq. (10) (Brown *et al.*, 2000):

$$RSR = \frac{\rho_{NIR}}{P_{RED}}\left[1 - \frac{\rho_{SWIR} - \rho_{SWIRmin}}{\rho_{SWIRmax} - \rho_{SWIRmin}}\right] \quad (10)$$

where ρ_{NIR}, ρ_{RED}, and ρ_{SWIR} are the reflectance in NIR, RED, and SWIR band, respectively. $\rho_{SWIRmin}$ and $\rho_{SWIRmax}$ are the minimum and maximum SWIR reflectance

found in each image and defined as the 1% minimum and maximum cutoff points in the histogram of SWIR reflectance. The major advantages of RSR over simple ration VI are (Chen *et al.,* 2002): (1) the difference between cover types is very much reduced so that the accuracy for LAI retrieval for mixed cover types can be improved or a single LAI algorithm can be developed without resorting to a co-registered land cover map as the first approximation, and (2) the background (understory, moss cover, litter, and soil) influence is suppressed using RSR because the SWIR band is most sensitive to the amount of vegetation containing liquid water in the background.

Results from Brown *et al.* (2000) and from a later study by Chen *et al.* (2002) and Stenberg *et al.* (2004), comprising data from the major boreal tree species in Canada and Finnish pine and spruce stands, showed that for both coniferous and deciduous stands RSR correlated better with LAI than did NDVI and SR. Different algorithms are applied to retrieve LAI using different vegetation indices of which RSR is selected for this study by determining the reduced effect of background reflectance and increase the sensitivity to changes in LAI throughout its natural range.

3. Methodology

3.1. Study Area

The study area for the validation of the remote sensing data (AHS imaging spectrometer) and ground measurements is located at a large flood-plain of the river Rhine, very close to the German-Dutch border called Millingerwaard (Fig. 2). The floodplain Millingerwaard is part of the Gelderse Poort nature reserve and was one of the first nature rehabilitation projects for river floodplains in the Netherlands. The Millingerwaard is located at a distance of approximately 10 km east of the city of Nijmegen (Barendregt *et al.*, 1998). It is located south of the river Waal, which is the main branch of the river Rhine in the Netherlands. Millingerwaard was established in 1986 for the purpose of development of natural ecosystem by restoring natural processes (Barendregt *et al.*, 1998) and covers approximately an area of 16 km^2. It is situated at 51.5^o N and 5^{o}E. The mean altitude of this site is 12 m a.s.l. with the minimum of 8.8 m a.s.l. and a maximum of 15.6 m a.s.l.

The Millingerwaard is a managed natural ecosystem which covers a wide range of species (Appendix 3) and softwood forests comprised of *Salix fragilis* L. (crack willow), *Salix alba* L. (white willow), *Populus nigra* L. (Lombardy poplar) with dense undergrowth of *Urtica dioica* L. (common nettle), *Calamagrostis epigejos* L. (wood small-reed), *Rubus caesius* L. (European dewberry). It consists also scrub and woodland species namely *Calamagrostis epigejos, Sambucus nigra, Rubus caesius* L. (European dewberry); and grass lands with dominating species of *Medicagini-Avenetun puescentis*, *Bromo inermis-eryngientum campestris* and mosaic of low and tall grasses (*Ranunculo alopecuretum*).

Fig. 2. Location of the study area, Millingerwaard. Source, http://home.wanadoo.nl/jelle.ferwerda/research/location.html

3.2. Methodological Conceptual Model

The general working methodology of this study followed the schema indicated by a conceptual model in Fig. 3. There are generally four input data sets: TRAC; LAI-2000; hemispherical photographs and AHS imaging spectrometer data. The ground measurements were used for calibration and validation of imaging spectrometer data. Finally, the outputs were compared for each plant functional type, methods and instruments employed.

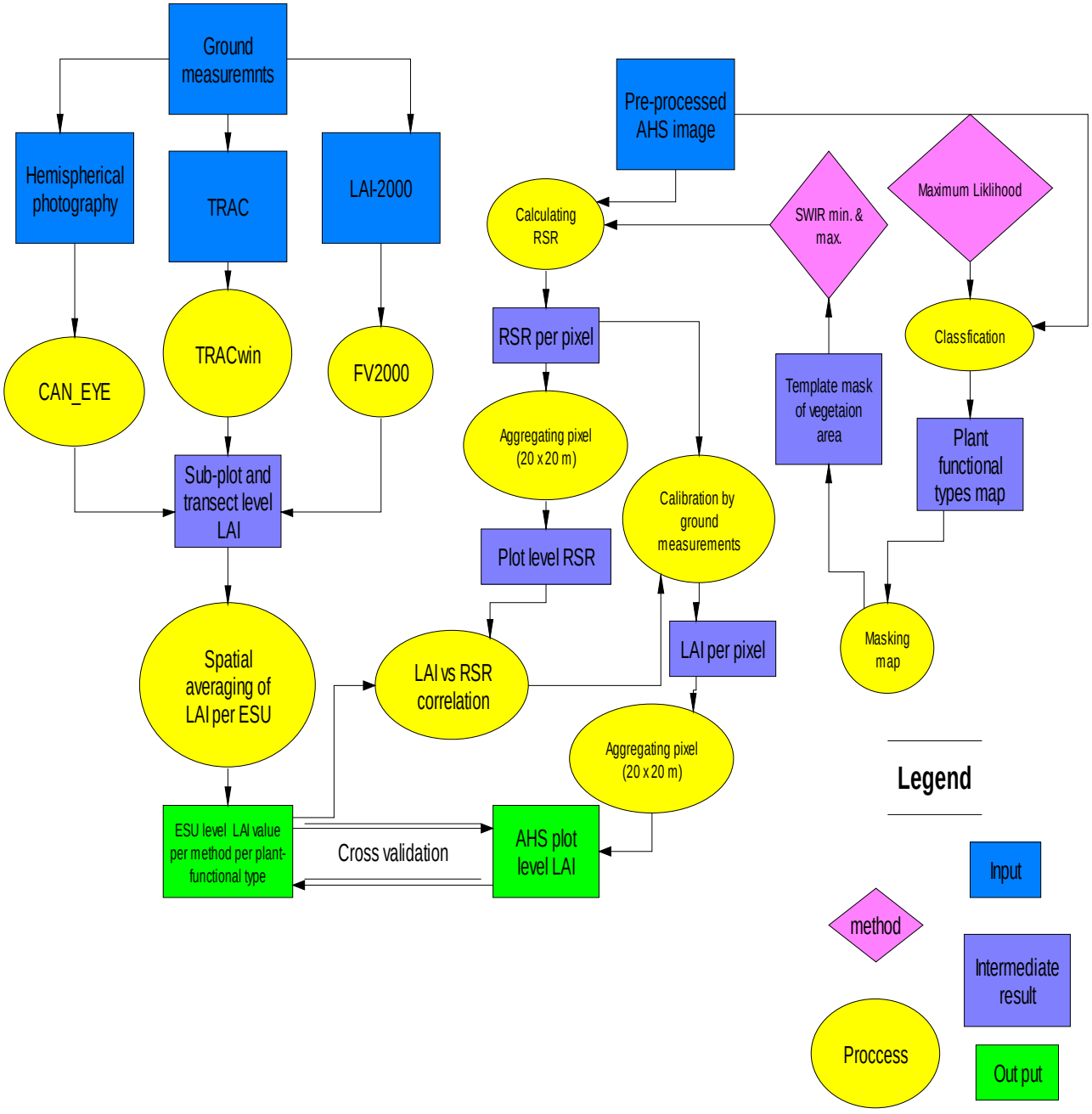

Fig. 3. Flow chart of working scheme to estimate leaf area index of forest, shrub and grass canopies using ground measurement techniques and imaging spectroscopy.

3.3. Ground Measurement Sampling Technique

A total of 19 plots were located within the study area covering the full range of plant-functional types present namely grass, shrub and softwood forest. The ground plots were selected based on a random sampling scheme to cover the representative soft wood forest, shrub and grass canopy densities. Originally, the locations were setup according to the VALERI protocol http://www.avignon.inra.fr/valeri/ as described hereafter. For each elementary sample unit (ESU), a square area of 20m x 20 m was defined by its 12 subplots starting from the center point and continues systematically (Fig. 4 (A)). However, because of the time constraint, only nine sub-plots were taken for hemispherical photography and LAI-2000 measurements (Fig. 4 (B)).

The location of each ESU was determined using global positioning systems (GPSs), which have an accuracy of about ±5 m. The ESUs are set randomly over the study area so that all plant-functional types are represented. The objective here is to set the minimum number of ESUs at the optimal location to get both: (1) a good and efficient description of the LAI value for the range of vegetation considered over the river floodplain in the Millingerwaard, and (2) to establish robust relationships between the ground based measured LAI value and the corresponding high spatial resolution radiometric values over an ensemble of ESUs. For these reasons, five ESUs in the softwood forest were selected for ground measurements with hemispherical photography and TRAC instruments. In grass and shrub plots, eight and six ESUs, respectively, selected for ground measurement with hemispherical photography, LAI-2000 and TRAC.

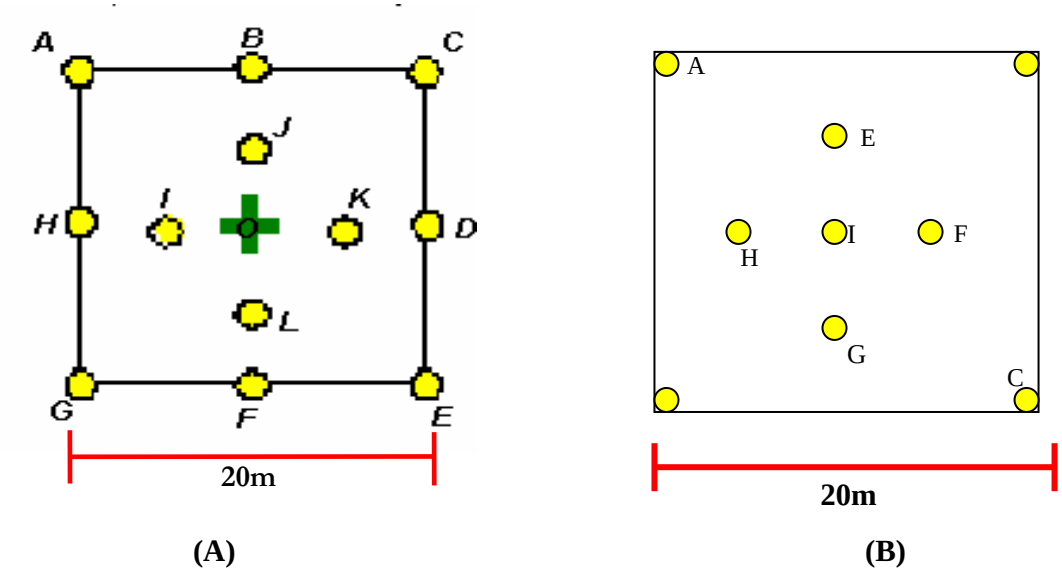

Fig. 4. Sampling method. (A) Experimental set-up of sampling plot according to VALERI-protocol (www.avignon.inra.fr/valeri/), and (B) sampling scheme used for this study.

From each ESU, 9 sub-plots were selected for the measurement of LAI-2000 and hemispherical photography for all plant functional types (Fig. 5 (B)). At each sub-plot in the VALARI ESU, two measurements were taken using hemispherical camera for shrub and forest plots. One measurement was taken with 180^{o} upward looking and the

other was taken downward looking with the same zenith angle away from the trunk. For grass plots only downward looking hemispherical photographs were taken. LAI-2000 measurement was taken only for grass and shrub canopy at each point of the ESUs.

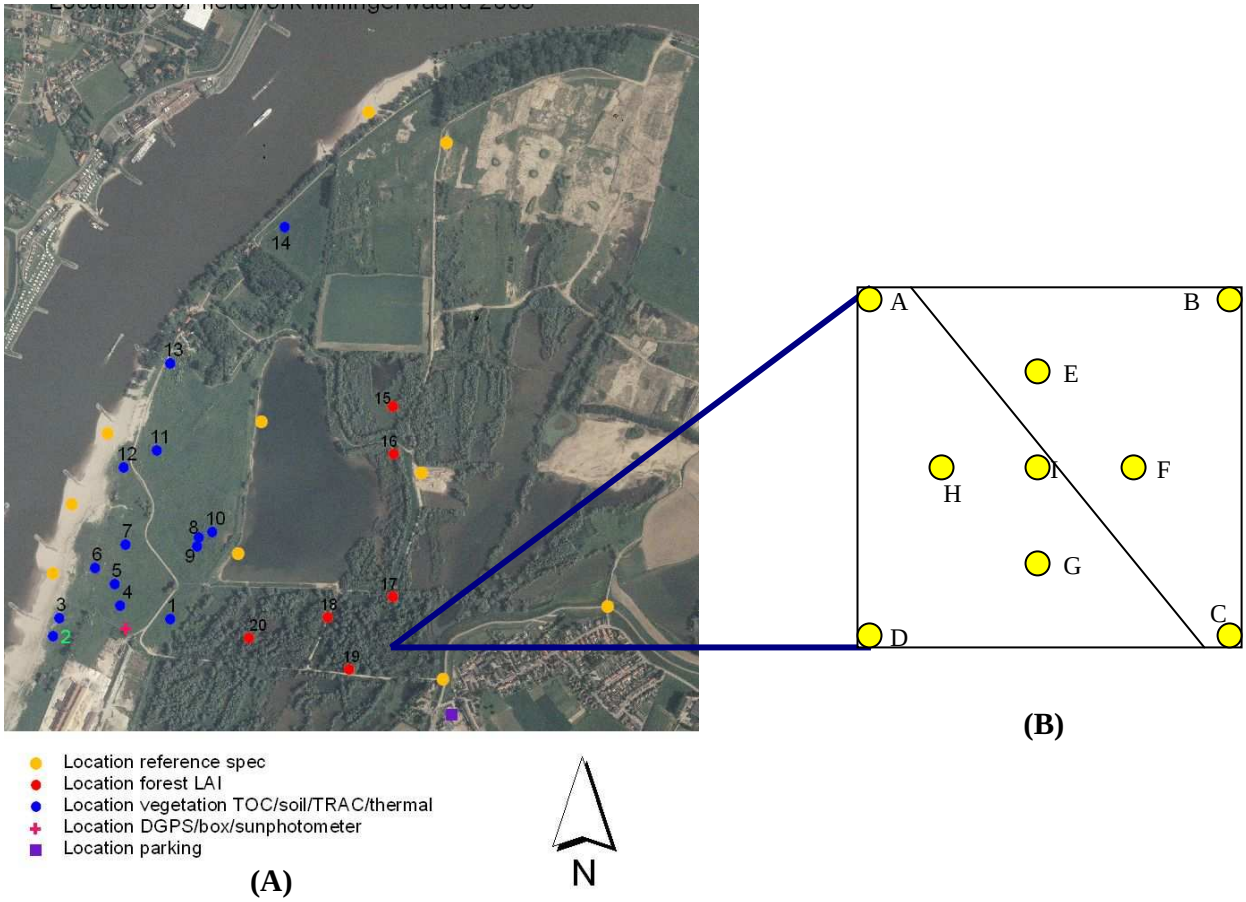

Fig. 5. Spatial distribution of ESUs. (A) Distribution of ESUs in the floodplain vegetation on top of HyMap (2004) image, and (B) the sampling scheme of ESU for digital hemispherical photography, LAI-2000 and TRAC (transect).

The TRAC data were collected by slowly walking along the transects, holding the instrument level to the ground (as much as possible) for understory of shrub and forest plots and grass plots, and holding above understory of shrub and forest plots with the TRAC instrument in front. One transect measurement with the TRAC were made at each plot with varying length and number of segments within ESUs. One additional understory transect was measured for shrub and forest plots.

3.4. LAI Estimation from Optical Field Instruments

3.4.1. LAI-2000 Plant Canopy Analyser

The LAI-2000 plant canopy analyzer is designed to be used in diffuse light conditions with either no cloud or complete cloud cover. In this study, all measurements were made in uniform overcast cloud condition to reduce the effect of scattered blue light in the canopy and to have diffuse radiation from all directions in the hemisphere. An azimuth mask of 180^o view caps were used on LAI-2000 sensor of both instruments all the time to block the bright sky near the sun's direction and to eliminate the shadowing effect of instrument operators.

Two instruments were used to measure shrub plots, one underneath the shrub canopy and the second mounted in a nearby open cleared area (with no obstruction) to provide an open-sky reference of radiation conditions. Finally, two data are merged using FV2000 software (http://www.licor.com/env/Products/AreaMeters/lai2000/2000_FV2000.jsp) by closest in time records to each other for the reference data which is made at the same day and by interpolating the records from existing reference measurements for those plots reference measurements were not available. For grass plots, only one instrument is used to measure reference irradiance above the canopy and under canopy measurement, since all grass plots have short canopy. Ground measurements using LAI-2000 plant canopy analyzer is made only for grass and shrub plots. No measurements were done for forest plots because the reference LAI-2000 plant canopy analyzer was not available on the later field days.

The within canopy measurements were made by placing the sensor on ground surface. Four records were made for each sub-plot of ESUs and one above canopy reference record was made for each sub-plot when there was no reference equipment. Finally, measurements were averaged per ESU to get plot level LAI.

In addition to full range of view zenith angle, LAIe, is also computed from the first two rings; 0.0^o-12.3^o and 16.7^o-28.6^o which are centered at 7^o and 23^o zenith angle, respectively. This is due to, the malfunctioning of the other rings of the instrument. Consequently, comparative computation of LAIe is done from hemispherical photography for the same range of view zenith angle.

3.4.2. Tracing Radiation and Architecture of Canopies (TRAC)

Ground measurement using TRAC was done for all plant functional types (grass, shrub and forest). One transect was selected for each grass plot to take the measurement, and one transect above understory and one transect below understory were selected for shrub and forest plots. The total leaf area index of each ESU for shrub and forest plots was obtained from below understory measurements. Leaf area index and clumping index were assessed from measurements using the TRACwin.exe version 3.7 software (Leblanc et al., 2002a). The clumping index obtained from TRAC is used to convert LAIe from hemispherical photography and LAI-2000 to

LAIt. For flat leaf and grass species the clumping index measured from TRAC includes the clumping effect at all scales (Chen et al., 1997).

To correct for clumping within a stand at all scales greater than the shoot, including within-crown clumping, Ω_e was obtained from TRAC (Leblanc et al., 2002a) as:

$$\Omega_e = [1 + \frac{(F_m - F_{mr})}{1 - F_m}] \frac{\ln F_m}{\ln F_{mr}} \quad (11)$$

where *F*m is the measured total canopy gap fraction and *F*mr is the gap fraction of an imaginary canopy with the same LAI as the clumped canopy, but where the foliage elements are considered spatially random (Chen and Cihlar, 1995). Averaging of clumping index is made per plant-functional type and applied for correction of LAI_e from hemispherical photography and LAI-2000, since TRAC measurements were not done for all ESUs and clumping index does not show significant variation with in the same type of vegetation class and stand (Chen *et al.,* 1997).

Woody-to-total area ratio was determined using digital hemispherical images, where the amount of woody material was estimated by means of image classification, assuming the stems and branches seen on the photographs were simple cone shapes (Barclay *et al.,* 2000). First, wood (including stems and un-shaded branches by foliage) area index is estimated using CAN_EYE software by classifying wood as green vegetation element, and leaves and soil/sky as gap. Then, wood area index (WAI) is divided by plant area index of the same plot to get α (Eq. (12)). This value is used for TRAC input parameter and for correction of LAI value from hemispherical photography. The value of woody area index (WAI) by considering the clumping of stems and branches ranges from 0 – 0.15 and 0.01 – 0.04 for shrub and forest plots, respectively. Then after, woody-to-total area ratio (α) is computed by dividing the WAI to LAIt which is computed from the same photographs. The computed α ranges from 0 – 0.02 and 0.001 – 0.008 for shrub and forest plots, respectively. This value is much lower than what was obtained by Chen *et al.* (1997) and Kucharik *et al.* (1998), woody components comprise between 0.1-0.25 of the total plant area index for pine species. Broad leaf species are believed to have less proportion of α than conifer species, Barclay *et al.* (2000) obtained value of α less than 0.1. In addition to this, α is also calculated only for the above story of shrub and forest canopy and ranges from 0 – 0.048 and 0.003 – 0.015, respectively.

$$\alpha = WAI / (WAI + LAI) \quad (12)$$

Mean element width (W) which is average width of the shadow of a foliage element projected on a horizontal surface is calculated from leaf scans of representative species per plot for TRACwin.exe input. Pre-processing of scans is done using Adobe Photoshop version 9, in order to set up the color threshold and prepare the scans for pixels2 software which calculates the area of each leaf with in scan. The scans are made from field collection of leaves using resolution of 600 x 600 dots per inch. This resolution size was found too big for pixel2 software and it was reduced to 300 x 300 dots per inch. All the scans had hole effect and filled using the stamp filter operation of Adobe Photoshop. The same steps have been carried out to the objects which have known area to validate the whole process and gave satisfactory value of area and dimensions of the objects (Appendix 11). W is calculated using the following equation which is proposed for broadleaf (Leblanc *et al.,* 2002a):

$$W = \sqrt{G(\theta)}A \quad (13)$$

where *A* is the projected (one-sided) leaf area. For crops and natural canopies, $G(\theta) = 0.5$ is valid in many cases, especially if the solar zenith angle is near 57.3°. Leaf scan is done for the dominant species of the representative plots per plant functional type (see Appendix 4). Percentage of each species exists in the plot is computed from species abundance field data (Appendix 3). Thereafter, the ratio of only dominant species abundance is used to compute mean *A*, per plot (Table 1).

Table 1 TRAC input parameters: average woody-to-total area ratio and mean element width (mm) per plant functional type.

Plant function type	**Woody-to-total area ratio (α)**	**Mean element width(mm) (W)**
Grass	-	25.02 (19.51 – 30.09)
Shrub	0.005 (0 – 0.02)	29.65 (28.45 – 30.09)
Overstory	0.015 (0 – 0.048)	29.65 (28.45 – 30.09)
Forest	0.0042 (0.001 – 0.008)	23.99
Overstory	0.0085 (0.003 – 0.015)	12.88

3.4.3. Hemispherical Photograph Acquisition and Processing

Hemispherical photographs were acquired after establishing ESUs for forest, shrub and grass canopies of the study area. The photographs were captured by the use of Nikon hemispherical digital camera. For the forested sites five ESUs, for shrub six ESUs and for grass areas eight ESUs were randomly selected to represent the river floodplain vegetation of Millingerwaard. For forest and shrub canopy, two series of hemispherical images were acquired: one looking downward to characterize understory, the other looking upward to estimate tree characteristics. The images captured were arranged in similar orders in a folder to be processed by software developed for this specific purpose. Accordingly, the images in one elementary sample unit were arranged in folders named UP and Down for upward and downward photos (Fig. 6) for the processing purpose. These procedures are implemented on the photographs arranged in folders according to the direction and the plot from which they are taken based on CAN- EYE soft ware (http://www.avignon.inra.fr/can_eye/). The two kind of images (upward and downward looking) were processed as two separate series and resulting characteristics been combined to represent the whole canopy of each plot.

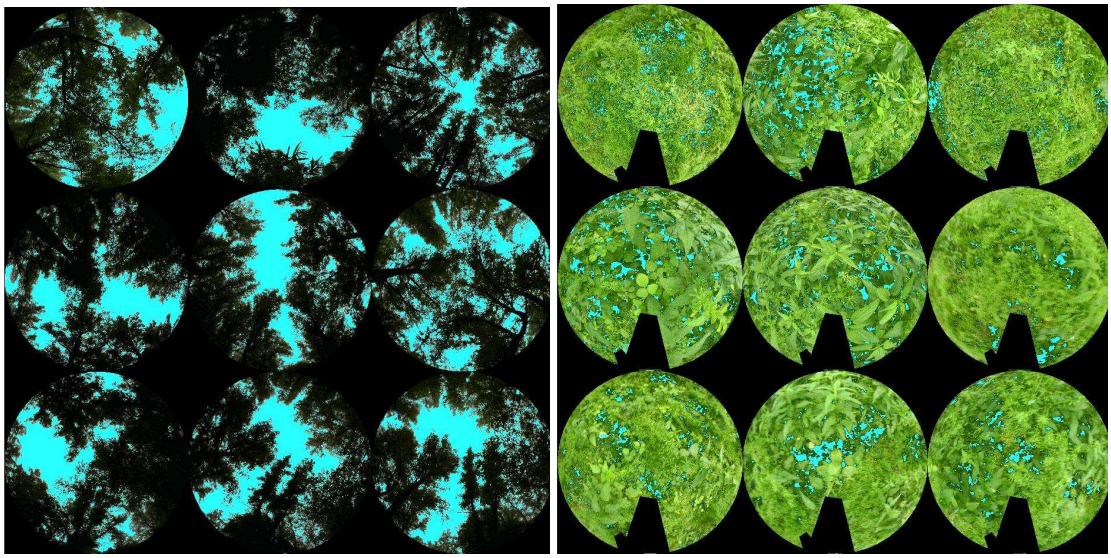

(A) **(B)**

Fig. 6. Hemispherical photographs of plot FR 18 after classification. (A) Upward looking hemispherical photographs, and (B) downward looking hemispherical photographs.

For grass canopy, the digital camera was placed looking down ward, in such a way not too close from the foliage, so that one leaf does not cover the whole field-of-view. Also, the camera was not placed too high to avoid the sky ring in the image.

The dedicated software, CAN_EYE, which was developed to process the color hemispherical photographs with special emphasis on green element, was used to do the classification and processing of a series of nine photographs at a time. The software processes with optimal performances a large number of photographs to derive canopy characteristics. This neural network system based CAN_EYE version 4.1 software was used to compute the gap fraction and LAI. As compared to currently existing software available for processing hemispherical images, CAN_EYE has a set of specific features that improves its efficiency, accuracy, flexibility, portability and traceability (Baret and Weiss, 2004). All the photographs were processed using the following calibration parameters and angular resolution of the CAN_EYE software:

- Image size (lines) = 2448,
- Image size (rows) = 3264,
- Optical center (lines) = 1224,
- Optical center (rows) = 1632,
- Horizon (pixel) = 2448,
- Radius = 90°,
- Sub-sampling factor = 2,
- Circle of interest = 60° and 30°
- Zenith angular resolution = 2.5°,
- Azimuth Angular Resolution = 5°, and
- fCover max zenith angle = 10°.

All the calibration parameters determined by the extent of the photographs i.e., size in pixel and field of view of the hemispherical camera used. Both the angular and the calibration parameters defined by default option of the software and those values were used for processing of the hemispherical photographs except the changes in sub sample factor and circle of interest. Because of the limited memory of the computer

used and the size of the photographs, the sub sample factor of computing was changed into two. Besides, the photographs were computed at 30^o in addition to 60^o circle of interest.

Images may include the legs of the observers, tripod and stars from the sun. These undesirable parts of the image were excluded during the preprocessing of the image through masking. In addition, the gamma factor was used to increase the brightness of the image or darkening the image to provide better visual discrimination between the vegetation elements and the background. At the end of preprocessing, the colors are reduced to a sufficient number to get good discrimination capacities. The classification step differentiates the leaf and the non leaf areas in to different classes. Then after, the gap fraction is computed to derive LAI. The technique to derive the canopy architecture variables leaf area index (LAI) and average leaf inclination (ALA) using CAN_EYE is based on the use of a look-up-table (LUT), i.e. a reference table composed of gap fraction value in different view zenith angles and the corresponding LAI and ALA parameters (details, Baret and Weiss (2004)).

Much care has been made to avoid the errors (Rich, 1988) during different processing steps of hemispherical photographs using CAN_EYE software. Photographs were investigated for the quality and another picture was captured when the quality was not good. Some pictures were affected by the moisture on the lens and were excluded from further processing. Since most of the shrub plots didn't have overstory for all sub-plots visited, the value of upward looking photographs from those sub-plots which didn't have overstory was set to the 0 in order to average the result to plot level. LAI is computed for range of $0\text{-}60^o$ view zenith angle to avoid mixed pixels which results from course resolution of near to horizontal zenith angles. In addition to this; LAI, is also computed for the range of $0\text{-}30^o$ view zenith angle to make comparison of the result from the first two annulus rings of LAI-2000 instrument (see section 3.4.1). Wood area index is calculated separately for the shrub and forest plots (see details of process in section 3.4.2).

3.4.4. Combination of Techniques

The suitability of each instrument to measure canopy variables are summarized in Table 2. All three instruments can measure gap fraction at different zenith angle. The hemispherical photography systems and LAI-2000 measure the gap fraction over a wide range of zenith angle. TRAC is limited by the local solar zenith angle available and requires half a day to produce such measurements. However, with the gap fraction, only the so called effective LAI (LAIe) or PAIe can be retrieved. To get an estimate of LAIt, gap size information is needed. The gap and the non-gap size information have been used in retrieving the clumping index (Leblanc, 2002) that is used in transforming the so-called effective LAI into LAIt (PAIt) based on Eq. (6) and (7). Thereafter, by applying woody-to-total area ratio, LAIt is transformed to LAI (Eq. (8) and (9)). The average clumping index per plant-functional type from TRAC based on Chen (1996b), and Chen and Cihlar (1996) and woody-to-total area ratio retrieved from hemispherical photography is used to correct LAIe which is estimated using LAI-2000, TRAC and hemispherical photography. Despite the fact that, hemispherical photography can be used to retrieve clumping index using CAN_EYE software (parenthesis in Table 2), the algorithm used is not documented and the performance is not validated unlike TRAC derived clumping index. In this report the

term LAI was used to describe; (1) the general term 'leaf area index', and (2) the leaf area index estimate which is corrected for clumping factor and non-leaf elements (stem and branch).

Table 2 Suitability of optical field instruments to measure canopy characteristics.

	LAI-2000	TRAC	Hemispherical photography	LAI-2000 &TRAC	Hemispherical photography & TRAC
Clumping index (Ω)		√	**(√)**	√	√
LAIe (PAIe)	√	√	√	√	√
LAIt (PAIt)		√	**(√)**	√	√
LAI			**(√)**		√
WAI			√		√

3.5. LAI Retrieval from AHS Hyperspectral Image

The AHS image is spatially clipped to study area and only the first 21 bands are selected for further process. Plant functional type map is produced using maximum likelihood classification algorithm. The end members are collected from the image for five possible classes of the area namely; soil, water, grass, shrub, and forest. The other cover types than plant functional types are merged together to class 'others' (Appendix 10). The 'others' land class was masked out to calculate the 1% minimum and maximum cutoff points in the histogram of SWIR reflectance (Fig. 7) for RSR vegetation index. The 1% histogram cut-off points of SWIR band reflectance were computed and resulted 0.015791 and 0.341475 as a minimum and maximum, respectively and used to compute RSR for Millingerwaard area. After computing RSR per pixel, the image is aggregated to the pixel size of ground plots (20 x 20 m); consequently, RSR was extracted for each ESU after identifying the ground plots in the scene.

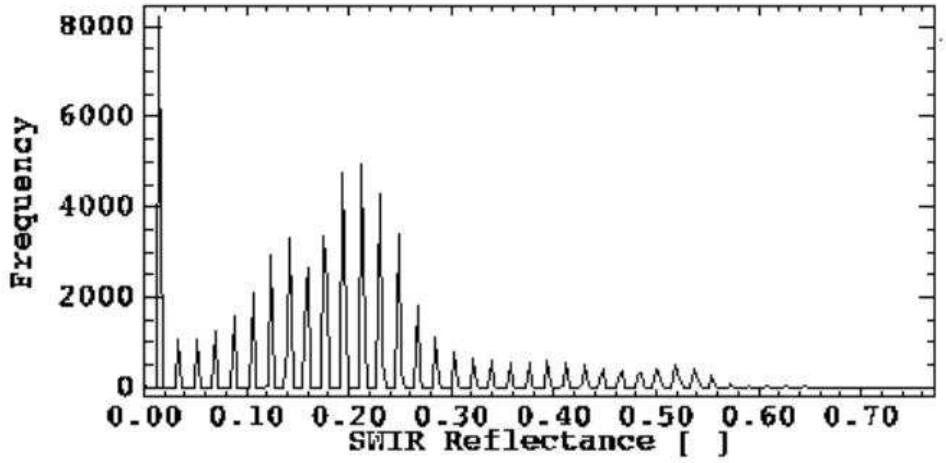

Fig. 7. Histogram of SWIR reflectance (band 21) of AHS image.

The relationship between LAI measured using optical field instruments and RSR vegetation index was made for each plant functional type. This vegetation index

considers SWIR band in addition to the RED and NIR bands (Eq. (10)). Least squares regression analysis with LAIe and LAI as independent variable was used to evaluate the relationships between RSR and LAI of each plant functional type. Linear, logarithmic and exponential models were investigated to asses best fit of LAI-RSR. To evaluate the relative influence of RED, NIR and SWIR reflectance on the LAI-RSR relationships, plots of LAI against reflectance of the aforementioned bands were also inspected.

In the analysis of this case the reflectance data of AHS spectral bands 8 (659 nm), 14 (833 nm) and 21 (1622 nm) were considered for RED, NIR and SWIR bands, respectively. The regression correlation was evaluated between the RSR and all ground measurements for each plant-functional type. After applying the regression coefficients for the RSR image to determine the LAI value, the pixel size is aggregated to 20 x 20 m which is the dimension of ground data VALERI plots.

3.6. Field and Airborne Data

The hyperspectral images were acquired by the AHS air-borne imaging spectrometer sensor on June 19, 2005. At the same time, a field work was coupled to this campaign and ground measurements were taken from June 19 – 30, 2005 and supposed that there is no significant variation of leaf area index during field data collection period.

3.6.1. Field Data

Ground Plot Description

Table 3 shows the plot codes, geographic location and summary of vegetation structural information of each ESU. The geographic Northing and Easting coordinates refer to the center of each ESU (sub-plot 'I' in Fig. 5 (B)). Because of time constraint, the stand minimum and maximum height measurements were done only for 16 ESUs. Stand height information was acquired for all grass plots. The grass/herbs height information of shrub and forest plots stands for the height of understory vegetation. From height information which is presented in Table 3, one can see high variation of vertical structure of each ESU. Besides this, Appendix 3 reveals high species richness of the study area. Generally, Millingerwaard vegetation is characterized by considerably heterogeneous managed ecosystem (Table 3 and Appendix 3).

Table 3 Plot code, location and summary of stand structural information at each ESU. (GH = Grass/herbs, SH = Shrub and FR = Forest. Projection system: UTM, Zone 31 North)

Plot Code	*Northing*	*Easting*	Plant functional type	Height (m)					
				Grass/herbs		Shrub		Tree	
				Min	Max	Min	Max	Min	Max
GH 1	5750334.330	706101.733	grass/herbs	1.6	2				
GH 2	5750262.254	705770.418	grass/herbs	0.05	1.5				
GH 3	5750294.722	705786.352	grass/herbs	0.05	1.5				
GH 4	5750370.623	705965.634	grass/herbs	0.01	1.5				
GH 5	5750428.011	705930.346	grass/herbs	1.5(mean)					
GH 6	5750444.447	705864.750	grass/herbs	0.2	1				
SH 7	5750532.409	705968.869	shrub	0.5	1.5	2.5	3		
SH 8	5750547.835	706180.251	shrub	0.1	1.5	2	3		

SH 9	5750535.831	706152.001	shrub	1	1.5	2	2.5		
SH 10	5750558.173	706193.240	shrub						
SH 11	5750801.567	706034.443	shrub						
GH 12	5750733.425	705947.289	grass/herbs	0	1				
SH 13	5751022.338	706072.596	shrub	1	2	5(mean)			
GH 14	5751428.314	706388.907	grass/herbs	0.05	1.2				
FR 15	5750921.008	706695.433	forest						
FR 17	5750405.864	706717.824	forest	0.2	2			20	29
FR 18	5750342.296	706579.805	forest	1.5	2			19	20
FR 19	5750219.780	706597.331	forest	0.5	2			15(mean)	
FR 20	5750231.410	706356.774	forest	1.5	2			10(mean)	

LAI-2000 Plant Canopy Analyzer

Field measurements using LAI-2000 were made only for grass and shrub plots, because the reference device was not available on later field days for forest plots. A total of 12 ESUs data was obtained using LAI-2000 instrument. However, for the measurements which were made in June 22, 2005 (GH 6, SH 7, SH 9 and GH 14) the outermost three rings of the instrument sensor was not functioning so that the measurements were obtained only for ring 1 & 2. Additionally, for the same date, only the within canopy measurements were obtained without reference measurements. Two instruments were used for June 21, 2005 measurements, one for the within canopy measurements and the other for reference measurements whereas only one instrument was used for both within canopy and reference measurements in June, 30, 2005. Four measurements were acquired for each of nine sub-plots (Fig. 5 (B)) of ESUs. However, for plot GH1, SH 7, SH 9 and GH 4 the measurements were made only for 5, 7, 6 and 7 sub-plots, respectively (Table 4).

Table 4 Summary of LAI-2000 data description.

Plot code	**Number of point measurements**		**Method**			**Date**
	2 rings (0.0^o-28.6^o)	**5 rings (0.0^o – 75^o)**	**1 instrument**	**2 instrument**	**1 instrument (with out reference measurement)**	
GH 1	20	20	√			June 30, 2005
GH 2	36	36		√		June 21, 2005
GH 3	36	36	√			June 30, 2005
GH 4	36	16		√		June 21, 2005
GH 6	36				√	June 22, 2005
SH 7	28				√	June 22, 2005
SH 8	36	36	√			June 30, 2005
SH 9	24				√	June 22, 2005
SH 11	36	36	√			June 30, 2005
GH 12	36	36	√			June 30, 2005
SH 13	36	36	√			June 30, 2005
GH 14	28				√	June 22, 2005

TRAC

Field measurements using TRAC were made for 6, 3 and 3 ESUs of grass, shrub and forest canopies, respectively. Because of time constraint, only a total of 12 ESUs data was obtained using TRAC instrument. The measurements were done at two levels of canopy strata for shrub and forest ESUs. From Table 5, 'below' measurements were made at ground surface by placing TRAC sensor beneath understory vegetation of shrub and forest ESUs so that it includes the LAI estimation of the whole vegetation of each ESU. The 'above' measurements were done above understory vegetation for shrub and forest ESUs so that it estimates LAI of overstory canopy. However, for shrub plot SH 8 only 'below' measurement was obtained, because there was no overstory canopy strata whereas since there was no understory vegetation for young willow forest plot FR 15, only 'below' measurement was obtained. Mean element width and woody-to-total area ratio were determined following the procedure explained in section 3.4.2 from field leaf scans and hemispherical photography, respectively.

Table 5 Summary of TRAC and input data description. (Below = measurements below understory, Above = measurements above understory).

Plot code		Mean solar zenith angle (^{o})	Number of segments	Mean element width (mm)	Woody-to-total area ratio (α)	Date
GH 1		59.85	1	24.65		June 21, 2005
GH 2		45.68	8	19.51		June 21, 2005
GH 3		43.68	2	20.28		June 21, 2005
GH 4		32.61	2	25.64		June 21, 2005
GH 5		34.22	11	29.95		June 21, 2005
GH 6		53.08	3	30.09		June 21, 2005
SH 8		54.49	5	28.45	0	June 20, 2005
SH 11	Below	42.66	1	31.39	0.006	June 20, 2005
	Above	41.97	1	31.39	0.025	June 20, 2005
SH 13	Below	38.71	2	28.67	0.021	June 20, 2005
	Above	38.97	1	28.67	0.048	June 20, 2005
FR 15		31.81	8	12.88	0.008	June 20, 2005
FR 19	Below	36.30	6	23.99	0.006	June 19, 2005
	Above	37.40	3	12.88	0.015	June 19, 2005
FR 20	Below	59.19	1	23.99	0.003	June 19, 2005
	Above	58.65	2	12.88	0.011	June 19, 2005

Hemispherical Photographs

Hemispherical photographs were taken from all of 19 ESUs sampled in the study area. One picture per sub-plot point was captured from each of grass ESUs whereas for shrub and forest canopies, two pictures per sub-plot point were captured one looking downward to understory and the other looking upward to overstory. Each picture has the dimension of 3264 by 2448 pixels storage capacity. Table 6 shows the number of

captured pictures for some of the upward looking photograph serous of shrub ESUs is less than the number of sub-plots (nine) sampled. This is because of the pictures were taken only if there was overstory vegetation in the view width of the camera for each sub-plot point. For ESU GH 3 and SH 13, some of the photographs were not in good quality so that they were excluded from further processing. All pictures were taken in June 22 and 26, 2005. However, additional pictures were taken in June 30, 2005 for those ESUs i.e., the picture quality of the previous days was not good and the best of the two serous was used for further process.

Table 6 Number and date of hemispherical photographs taken. (Down = downward looking photographs for grass plots and understory of shrub and forest plots, Up = upward looking photographs for overstory vegetation of shrub and forest plots).

Plot Code		**Number of photographs taken (out of 9 sub-sample points)**	**Number of photographs processed**	**Date picture taken**
GH 1		9	9	June 26, 2005
GH 2		9	9	June 26, 2005
GH 3		9	8	June 26, 2005
GH 4		9	9	June 30, 2005
GH 5		9	9	June 26, 2005
GH 6		9	9	June 26, 2005
SH 7		9	9	June 22, 2005
SH 8	Down	9	9	June 30, 2005
	Up	4	4	June 30, 2005
SH 9	Down	9	9	June 22, 2005
	Up	4	4	June 22, 2005
SH 10	Down	9	9	June 22, 2005
	Up	7	7	June 22, 2005
SH 11	Down	9	9	June 22, 2005
	Up	5	5	June 22, 2005
GH 12		9	9	June 22, 2005
SH 13	Down	9	7	June 30, 2005
	Up	9	8	June 30, 2005
GH 14		9	9	June 30, 2005
FR 15	Down	9	9	June 30, 2005
	Up	9	9	June 30, 2005
FR 17	Down	9	9	June 30, 2005
	Up	9	9	June 30, 2005
FR 18	Down	9	9	June 30, 2005
	Up	9	9	June 30, 2005
FR 19	Down	9	9	June 22, 2005
	Up	9	9	June 22, 2005
FR 20	Down	9	9	June 22, 2005
	Up	9	9	June 22, 2005

3.6.2. AHS Data Description

The hyperspectral images were acquired by the AHS air-borne imaging spectrometer sensor on June 19, 2005. The flight specification is given in Table 7. The Airborne Hyperspectral System (AHS) data are delivered in surface reflectance after radiometrical, atmospherical and geometrical correction (VITO, 2005).

Table 7 AHS 2005 flight specification. (Adapted from, http://campaigns.vgt.vito.be/quicklook2005.htm).

Acquisition date	Scene Title	Location	Acquisition time (UTC)	Coordinates Flightlines (UTM/WGS84)				Altitude (feet/m, AGL)
				Start_Lat	Start_Lon	End_Lat	End_Lot	
19/06/2005	Millingerwaard 27	Millingerwaard (NL)	10:38	51.89209	5.95387	51.84386	6.03069	6000/1834
19/06/2005	Millingerwaard 28		10:46	51.83168	5.99209	51.90359	5.99306	6000/1834
19/06/2005	Millingerwaard 29		10:56	51.86781	5.95627	51.86744	6.02886	6000/1834
19/06/2005	Millingerwaard 30		11:04	51.84496	5.95460	51.88960	6.02983	6000/1834

The metadata of the AHS image used in this study has the general parameters and metadata explained in Table 8. In Appendix 1, the band positions and FWHM (Full Width at Half the Maximum) band of the AHS sensor are presented, while Appendix 2 shows the quicklooks for the acquired AHS images over the Millingerwaard. AHS image of scene one (Appendix 2) was used in this study to compute LAI from imaging spectroscopy.

Table 8 AHS 2005 Imaging spectrometer parameters and metadata. (Source for general parameters, http://campaigns.vgt.vito.be/documents/)

General Parameters**	**Description/unit**
Field of View	90°
Instantaneous field of view	2.5 mrad
No. of Channels	80
No. of Samples/line	750
Scan Principle	whiskbroom
Scan Frequency	variable
Ground Resolution	2.5 - 10 m
Radiometric Resolution	12 bit
Spectral Configuration**	
Visible and Near Infrared	
Number of bands	20
Spectral region	430 to 1030 nm
Band width	30 nm
1A Short Wave Infrared	
Number of bands	1
Spectral region	1550 to 1750 nm
Band width	200 nm
2 Short Wave Infrared	
Number of bands	42
Spectral region	1994 to 2540 nm

Band width	13 nm
Mid Infrared	
Number of bands	7
Spectral region	3300 to 5400 nm
Band width	300 nm
Long Wave Infrared	
Number of bands	10
Spectral region	8200 to 127002540 nm
Band width	400 nm
Sampling: Millingerwaard area	
Pixel size	5.375025 x 6.000464 Meters
Projection	UTM, Zone 31 North
Datum	North America 1927
Dimensions (x, y, and spectral bands)	2523 x 2155 x 80
Size: (Floating Point)	1.739 GB

For the AHS image taken on June 19, 2005, the histogram of the image over the whole spectral range is computed. The minimum, maximum, mean and standard deviation of the reflectance is plotted in Fig. 8. AHS bands more than 1622nm were not completed for preprocessing and were not used for further processes. Fig. 8 confirms the unreliability of these bands.

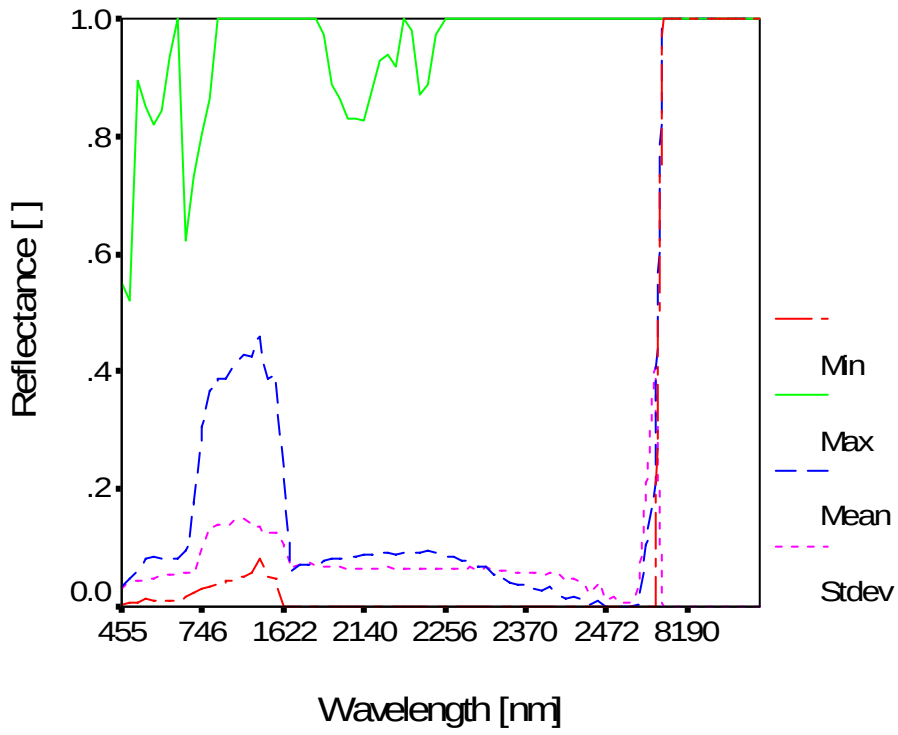

Fig. 8. AHS minimum, maximum, mean and standard deviation reflectance.

4. Results and Discussion

4.1. Ground Measurements

The over all processing results of each optical method are presented and discussed in the following sections.

4.1.1. LAI-2000 Plant Canopy Analyzer

Estimation of leaf area index using LAI-2000 plant canopy analyzer was done only for grass and shrub VALERI plots. Since the instrument is limited to compute gap fraction with assumption of random distribution of foliage elements, only the so-called effective leaf area index (LAIe) can be retrieved. The estimation of LAIe was made using ring 1-2 and ring 1-5 in 12 and 8 VALERI plots, respectively. Summary of LAI-2000 measurement results are given in Appendix 5. The result of the analysis of LAIe from the grass canopy ranges from 1.69 – 7.51 m^2/m^2 and 2.01 – 5.28 m^2/m^2 from ring 1-2 and 1-5, respectively (Table 9). Shrub plots exhibit the highest average LAIe value which ranges from 6.47 – 10.99 m^2/m^2 and 4.34 – 5.87 m^2/m^2 from ring 1-2 and 1-5, respectively.

Table 9 Summary of LAIe in the 12 VALERI ESUs as estimated using LAI-2000 plant canopy analyzer. (NA = not applicable, measurements from ring 3-5 were not obtained due to malfunctioning of the instrument).

Plot code.	LAIe 1-2 rings	LAIe 1-5 rings
	GRASS/HERBS	
GH 1	4.93	3.91
GH 2	2.46	2.01
GH 3	1.69	1.42
GH 4	7.51	5.28
GH 6	3.35	NA
GH 12	4.90	3.20
GH 14	3.31	NA
Mean	4.02	3.16
Minimum	1.69	1.42
Maximum	7.51	5.28
	SHRUB	
SH 7	10.99	NA
SH 8	6.47	4.34
SH 9	10.46	NA
SH 11	9.50	5.87
SH 13	8.89	5.02
Mean	9.26	5.08
Minimum	6.47	4.34
Maximum	10.99	5.87

Fig. 9 reveals that the systematic increase of LAIe from rings 1-2 than the five annulus rings for all grass and shrub plots. This confirms the general case obtained by

other studies (Chen, 1996b; Leblanc and Chen, 2001) and resulted because of the multiple scattering effect on the measurement is most serious at larger zenith angles.

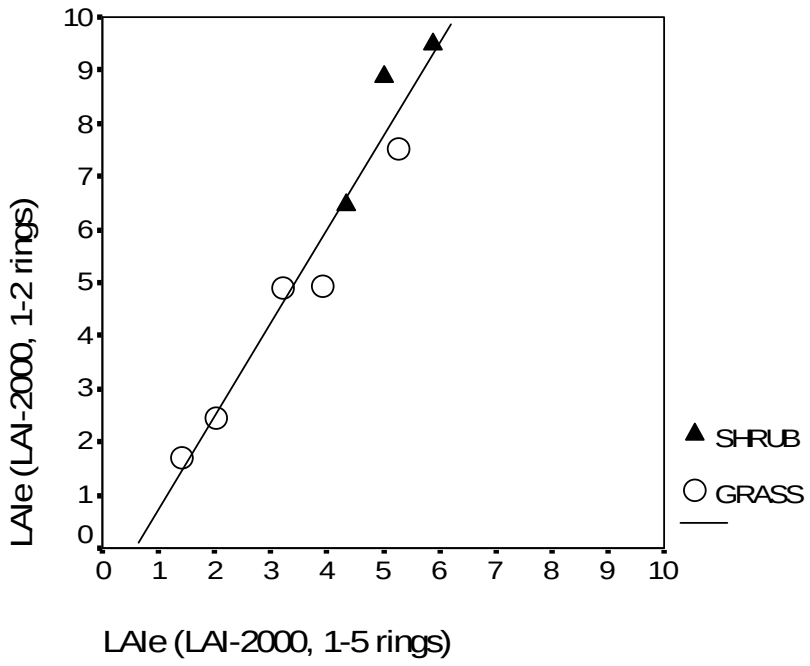

Fig. 9. Comparison between LAI-2000 effective LAI retrieved using 5 annulus rings and from only the first 2 rings. The fit is almost perfect ($y = -0.999 + 1.75x$, $R^2 = 0.95$, $p < 0.05$).

In addition, the spatial variation of LAIe within each plot using the thirty six (four measurements for each nine sub-plot ESUs) independent measures were computed (Appendix 5). The highest variation was observed in shrub plot (stdev = 2.63) and grass plots show relatively low (minimum stdev = 0.39) variation of LAIe within ESUs. Even though, LAIe for plot GH 6, SH 7, SH 9 and GH 14 was obtained by interpolation of the reference measurements from different days than with in canopy measurements, resulted lowest variation with stdev ranging from 0.44 to 0.74 than other methods (Appendix 5). One benefit of the LAI-2000 unit is ease of use when estimating LAIe with the hand-held unit providing an immediate readout of LAIe. The disadvantage is that the effect of varying conditions, such as direct sunlight resulting multiple scattering. However, an alternative method, employing a Tracing Radiation and Architecture of Canopies (TRAC) instrument to characterize and account for light scattering under variable illumination conditions, has recently been proposed by Leblanc and Chen (2001) which used in tandem with a LAI-2000 PCA, may overcome many of these challenges. Using this method, it was concluded that estimates of LAIe vary by up to 20% as a result of changes in direct and diffuse lighting conditions. In this study, TRAC measurements were done only for one solar zenith angle and the evaluation of scattering effect was not assessed. However, the scattering effect can be easily evaluated based on the comparison of two view zenith angle ranges measurements (Fig. 9) by assumption of high scattering effect on more horizontal rings (Leblanc et al., 2002a) even if all rings of the LAI-2000 PCA can be affected by multiple scattering. Based on this study, the change of the result for grass plots is 20% and in agreement with Leblanc and Chen (2001), but shrub plots show change of 45%. The big change obtained in shrub plot can be also due to the high heterogeneity of vegetation in shrub plots (Table 3) so that difference of footprint from two ranges of view zenith angle measurements could be more pronounced than

grass plots for LAI estimation. This is not significant problem for most of grass plots because of short canopy height and doesn't result reasonable difference of footprint for two ranges of view zenith angle.

4.1.2. TRAC

Table 10 shows the summary of corrected LAI for wood and stem contribution, effective LAI and clumping factor. The LAI estimation is made above and blow understory of shrub and forest plots, summary of analysis results using TRACwin is given in Appendix 6, for both measurements. The range of LAI across all VALERI plots was from 0.7 – 5.91 m^2/m^2. The lowest LAI and LAIe were found in grass plots. The forest plots gave the highest value clustered around an LAI value of 5.5m^2/m^2. All plots show spatial clumping of foliage elements with clumping factor ranging from 0.76-0.94, with the mean value of 0.89, 0.85 and 0.86 for grass, shrub and forest plots, respectively. The mean clumping factor per plant functional type is used to correct LAIe value from hemispherical photography and LAI-2000 since TRAC measurements were not made for all VALERI plots.

Table 10 Summary of LAI in the 12 VALERI ESUs as estimated using TRAC.

Plot code.	LAI	LAIe	Clumping index (Ω)
	GRASS/HERBS		
GH 1	2.44	2.21	0.91
GH 2	1.20	1.06	0.88
GH 3	0.70	0.65	0.93
GH 4	2.85	2.33	0.82
GH 5	4.28	3.76	0.88
GH 6	1.41	1.32	0.94
Mean	2.15	1.89	0.89
Minimum	0.70	0.65	0.82
Maximum	4.28	3.76	0.94
	SHRUB		
SH 8	1.82	1.48	0.81
SH 11	1.48	1.22	0.80
SH 13	5.58	5.51	0.94
Mean	3.02	2.74	0.85
Minimum	1.51	1.22	0.80
Maximum	5.34	5.51	0.94
	FOREST		
FR 15	5.25	4.65	0.88
FR 19	5.59	4.29	0.76
FR 20	5.91	5.54	0.93
Mean	5.59	4.82	0.86
Minimum	5.25	4.29	0.76
Maximum	5.96	5.54	0.93

Following the method of Chen and Cihlar (1995), visible direct solar irradiance measured along transects beneath the understory was used to derive the element clumping index quantifying the effect of canopy architecture on LAI measured by the TRAC instrument itself, hemispherical photography and LAI-2000 PCA. The element clumping index includes the effects of clumping at scales larger than the foliage elements (shoots). Appendix 7 and Fig. 10 show the instantaneous values and mean of ground level photosynthetic photon flux density (PPFD) in sampled VALERI plots. From the plot of PPFD, one can easily tell the difference in the canopy architecture. Mean PPFD of forest plots (FR 15, FR 19 and FR 20) show relatively lower values. This indicates that high canopy closure results from understory and/or overstory.

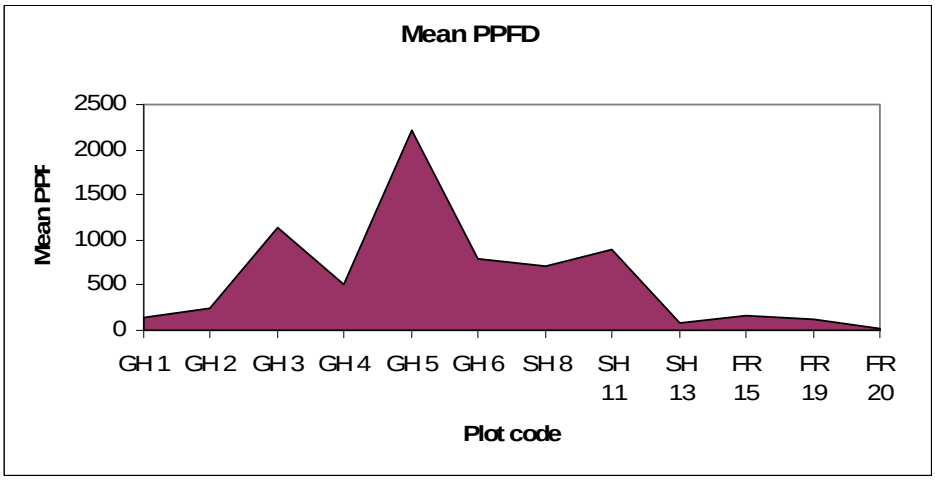

Fig. 10. Plot of average photosynthetically active photon flux density (PPFD) measured on transect of each VALERI plots.

Because the with-in plant functional type variation of clumping index is small and TRAC measurements were not done for all ESUs, the average clumping factor per plant functional type was used to compute foliage spatial distribution for the correction of LAI measurements. Chen and Cihlar (1995) found that inaccuracy in determining the gaps becomes serious only when the solar zenith angle is greater than 60^o. In this study the range of mean solar zenith angle is between 31.81^o – 59.19^o (Appendix 6). The range of forest plot clumping index (0.76-0.93) is in good agreement with the index value (0.86-0.96) found by Leblanc and Chen (2001) for deciduous forest of Canada.

Leblanc *et al.* (2002a) emphasized, the length of the transect should be theoretically at least ten times the average distance between the major foliage structures such as crowns. Transects of 100-300 m are recommended Leblanc *et al.* (2002a) to consider the patchiness of stands. However, the maximum transect length with in VALERI plots of this study was 20 m and may have effects on the result of LAI to consider the whole patchiness of the vegetation. In addition, the instrument did not measure vegetation below the sensor height as with LAI-2000 PCA; therefore, the true LAI values might be higher. Results for grass plots are questionable since most of the vegetation at that site was below the TRAC sensor height. Comparison with other instruments and correlation with RSR vegetation index was made only with LAI of TRAC instrument, not with LAIe since the measurements are made only using one solar zenith angle.

4.1.3. Hemispherical Photography

The hemispherical images were processed using the CAN_EYE software (version 4.1) to derive leaf area index for Millingerwaard floodplain vegetation. Table 11 shows an estimation of both effective and true LAI over all 19 VALERI plots. As there was understory in most of the forest and shrub canopy plots, hemispherical photographs were acquired downward looking above the understory and upward looking below the canopy (trees and shrubs). The two sets of acquisition were processed separately to derive LAIt and LAIe (summary results in Appendix 8 and 9). This assumes that independency of the gaps inside the understory and the gaps inside the trees/shrubs (Weiss, 2004). Finally, the leaf area index is computed for each VALERI plot by summing up the understory and overstory LAI estimates.

Table 11 Summary of LAI in the 19 VALERI ESUs as estimated using hemispherical photography. (NA = Not applicable, hemispherical photographs using 30^{o} view zenith angle are processed only for the corresponding plots which have 1-2 rings of LAI-2000 measurements)

Plot code.	HP LAI	HP LAIe	HP30 LAI	HP30 LAIe	HP WAIt
			GRASS/HERBS		
GH 1	10.00	8.60	5.80	7.50	-
GH 2	5.90	2.70	8.90	5.10	-
GH 3	5.10	2.30	6.90	2.80	-
GH 4	3.80	3.20	5.70	5.00	-
GH 5	5.60	3.70	4.30	4.20	-
GH 6	6.80	2.70	10.00	4.80	-
GH 12	6.90	4.10	9.60	5.70	-
GH 14	5.30	4.10	6.30	5.20	-
Mean	6.18	3.93	7.19	5.04	
Minimum	3.80	2.30	4.30	2.80	
Maximum	10.00	8.60	10.00	7.50	
			SHRUB		
SH 7	6.50	3.90	10.00	8.40	0
SH 8	3.71	2.40	4.62	4.40	0
SH 9	4.12	2.44	9.86	6.24	0
SH 10	6.66	3.43	NA	NA	0
SH 11	6.16	4.00	11.60	7.87	0.03
SH 13	8.82	4.90	12.15	6.70	0.15
Mean	5.99	3.51	9.65	6.72	0.03
Minimum	3.71	2.40	4.62	4.40	0
Maximum	8.82	4.90	12.15	8.40	0.15
			FOREST		
FR 15	5.75	3.80	NA	NA	0.04
FR 17	10.58	6.00	NA	NA	0.02
FR 18	10.49	6.50	NA	NA	0.01
FR 19	10.14	5.80	NA	NA	0.04

FR 20	8.77	4.30	NA	NA	0.03
Mean	9.15	5.28	NA	NA	0.03
Minimum	5.75	3.80	NA	NA	0.01
Maximum	10.58	6.50	NA	NA	0.04

The result of the analysis from the grass canopy results the value ranging from 3.8 – 10 m^2/m^2 and 2.3 – 8.6 m^2/m^2 for LAI and LAIe, respectively (Table 11). Forest plots exhibit the highest average value which ranges from 5.75 – 10.58 m^2/m^2 and 3.8 – 6.5 m^2/m^2 for LAI and LAIe, respectively. The result reveals that there is dense understory beneath forest and shrub canopy (Appendix 8). Along with, shrub plots results lowest variation of effective LAI with standard deviation of 0.97, and LAI and LAIe value ranging from 3.71 – 8.82 m^2/m^2 and 2.4 – 4.9 m^2/m^2, respectively. In plot GH 1, the value of LAIe is greater than LAI which is calculated from 30^o view zenith angle, this happens in extreme case when leaves are regularly distributed (leaves are all laid side by side) and results Ω larger than unity (Chen *et al.,* 1997). LAI value of forest plots show large increase of both LAIe and LAI from previous year. The result of previous year by Mengesha (2005) from the softwood forest resulted in LAI values ranging from 4.7 - 6.5 m^2/m^2 and 2.9 - 4.0 m^2/m^2 for true and effective LAI, respectively. However, no explanation for this difference is evident, and there remains a need for further testing.

The value of leaf area index that is derived from simple gap fraction measurements is really a plant area index, because all tissues, including stems and branches, intercept light and contribute to the measured gap fraction value. Therefore, wood area index is determined using digital hemispherical images, where the amount of woody material was estimated by means of image classification, assuming the stems and branches seen on the photographs were simple cone shapes (Barclay *et al.,* 2000). Then LAIt from hemispherical photographs and TRAC measurements are corrected using this value to obtain LAI, assuming that stems and branches are positioned randomly with the respect to other foliage in the canopy. Only uncovered stems and branches by leaf were computed as WAI, the result reveals significantly low value ranging for 0 – 0.15 $m^2/m^2$and 0.01 – 0.04 m^2/m^2 for shrub and forest canopy, respectively. Generally, woody material, on hemispherical area basis, comprises 0-2% and 0.1-0.8% in shrub and forest canopy, respectively. See for the details of comparison of WAI in section 3.4.2

Hemispherical photographs are also processed at view zenith angle of 30^o in order to make comparison with LAI value obtained using the first two rings of LAI-2000 plant canopy analyzer. Ring 1 and 2 of LAI-2000 corresponds to the zenith view range of 0^o-$28.6^{o.}$ Analysis of hemispherical photography at the view range of 30^o is made only for those plots which have LAI-2000 measurements so that the result can be compared roughly at the same foot print of both instruments.

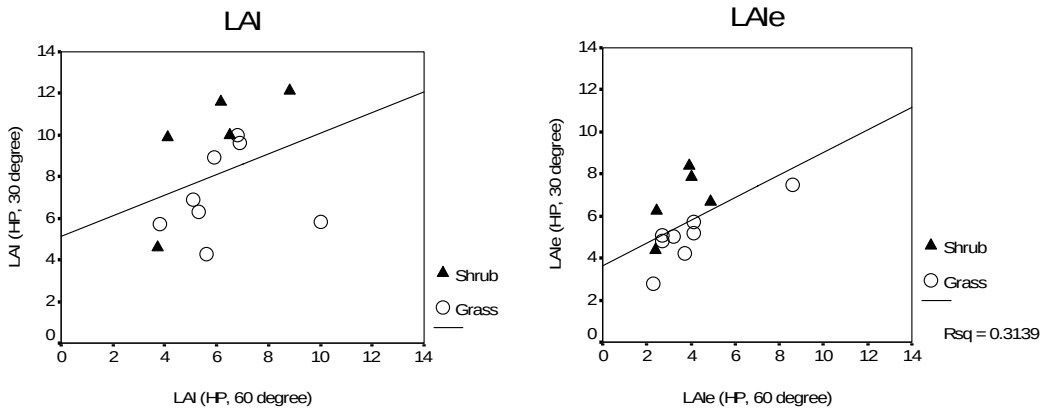

(A) **(B)**

Fig. 11. Relationships of LAI and LAIe using hemispherical photography from two view zenith angles. (A) Comparison of LAI, and (B) comparison of LAIe. HP 60° LAI and effective LAI computed from the range 0-60° view zenith angle. HP 30° LAI and effective LAI computed from the range 0-30° view zenith angle.

Fig. 11 (A) and (B) indicate a weak relationship between LAI and effective LAI estimates using the two view zenith angles for both relationships. Because of short canopy height, relatively grass plots show small variability of LAI andeffective LAI than shrub ones. Generally, both LAIe and LAI from 30° gave higher value than 60° view zenith angle. This could happen because of the scattering effect which is significant near horizontal view zenith angles. The effect is much pronounced in shrub plots and resulted 38% difference of LAI from two view angles than grass plots which show 14% difference. The big change obtained in shrub plot can be also due to the high heterogeneity of vegetation in shrub plots (Table 3) so that difference of footprint from two ranges of view zenith angle measurements could be more pronounced than grass plots for LAI estimation. This is not significant problem for grass plots because of short canopy height and doesn't result reasonable difference of footprint for two ranges of view zenith angle. The difference obtained is in good agreement with those of LAI-2000 PCA (section 4.1.1).

Leaf area index estimation using hemispherical photography could be liable to different sources of errors. Jonckheere *et al.* (2004a) mentioned the possibility of errors as with any remote sensing technique, at any stage of image acquisition, analysis or violation of model assumption. Rich (1988) discussed the problems of image acquisition, which includes camera positioning, horizontal/ vertical positioning, exposure, evenness of sky lighting, evenness of foliage lighting (reflections), direct sunlight, and optical distortion. He further mentioned errors occurring during image analysis while distinguishing foliage from canopy openings, assumed direct sunlight distribution, assumed diffuse skylight distribution, assumed surface of interception, image editing/enhancement, consideration of missing areas and finally in the case of violation of model assumptions like assessment of G-function variations, leaf angle variability and consideration of clumping factors.

4.1.4. Combined Method

Leaf area index is calculated using the combination of effective leaf area index (LAIe) from hemispherical photography or LAI-2000 and the element clumping index from TRAC. Table 12 shows the final results of leaf area index estimated using the hybrid method of optical instruments.

Table 12 Summary of LAI using the combination of TRAC and hemispherical photography/LAI-2000. (*NA= not applicable, no measurements were done for forest plots because the reference LAI-2000 PCA was not available. **See Table 9).

Plot code	*HP-TRAC*	*LAI-2000 (1-2 rings)-TRAC*	*LAI-2000(1-5 rings)-TRAC*
		GRASS/HERB	
GH 1	9.64	5.53	4.38
GH 2	3.03	2.76	2.25
GH 3	2.58	1.90	1.59
GH 4	3.59	8.42	5.92
GH 5	4.15	NA*	NA**
GH 6	3.03	3.75	NA
GH 12	4.60	5.49	3.59
GH 14	4.60	3.71	NA
Mean	4.40	4.51	3.55
Minimum	2.58	1.90	1.59
Maximum	9.64	8.42	5.92
		SHRUB	
SH 7	4.58	12.91	NA
SH 8	2.82	7.60	5.10
SH 9	2.87	12.29	NA
SH 10	4.03	NA	NA
SH 11	4.70	11.15	6.90
SH 13	5.76	10.45	5.90
Mean	4.12	10.88	5.97
Minimum	2.82	7.60	5.10
Maximum	5.76	12.91	6.90
		FOREST	
FR 15	4.45	NA*	NA*
FR 17	7.02	NA	NA
FR 18	7.61	NA	NA
FR 19	6.79	NA	NA
FR 20	5.03	NA	NA
Mean	6.18	NA	NA
Minimum	4.45	NA	NA
Maximum	7.61	NA	NA

Fig. 12 shows the relationship between the combined optical methods. Since the within plant functional type variation of the clumping index was small for all the plots investigated (see Table 10), only an average clumping index was determined for each plant functional type for the calculation of LAI. Even if, there obtained good agreement (R^2 = 0.96) between the hybrid methods of two ranges of view angles of

LAI-2000 PCA with TRAC, there is no real relation between LAI-2000-TRAC and hemispherical photography-TRAC. Fig. 12 (A) and (B) indicate that the relationships between the combined method of TRAC and hemispherical photography/LAI-2000 resembles to the relationship of LAIe between hemispherical photography and LAI-2000 which is further discussed in section 4.2.1. The relation is highly affected by the outlier effect of GH 1 plot and discussed in section 4.2.2.

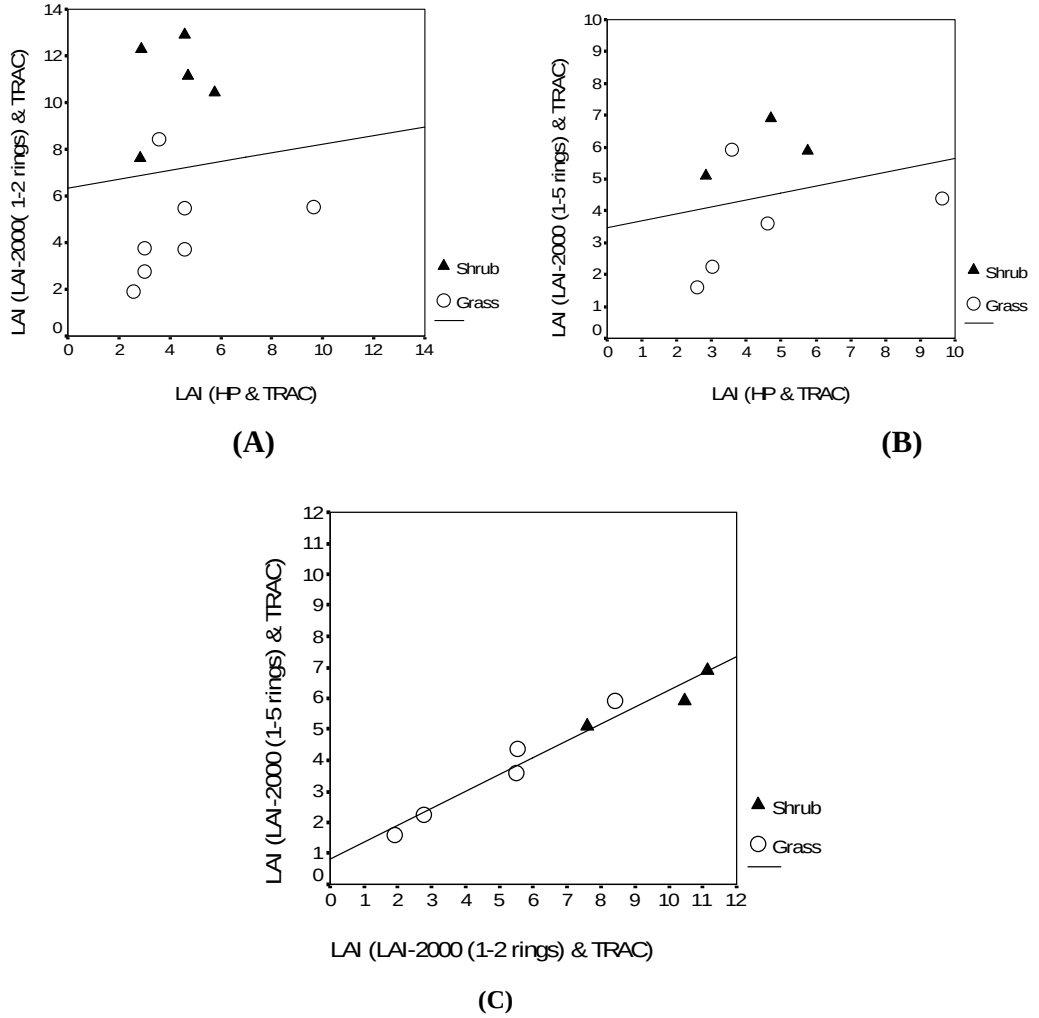

Fig. 12. Comparison between LAI estimated using the combine method of TRAC and hemispherical photography/LAI-2000. (A) The relationship between the combined LAI value from Hemispherical photography & TRAC and LAI-2000(1-2 annulus rings) & TRAC, (B) the relationship between the combined LAI value from Hemispherical photography & TRAC and LAI-2000(1-5 annulus rings) & TRAC, and (C) the relationship between the combined LAI value from LAI-2000(1-2 annulus rings) & TRAC and LAI-2000(1-5 annulus rings) & TRAC, the fit is, $R^2 = 0.96$.

From comparisons of optical methods with destructive sampling results, it is believed that optical LAI estimates can generally be better than allometric LAI through laborious destructive sampling (Chen, 1996b). The critical improvement in the optical measurements in such cases is the use of the TRAC which removes the effect of canopy architecture on LAI measurements. Clumping factors estimated by the TRAC have recently been validated (Chen and Cihlar, 1995; Chen, 1996b; Chen *et al.*, 1997; Kucharik *et al.*, 1998; Leblanc and Chen, 2001).

4.2. Comparison of LAI results from optical field instruments

4.2.1. Comparison of the Effective LAI

Point estimates of LAIe, obtained using hemispherical photography and LAI-2000 showed a better relation, (R^2 = 0.51, Fig. 13 (A)) for 30 degree zenith view angle of hemispherical photography and the corresponding view zenith angle (ring 1 - 2 (0-28.6^o)) of LAI-2000 than the full range of view zenith angle of LAI-2000 and corresponding view zenith angle of hemispherical photography (Fig. 13 (B)). The result of the relationship found between hemispherical photography using 30 degree zenith view angle and LAIe from the first two rings of LAI-2000 were in good agreement with other studies; for example, Coops *et al.* (2004) found R^2 = 0.65. Both techniques can suffer from the same problem: scattering of light within the canopy. In order to minimize this effect, LAI-2000 measures in the blue wavelength only (400-490 nm) and assumes all diffuse blue light originates directly from the sky (i.e., leaves in the blue band are totally black). Although blue reflectance of leaves is the smallest in the solar spectrum, it is still significantly larger than zero (about 3-6%) (Chen *et al.*, 1997). In open canopies the contribution of scattered blue light is small compared to that from the sky; therefore the problem is less serious. In photographs the scattering effect also exists but in a different way. Leaves at the top of a canopy under bright light appear to be much brighter than the foliage below. These bright leaves are more easily seen at small zenith angles than at large zenith angles, and therefore the absolute distortion of the gap fraction is larger at smaller zenith angles when a fixed threshold value is used to distinguish leaves from the sky.

In both view angle ranges, the average value of LAIe from hemispherical photography is relatively higher (28%-32%) for grass plots and lower for shrub plots (26%) than LAIe estimated from LAI-2000. This could be due to the difficulties in distinguishing gap (soil) and shade during the classification of the downward looking hemispherical photographs of shrub plots. Since, most of the shrub plots have dense undergrowth, shade of foliage being classified as a gap may result in an underestimation of LAIe. Contrary, higher values of LAIe are observed for hemispherical photography than LAI-2000 for the grass plots. The sensor head of the LAI-2000 instrument has a cross section of 3cm which does not allow to measure any LAI below this reference height, and additionally creates a significant artificial gap in dense canopies. These effects lead to an underestimation of the derived LAI and thus to the recommendation not to use the LAI-2000 instrument for dense, short canopies lower than 3 cm.

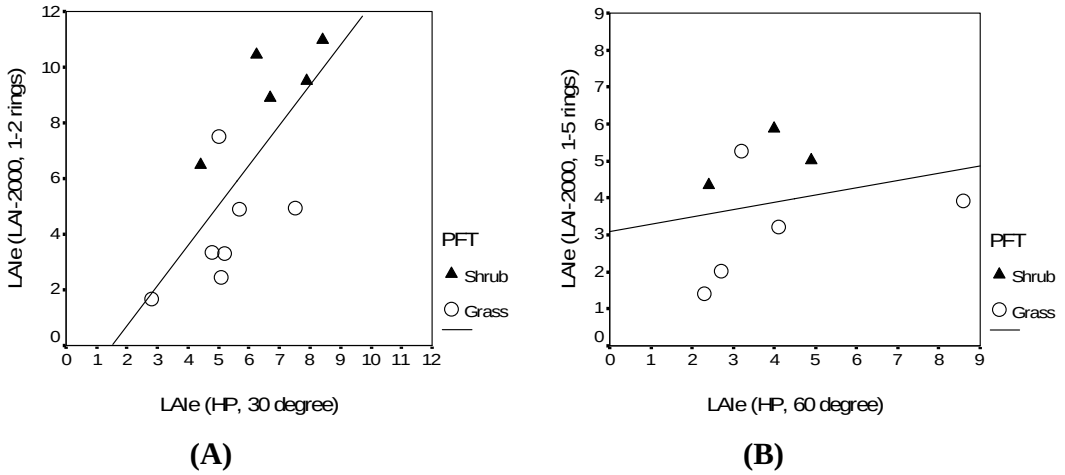

Fig. 13. Comparison of individual effective LAI measurements in two plant functional types using hemispherical photography and the LAI-2000. (A) Relationship between LAIe from 30 degree view zenith angle using hemispherical photography and the corresponding first two rings of LAI-2000, and (B) relationship between LAIe from 60 degree view zenith angle using hemispherical photography and the full view range of LAI-2000.

Fig. 14 shows the comparison between LAIe from TRAC and hemispherical photography. The conditions of measurement and the difference in foot print (see section 2.3.3) of both instruments can affect the agreement between the two instruments, but no significant correlation could be identified between TRAC and hemispherical photography LAIe measurements. However, from hemispherical photography higher LAIe was obtained than TRAC for all grass plots. This is because of majority of vegetation in most grass plots is below the sensor height of TRAC instrument. For instance, from TRAC measurement, 1.06 m^2/m^2 and 0.65 m^2/m^2 (Table 10) LAIe was obtained for grass plots GH 2 and GH 3, respectively. These plots have height ranging from 5 cm to 150 cm (Table 3) and from hemispherical photography, 2.7 m^2/m^2 and 2.6 m^2/m^2 (Table 11) LAIe was obtained for grass plots GH 2 and GH 3, respectively. Comparison of LAI and LAIe from hemispherical photography with other methods is computed from the 60 degree view zenith angle except for comparison with LAIe from LAI-2000 PCA.

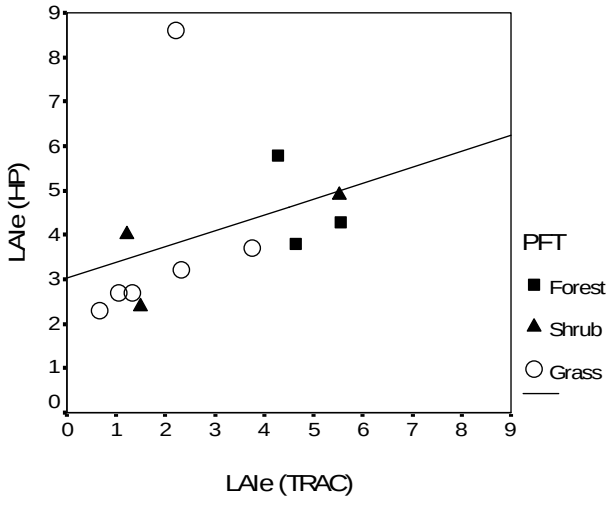

Fig. 14. Comparison of LAIe measurements from hemispherical photography and TRAC.

4.2.2. Comparison of LAI Measurements

Measurement of LAIe is a key step in optical measurement of LAI, but to obtain LAI, other parameters need to be quantified. These include the woody-to-total area ratio (α) and the element clumping index (Ω). The full detail of the methods for obtaining these parameters are given by Chen (1996a) and Chen *et al.* (1997). Table 5 and 10 show woody-to-total area ratio per plot and the average values of clumping index per plant functional type leading to the LAI estimates based on optical measurements, respectively. A total of 19 plots data acquisitions were made using hemispherical photography, 12 plots acquisitions were made using LAI-2000 and 12 plots acquisition were made using TRAC. Statistics of estimated LAI for each instrument are shown in Table 13. LAI-2000 estimates only effective leaf area index (LAIe), therefore the result is not comparable with other instruments for LAI.

Table 13 Number of collections and overall means for estimated LAI for this study.

PFT	**Hemispherical Photography**		**TRAC**		**Hemispherical Photography and TRAC**	
	n	Mean(range)	n	Mean(range)	n	Mean(range)
Grass	8	6.18(3.8-10)	6	2.15(0.70-4.28)	8	4.40 (2.58-9.64)
Shrub	6	5.99(3.7-8.81)	3	3.02(1.51-5.74)	6	4.13 (2.82-5.76)
Forest	5	9.15(5.75-10.58)	3	5.59(5.25-5.96)	5	6.18 (4.45-7.61
All	19	6.90(3.7-10.58)	12	3.23(0.70-5.96)	19	4.78 (2.58-9.64)

Comparison statistics for the data acquisitions using hemispherical photography and TRAC instruments (Table 13 and Fig. 15) show that, overall, the correlation between the retrievals is low ($R^2 = 0.26$), but results for different plant functional types vary. On average, the hemispherical photography retrieval was 50% higher than LAI derived from the TRAC. The magnitude of the discrepancy did not have a significant trend (e.g., heteroscedasticity) with LAI magnitude of different plant functional type. The hemispherical photography shows highest average value of LAI per plant functional type followed by the combined method of hemispherical photography-TRAC, whereas TRAC shows the lowest average LAI value for all plant functional types. The highest LAI values are obtained in forest plots for all three methods (Table 13). Average LAI of grass plots ranked next to forest for hemispherical photography and combined method of hemispherical photography-TRAC and shrub plots resulted the lowest average LAI per plant functional type using these two methods. LAI values using TRAC measurements for grass plots resulted low values ranging from 0.7-4.28 compared to the other methods. This is due to the limited canopy height of most grass plots being below the sensor head of the TRAC instrument. This experiment was not suitable to determine a canopy height threshold for TRAC and LAI-2000 measurements. Other studies such as Privette and Mukelabai (2000) and Privette *et al.* (2002) also suggested that TRAC derived LAI is least accurate for grass transects.

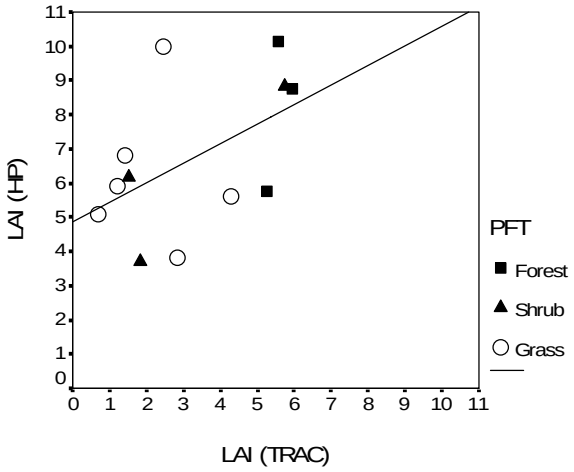

Fig. 15. Relationship between LAI as estimated from Hemispherical Photography and TRAC.

Tests for correlation of the combination of hemispherical photography and TRAC (Fig. 16 and 17) suggest that high correlation (R^2 = 0.74) with hemispherical photography and low correlation (R^2 = 0.17) with TRAC instrument. An obvious goal of using indirect techniques and approaches to estimate LAI is to be able to compare favorably with direct, destructive measurements, which are usually assumed to be more accurate and are typically the standard for comparisons. In the other hand direct methods are time consuming and can not be applied for extensive area. Currently, combined method of TRAC and hemispherical photography/LAI-2000 are used for quick and accurate LAI assessment of a canopy (see section 2.3.5 and 4.1.4 for literature) so that are being used for calibration and validation of other techniques. White *et al.* (2000) concluded that hemispherical photography is the most accurate and efficient way, as compared to LAI-2000 for long term monitoring of arid ecosystems. This was in good agreement with the recent results of Leblanc *et al.* (2002c), who concluded that hemispherical photographs in a grid offer a good potential to replace LAI-2000 and TRAC devices for canopy structure measurement. In this study, hemispherical photography is reported as the most efficient method specially to measure LAI of grass and understory of forest plots because of downward looking capability to encompass the estimation of the whole LAI which is below the sensor height of LAI-2000 and TRAC instrument. Additionally, LAI values estimated using hemispherical photography was most correlated with the combined method of hemispherical photography & TRAC than other methods. This indicates that the reliability of LAI estimates using hemispherical photography based on the comparison result with most validated combined method.

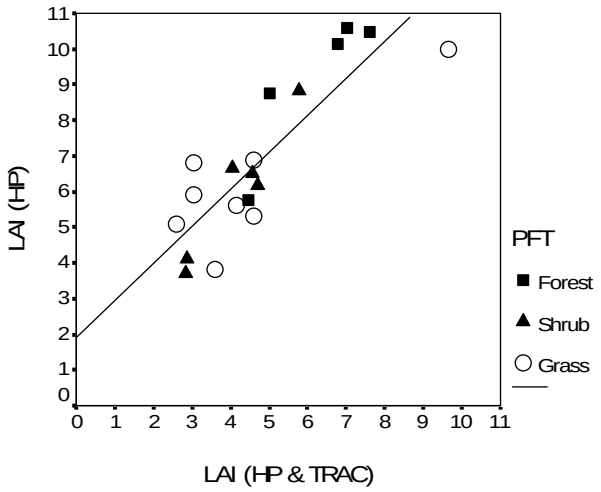

Fig. 16. Relationship between LAI as estimated from Hemispherical Photography and combination of Hemispherical Photography and TRAC.

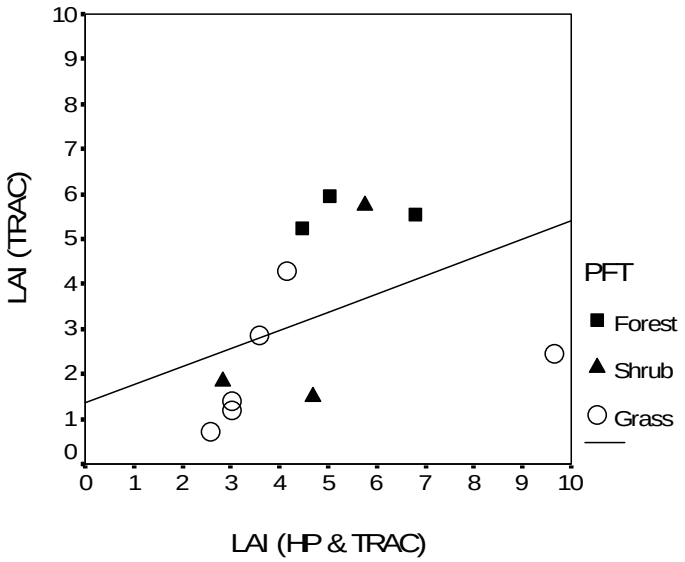

Fig. 17. Relationship between LAI as estimated from TRAC and combination of Hemispherical Photography and TRAC.

In both comparisons i.e. LAIe and LAI from ground measurements, the leaf area index value obtained using hemispherical photography from plot GH 1 was reasonably higher than TRAC and LAI-2000 plant canopy analyzer measurement for the same plot. It is the densest plot of grass plots with average height nearly 1.85 m and found to be difficult to be measured accurately with optical instruments. It was noticed that classification of downward looking hemispherical photographs into gaps and foliage elements found difficult from this plot because of the difficulty to distinguish real gaps (soil) and shadow caste by foliage elements. The LAI result obtained using hemispherical photography from this plot has significantly affected the comparison of ground-based LAI measurements. For example removal of this plot from comparison of LAI between hemispherical photography and TRAC improves R^2 from 0.26 to 0.42 and comparison of LAIe between hemispherical photography and LAI-2000 resulted the R^2 change from 0.007 to 0.32. Fig. 13, 14 and 15 show the outlier effect of this plot.

4.3. Relationships between Vegetation Indices and Ground-based LAI

The relationships between RSR and ground-based LAI measurement of each instrument are assessed for both, all plant functional types together and separately. The ground based LAI data were separated into three major plant functional types: forest, shrub and grass. The relationships between RSR versus LAI effective and LAI of these three plant functional types are shown in Fig. 18 and 19, respectively. The correlation between RSR versus LAI effective was made only from LAI-2000 and hemispherical photography ground measurements, since TRAC measurements were done only for one solar zenith angle, the correlation of RSR with LAIe from TRAC measurements were not made. RSR with LAIe from ring one and two, and all five rings of LAI-2000 plant canopy analyzer of two pant functional types show negative slope (Table 14) and doesn't have real relations. Shrub shows strong negative slope specially LAIe from five rings of LAI-2000 even if the number of ESUs are low. Contrary, the relationships between RSR and LAIe from hemispherical photography show positive slope with very low correlation for all plant functional types.

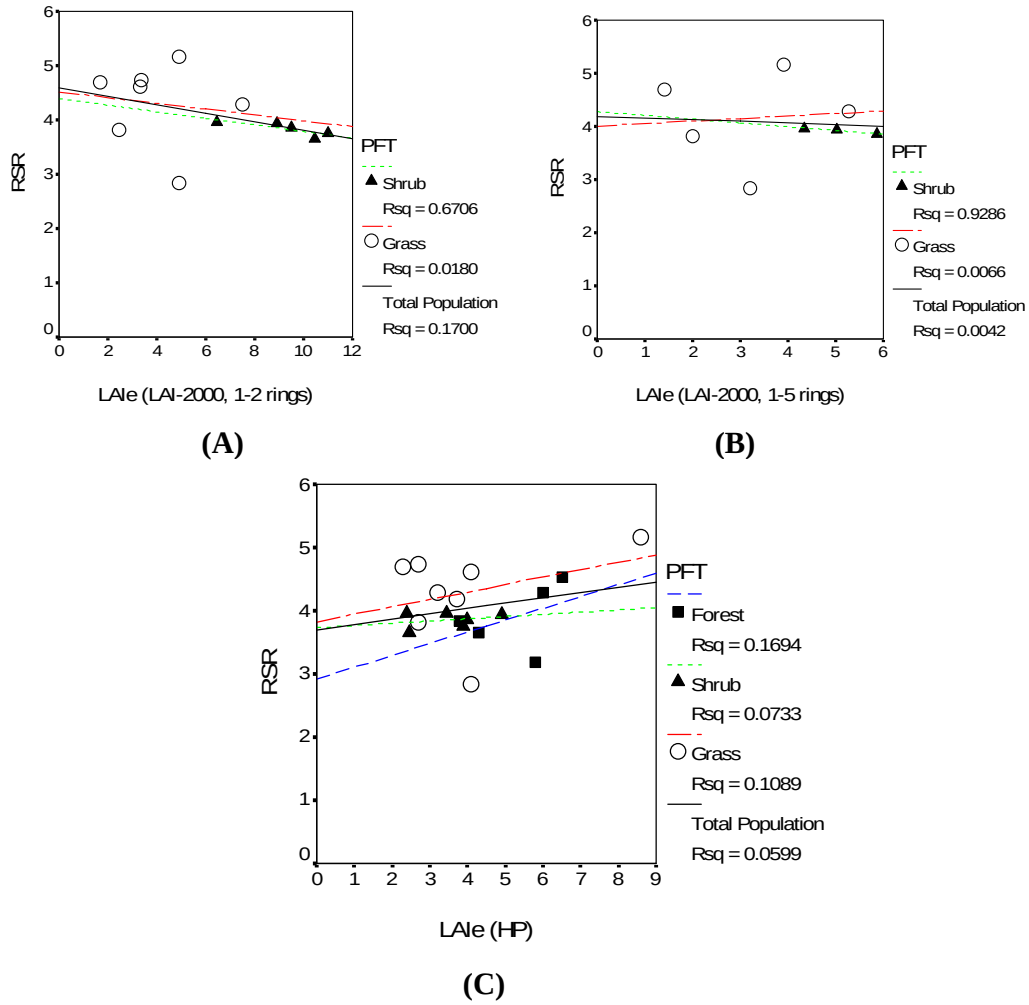

Fig. 18. Correlation of RSR vegetation index derived from AHS with ground measurements of LAI effective for three plant functional types. (A) LAIe (LAI-2000, 1-2 rings)–RSR, (B) LAIe (LAI-2000, 1-5 rings)–RSR, and (C) LAIe (Hemispherical photography)–RSR.

Table 14 Regression equations for the dependent variable effective LAI and RSR.

RSR with	*PFT*	*Model*	*RMSE*	R^2
LAI-2000 LAIe(1-2 rings)	All	y = -2.1386x + 14.988	2.947	0.17
	Shrub	y = -11.104x + 51.815	1.011	0.671
	Grass	y = -0.3375x + 5.4738	1.923	0.018
LAI-2000 LAIe(1-5 rings)	All	y = -0.1497x + 4.4903	1.575	0.004
	Shrub	Y = -13.078x + 56.328	0.145	0.927
	Grass	y = 0.14x + 2.5819	1.156	0.007
Hemispherical photography LAIe	All	y = 0.7149x + 1.2562	1.575	0.06
	Forest	y = 0.9092x + 1.7322	1.062	0.169
	Shrub	y = 2.0582x - 4.4205	0.934	0.073
	Grass	y = 0.9253x - 0.0424	1.893	0.109

Likewise the effective LAI, the relationships between RSR and LAI from TRAC, hemispherical photography and combined method of hemispherical photography-TRAC were assessed. There appeared no real correlation of RSR with LAI of all three ground measurements (Fig. 19 and Table 15). Even though very low R squares are obtained for all relationships of RSR and LAI, positive slops are achieved for all plant functional types but TRAC measurements. The result from previous year study by Mengesha (2005) show also low correlation (R^2 = 0.36) between hemispherical photography LAI and RSR from HyMap2004 for softwood forest of Millingerwaard (Fig. 19 (D)).

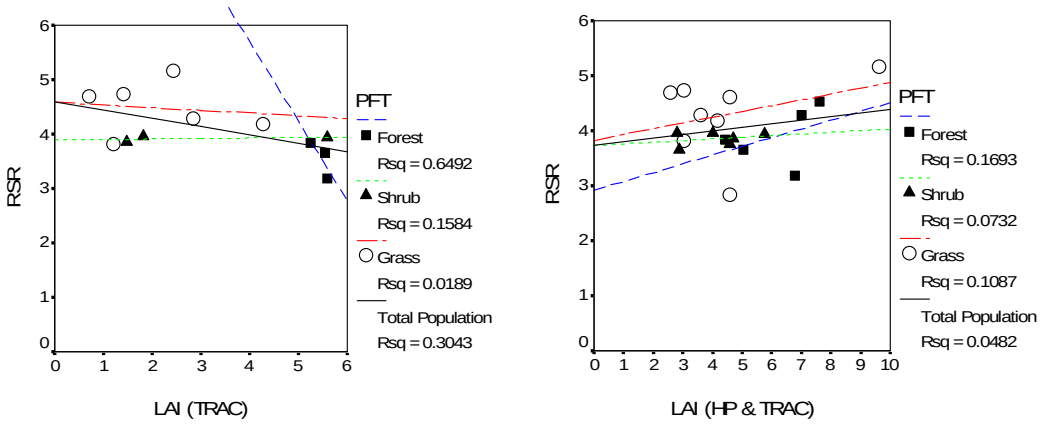

(A) **(B)**

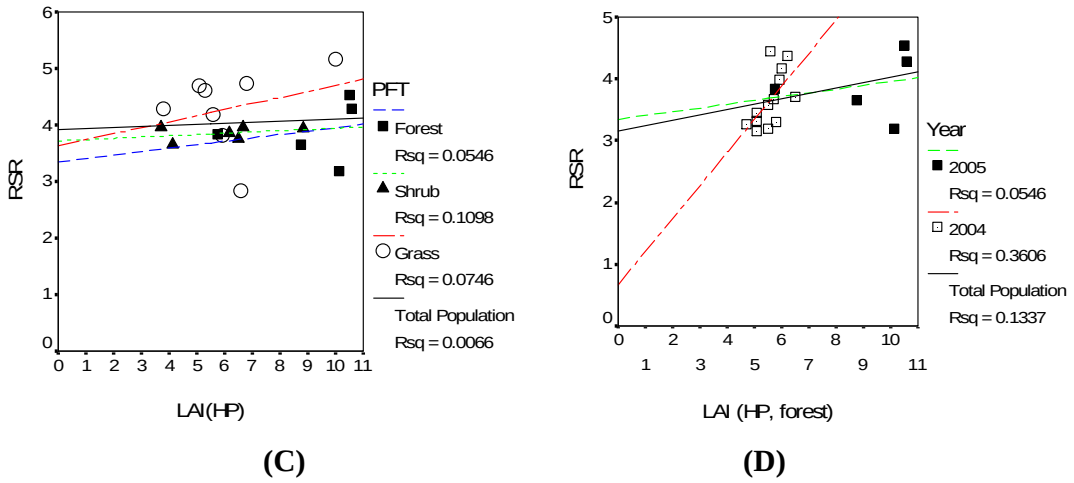

Fig. 19. Correlation of RSR vegetation index derived from AHS with ground measurements of LAI for three plant functional types. (A) LAI (TRAC)–RSR, (B) LAI (Hemispherical photography and TRAC)–RSR, (C) LAI (Hemispherical photography)–RSR, and (D) LAI (HP)-RSR for forest plots from 2004 data (Mengesha, 2005) and this study.

Table 15 Regression equations for the dependent variable LAI and RSR.

RSR with	***PFT***	***Model***	***RMSE***	***R^2***
TRAC LAI	All	y = -1.986x + 11.339	1.615	0.304
	Forest	y = -0.4442x + 7.0428	0.11	0.649
	Shrub	y = 16.032x - 59.869	2.087	0.158
	Grass	y = -0.3794x + 3.8451	1.303	0.019
Hemispherical photography-TRAC LAI	All	y = 0.7375x + 1.797	1.822	0.048
	Forest	y = 1.064x + 2.0279	1.243	0.169
	Shrub	y = 2.4165x - 5.1862	1.097	0.073
	Grass	y = 1.036x - 0.0394	2.121	0.109
Hemispherical photography LAI	All	y = 0.3304x + 5.5465	2.252	0.007
	Forest	y = 0.9004x + 5.6325	1.976	0.055
	Shrub	y = 4.8506x - 12.699	1.762	0.11
	Grass	y = 0.6951x + 3.1572	1.75	0.075

Test of non-linear regressions such as; exponential and logarithmic were performed when simple linear model were apparently inadequate or inappropriate. Unfortunately, no real correlation could be obtained of both LAIe and LAI from all ground measurements with RSR. It can be suggested several explanations for the observed results. First, the negative relationships noted between RSR vs. LAIe and LAI from LAI-2000 and TRAC in the current study may not be only due to RSR insensitivity to explain the LAI variation, but rather to the factors which can increase the uncertainty of these ground measurements. Half of the LAIe from LAI-2000 plant canopy analyzer is obtained using interpolation of the preceding day reference measurements. TRAC measurements are done using only one sun zenith angle and may not represent the corresponding plot of AHS image. In addition to these, most of the grass plots have short canopy and forest plots have dense understory, leaves which are close to the instruments sensor may affect the results obtained from these instruments. As a result, these factors may affect the relationships between LAI from TRAC and LAI-2000 with RSR.

All of the LAI value obtained using hemispherical photography was higher than 3.7, suggesting that the majority of data for this category may have fallen within the region of saturation for the bands used to calculate RSR. Chen *et al.* (2002) reported the saturation of vegetation indices signal at fairly low level of LAI of about 2–3. Other scientists have reported that the signal received by a sensor saturates at an LAI of 3-8 depending on the wavelength (Peterson *et al.*, 1987). Plots of AHS band used to compute RSR (Fig. 20) show general insensitivity with regard to in situ measured LAI. The relationships between LAI and all three bands of AHS image were virtually flat with little correlation between LAI-RED (R^2 = 0.034), LAI-NIR (R^2 = 0.176) and LAI-SWIR (R^2 = 0.194). It was also reported by (Lee *et al.*, 2003) this unusual low correlations between LAI and spectral reflectance in the near infrared bands (ETM+ 4) for mixed deciduous and coniferous forest. The variations in the near infrared band were supposed to be the dominant factor contributing to change of RSR for the whole range of LAI. Contrary, higher NIR reflectance was obtained for the lower LAI values of hemispherical photography. This contradicts to the general case of other studies(Clevers, 1989; Law and Waring, 1994; Fassnacht *et al.*, 1997; Turner *et al.*, 1999) of LAI-NIR reflectance relations. Scientists have noted a strong relationship between LAI and the response in the red band (Peterson *et al.*, 1987; Spanner *et al.*, 1990; Spanner *et al.*, 1994); however, it was not observed this relationship in the current study nor in LAI-SWIR relationship. The absence of trends in SWIR reflectance for various plant functional types and observed LAI ranges, contradicts the general fact that large sensitivity of the SWIR to LAI obtained in other study (Brown *et al.*, 2000).

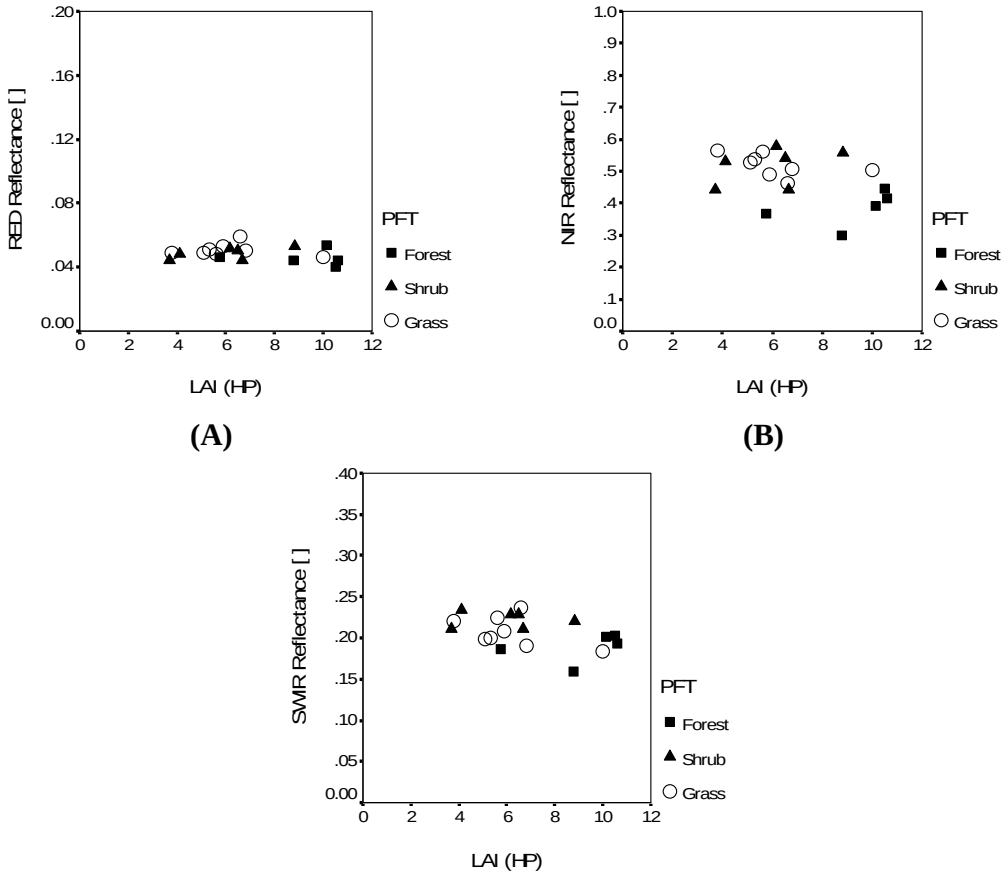

Fig. 20. Relationship between Hemispherical photography LAI and Reflectance. (A) Red (AHS band 8), (B) near-infrared (AHS band 14), and (C) short wave infrared (AHS band 21)

In addition to the aforementioned factors which affect LAI-RSR relationships, dislocation of ground plots from AHS image could affect the relationships although the area represented by the field instrument readings cannot be precisely defined. Regarding the calculation of RSR from AHS image, the presence of water in some forest plots could affect the resulting index values. In this study the ground-based information was not available on canopy closure and therefore the 1% cut-off point of SWIR reflectance histogram were used to obtain SWIR minimum and maximum from the AHS image after masking out the water and bare soil. Even though it is preferable not to determine the minimum and maximum SWIR reflectance from the image as the presence of water affects the SWIR reflectance (Nemani *et al.*, 1993; Brown *et al.*, 2000), the obtained values i.e. SWIR minimum and SWIR maximum may not represent the reflectance from completely closed and an open canopy of the Millingerwaard vegetation, respectively. Further, the quality of the used AHS image also is questionable, as the data provider gave lately notice of recalibrating and reprocessing the entire image with new sensor calibration parameters (VITO, 2005).

Generally, the performance of RSR in this study was remarkably weak unlike other studies (Brown *et al.*, 2000; Chen *et al.*, 2002; Stenberg *et al.*, 2004) which obtained strong relationships of LAI-RSR in forest and mixed vegetations. Among plant functional types existing in the study area, shrub plots show very low variation of RSR range. This could happen because of half of the shrub plots are located near to each other and plot SH8 and SH10 overlaps in the same pixel of aggregated RSR map. In addition to these, the absence of sufficient lower LAI plots from ground measurements complicated the comparison of the AHS image utility for remotely estimating the LAI of the Millingerwaard vegetation.

5. Conclusions and Recommendations

5.1 Conclusions

The present study shows that in the studied floodplain vegetation of the Netherlands, a number of methods can be used to estimate LAI. However, the comparison of LAI from optical field instruments demonstrated that TRAC and LAI-2000 plant canopy analyzer underestimates the LAI for grass plots when compared to hemispherical photography. The dimension of the sensor of TRAC and LAI-2000 plant canopy analyzer may affect the estimation of LAI for short canopy vegetation such as grasses and herbs. Leaf area index which is measured using these two instruments does not encompass the LAI value which is less than the sensor height. In addition to this, the closeness of foliage element to the sensor affects the LAI result from these instruments. Downward looking hemispherical photography was found to be an appropriate optical indirect method to estimate short canopy vegetation. However, for dense and tall grass plots, it was difficult to distinguish between gaps and shadow casted by foliage elements using hemispherical photography. Additionally, because of high humidity during ground data collection days, the moisture effect blurred some of the hemispherical photographs.

Regarding the evaluation of the feasibility of optical field instruments for shrub and forest plots, some of the points which impacted the successful assessment are discussed in the following. Because of time constraints, TRAC measurements were not performed for all ESUs and measurements were made only at one sun zenith angle. LAI-2000 reference measurements were interpolated for four ESUs from the reference device which were acquired one day before the within canopy measurements. The outermost three rings of LAI-2000 device were not recorded for some ESUs and LAI measurement for forest plots were not acquired because the LAI-2000 reference device was not available. Based on the aforementioned reasons and the absence or insufficient measurements using TRAC and LAI-2000 for shrub and forest plots, it is difficult to conclude the comparisons of the three field instruments used in this study for shrub and forest canopies. However, the comparison of LAI from hemispherical photography alone and the combined method of hemispherical photography-TRAC shows good agreement (R^2 = 0.74), indicating their comparable performance.

These estimate of LAI using the aforementioned instruments, however, are all indirect estimates; therefore, a possible bias in all of these measurements is not accounted for in this comparison. Additional work at the study site investigating direct methods could provide more of an unbiased estimate in the future. This study also demonstrates that each method has its strengths and can provide significant additional information that can be important for ecological modeling. Hemispherical photography has proven to be an appropriate method to measure LAI, especially for short canopy vegetation and improved classification techniques in CAN_EYE gave a good discrimination possibility for classification of foliage elements and gaps. The TRAC is also more reliable in determining the effect of foliage clumping and proved in various studies(Chen and Cihlar, 1995; Chen, 1996b; Chen *et al.*, 1997; Breda, 2003; Leblanc and Fournier, 2005). A key advantage of all of these estimation methods is that observations can be collected in a short period of time in contrast to

weeks, months or even years required for direct estimation (e.g. litterfall or harvest), which is a major benefit, particularly for remote sensing investigations, where timely ground reference data collection of adequate size and spatial distribution is often a constraint.

A poor correlation of RSR and all three methods of ground measurements were obtained in this study for all plant functional types. Besides the insufficient number of plots with a small LAI, the majority of plots covered by the ground-based measurements show high LAI values which cause a saturation in the wavelength regions of the spectral bands which are required to calculate the RSR. Further, the uncertainty in the quality of AHS image and the unsuitability of TRAC and LAI-2000 instruments for LAI measurements of grass canopies could be the major factors which resulted in the poor relationship between RSR and ground-based LAI.

5.2 Recommendations

Based on the present study, the following points are mentioned to be considered for future studies.

There is a need for further studies on the usability of LAI estimations based on optical field instruments and validated with distractive sampling methods for natural and heterogeneous vegetation canopies. The number of sample plots has to be sufficient to represent all ranges of LAI and existing plant functional types, and need not to be located to the edge of vegetation boundary or road side. In this study, it was noticed that the documentation and quality of field measurements have created considerable difficulties. In future study, field measurements have to be well documented and have to be checked for the quality before the end of field days so that the missing or poor quality data can be re-measured in time.

Hemispherical photographs produce a permanent record of the plot that can be reanalyzed when the understanding of theory improves such as when CAN_EYE includes the possibility of computing gap size distribution.

A satisfactory technique for estimating LAI using imaging spectroscopy for the plant functional types in the Millingerwaard floodplain vegetation has not been clearly identified. The results of LAI-RSR relationship from this study are inconclusive, and further studies of the performance of ground-based LAI and RSR should include sufficient number of ground data in order to better determine the spectral characteristics of Millingerwaard vegetation, and field canopy closure measurements to improve the calculation of RSR. The quality of imaging spectroscopy data has to be assessed regarding the uncertainties in sensor calibration and atmospheric correction.

Additionally, it is reasonable to say on the basis of these results that exploring the applicability of different vegetation indices alongside developing physical reflectance models remains an important field of research.

References

Barclay, H. J. (1998). "Conversion of total leaf area to projected leaf area in lodgepole pine and Douglas-fir." Tree Physiology **18**(3): 185.

Barclay, H. J., J. A. Trofymow and R. I. Leach (2000). "Assessing bias from boles in calculating leaf area index in immature Douglas-fir with the LI-COR canopy analyzer." Agricultural and Forest Meteorology **100**(2-3): 255.

Barendregt, A., B. Beltman and K. Sykora (1998). Nature development in the Millinger Waard. Selected restoration objects in the Netherlands and NW Germany. A. Grootjans and R. v. Diggelen. Groningen, Laboratory of Plant Ecology**:** 85-91.

Baret, F. and M. Weiss (2004). Can_eye Processing Digital Photographs for Canopy Structure Characterization Tutorial, Avignon.

Baret, F., M. Weiss, D. Allard, S. Garrigue, M. Leroy, H. Jeanjean, R. Fernandes, R. Myneni, J. Privette, J. M. H. Bohbot, R. Bosseno, G. Dedieu, C. D. Bella, B. Duchemin, M. Espana, V. Gond, X. F. Gu, D. Guyon, C. Lelong, P. Maisongrande, E. Mougin, T. Nilson, F. Veroustraete and R. Vintilla (2005) "VALERI: a network of sites and a methodology for the validation of medium spatial resolution land satellite products." www. avignon.inra.fr/valeri/ **Volume**, DOI:

Berterretche, M., T. Andrew T. Hudak, W. B. Cohen, T. K., Maierspergera, S. T. Gower and J. Dungan (2005). "Comparison of regression and geostatistical methods for mapping Leaf Area Index (LAI) with Landsat ETM+ data over a boreal forest." Remote Sensing of Environment **96**: 49-61.

Breda, J. J. N. (2003). "Ground-based measurements of leaf area index: a review of methods, instruments and current controversies." Journal of Experimental Botany. **54**(392): 2403-2417.

Broge, N. H. and E. Leblanc (2001). "Comparing prediction power and stability of broadband and hyperspectral vegetation indices for estimation of green leaf area index and canopy chlorophyll density." Remote Sensing of Environment **76**(2): 156.

Brown, L., J. M. Chen, S. G. Leblanc and J. Cihlar (2000). "A shortwave infrared modification to the simple ratio for LAI retrieval in boreal forests: An image and model analysis." Remote Sensing of Environment **71**(1): 16.

Campbell, G. S. (1986). "Extinction coefficients for radiation in plant canopies calculated using an ellipsoidal inclination angle distribution." Agricultural and Forest Meteorology **36**(4): 317.

Campbell, G. S. and J. M. Norman (1990). The description and measurement of plant canopy structure.

Chason, J. W., D. D. Baldocchi and M. A. Huston (1991). "A comparison of direct and indirect methods for estimating forest canopy leaf area." Agricultural & Forest Meteorology **57**(1-3): 107.

Chen, J. M. (1996a). "Evaluation of vegetation indices and a modified simple ratio for boreal applications." Canadian Journal of Remote Sensing **22**(3): 229.

Chen, J. M. (1996b). "Optically-based methods for measuring seasonal variation of leaf area index in boreal conifer stands." Agricultural and Forest Meteorology **80**(2-4): 135.

Chen, J. M. and T. A. Black (1991). "Measuring leaf area index of plant canopies with branch architecture." Agricultural & Forest Meteorology **57**(1-3): 1.

Chen, J. M. and T. A. Black (1992). "Defining leaf area index for non-flat leaves." Plant, Cell & Environment **15**(4): 421–429.

Chen, J. M. and J. Cihlar (1995). "Quantifying the effect of canopy architecture on optical measurements of leaf area index using two gap size analysis methods." IEEE Transactions on Geoscience and Remote Sensing **33**(3): 777.

Chen, J. M. and J. Cihlar (1996). "Retrieving leaf area index of boreal conifer forests using Landsat TM images." Remote Sensing of Environment **55**(2): 153.

Chen, J. M., G. Pavlic, L. Brown, J. Cihlar, S. G. Leblanc, H. P. White, R. J. Hall, D. R. Peddle, D. J. King, J. A. Trofymow, E. Swift, J. Van der Sanden and P. K. E. Pellikka (2002). "Derivation and validation of Canada-wide coarse-resolution leaf area index maps using high-resolution satellite imagery and ground measurements." Remote Sensing of Environment **80**(1): 165.

Chen, J. M., P. M. Rich, S. T. Gower, J. M. Norman and S. Plummer (1997). "Leaf area index of boreal forests: Theory, techniques, and measurements." Journal of Geophysical Research D: Atmospheres **102**(24): 29429.

Clevers, J. G. P. W. (1989). "The Application of a Weighted Infrared-Red Vegetation Index for Estimating Leaf Area Index by Correcting for Soil Moisture." Remote Sensing of Environment **21**: 25-37.

Coops, N. C., M. L. Smith, K. L. JACOBSEN, M. MARTIN and S. OLLINGER (2004). "Estimation of plant and leaf area index using three techniques in a mature native eucalypt canopy." Austral Ecology **29**: 332-341.

Eriksson, H., L. Eklundh, K. Hall and A. Lindroth (2005). "Estimating LAI in deciduous forest stands." Agricultural and Forest Meteorology **129**: 27-37.

Fassnacht, K. S., S. T. Gower, E. V. Nordheim, T. M. Lillesand and M. D. MacKenzie (1997). "Estimating the leaf area index of North Central Wisconsin forests using the landsat thematic mapper." Remote Sensing of Environment **61**(2): 229.

Frazer, G. W., R. A. Fournier, J. A. Trofymow and R. J. Hall (2001). "A comparison of digital and film fisheye photography for analysis of forest canopy structure and gap light transmission." Agricultural and Forest Meteorology **109**(4): 249.

FV2000 (2005). FV2000: The LAI-2000 Data File Viewer manual. Lincoln, Nabraska, USA, LI-COR, inc.

Gong, P., R. Pu, G. S. Biging and M. R. Larrieu (2003). "Estimation of Forest Leaf Area Index Using Vegetation Indices Derived From Hyperion Hyperspectral Data." IEEE Transactions on Geoscience and Remote Sensing **41**(6).

Gower, S. T., C. J. Kucharik and J. M. Norman (1999). "Direct and Indirect Estimation of Leaf Area Index, fAPAR, and Net Primary Production of Terrestrial Ecosystems." Remote Sensing of Environment **70**: 29-51.

Hale, S. E. and C. Edwards (2002). "Comparison of film and digital hemispherical photography across a wide range of canopy densities." Agricultural and Forest Meteorology **112**(1): 51.

Hall, R. J., D. P. Davidson and D. R. Peddle (2003). "Ground and remote estimation of leaf area index in Rocky Mountain forest stands, Kananaskis, Alberta." Canadian Journal of Remote Sensing **29**(3): 411.

Hu, J., B. Tan, N. Shabanov, Y. Knyazikhin, R. B. Myneni, K. A. Crean, J. V. Martonchik and D. J. Diner (2003). "Performance of the MISR LAI and FPAR algorithm: A case study in Africa." Remote Sensing of Environment **88**(3): 324.

Jacquemoud, S., C. Bacour, H. Poilve´ and J.-P. Frangi (2000). "Comparison of Four Radiative Transfer Models to Simulate Plant Canopies Reflectance: Direct and Inverse Mode." Remote Sensing of Environment **74**(471-481).

Jonckheere, I., S. Fleck, K. Nackaerts, B. Muysa, P. Coppin, M. Weiss and F. Baret (2004a). "Review of methods for in situ leaf area index determination Part I. Theories, sensors and hemispherical photography." Agricultural and Forest Meteorology **121**: 19-35.

Jonckheere, I., B. Muys and P. Coppin (2004b). "Allometry and evaluation of in situ optical LAI determination in Scots pine: a case study in Belgium." Tree Physiology **25**: 723-732.

Knyazikhin, Y., J. V. Martonchik, R. B. Myneni, D. J. Diner and S. W. Running (1998). "Synergistic algorithm for estimating vegetation canopy leaf area index and fraction of absorbed photosynthetically active radiation from MODIS and MISR data." Journal of Geophysical Research **103**(D24): 32,257-32,276.

Kucharik, C. J., J. M. Norman and S. T. Gower (1998). "Measurements of branch area and adjusting leaf area index indirect measurements." Agricultural and Forest Meteorology **91**(1-2): 69.

LAI-2000 (2005). The LAI-2000 pant canopy analyser, manual. Lincoln, Nebraska, USA, LI-COR, inc.

Law, B. E. and R. H. Waring (1994). "Remote sensing of leaf area index and radiation intercepted by understory vegetation." Ecological Applications **4**(2): 272.

Leblanc, S. G. (2002). "Correction to the plant canopy gap-size analysis theory used by the tracing radiation and architecture of canopies instrument." Applied Optics **41**(36): 7667.

Leblanc, S. G. and J. M. Chen (2001). "A practical scheme for correcting multiple scattering effects on optical LAI measurements." Agricultural and Forest Meteorology **110**(2): 125.

Leblanc, S. G., J. M. Chen, R. Fernandes, D. W. Deering and A. Conley (2005). "Methodology comparison for canopy structure parameters extraction from digital hemispherical photography in boreal forests." Agricultural and Forest Meteorology **129**: 187-207.

Leblanc, S. G., J. M. Chen and M. Kwong (2002a). Tracing Radiation and Architecture of Canopies TRAC MANUAL Version 2.1.3. Natural Resources Canada. Ottawa, Canada, Canada Centre for Remote Sensing**:** 25.

Leblanc, S. G., J. M. Chen, H. P. White, R. Latifovic, R. Fernandes, J. L. Roujean and R. Lacaze (2002b). Mapping leaf area index heterogeneity over Canada using directional reflectance and anisotropy canopy reflectance models. International Geoscience and Remote Sensing Symposium (IGARSS).

Leblanc, S. G., R. Fernandes and J. M. Chen (2002c). Recent advancements in optical field leaf area index, foliage heterogeneity, and foliage angular distribution measurements. International Geoscience and Remote Sensing Symposium (IGARSS).

Leblanc, S. G. and R. A. Fournier (2005). Towards a better understanding of in-situ canopy measurements used in the derivation and validation of remote sensing leaf area index products. Natural Resources Canada. Québec,Canada, Canada Centre for Remote Sensing**:** 4.

Lee, K.-S., S.-H. Kim, Y.-I. Park and K.-C. Jang (2003). "Generation of Forest Leaf Area Index (LAI) Map Using Multispectral Satellite Data and Field Measurements." Korean Journal of Remote Sensing **19**(5): 371-380.

Lee, K. S., W. B. Cohen, R. E. Kennedy, T. K. Maiersperger and S. T. Gower (2004). "Hyperspectral versus multispectral data for estimating leaf area index in four different biomes." Remote Sensing of Environment **91**(3-4): 508.

Levy, P. E. and P. G. Jarvis (1999). "Direct and indirect measurements of LAI in millet and fallow vegetation in HAPEX-Sahel." Agricultural and Forest Meteorology **97**(3): 199.

Liu, J., J. M. Chen, J. Cihlar and W. M. Park (1997). "A process-based boreal ecosystem productivity simulator using remote sensing inputs." Remote Sensing of Environment **62**(2): 158.

Manninen, T., P. Stenberg, M. Rautiainen, P. Voipio, H. Smolander and K. Andersson (2005). LAI estimation of boreal forest with ENVISAT ASAR. European Space Agency, (Special Publication) ESA SP.

Mengesha, T. G. (2005). Validation of ground biophysical products using imaging specroscopy in a soft wood forest. Geo-Information Science. Wageningen, Wageningen University and Research Centre. **MSc thesis report:** 78.

Miller, J. B. (1967). "A formula for average foliage density." Aust. J. Bot. **15**: 141-144.

Morisette, J. T., F. Baret, J. L. Privette, R. B. Myneni, J. Nickeson, S. Garrigues, N. Shabanov, M. Weiss, R. Fernandes, S. Leblanc, M. Kalacska, G. A. Sánchez-Azofeifa, M. Chubey, B. Rivard, P. Stenberg, M. Rautiainen, P. Voipio, T. Manninen, A. Pilant, T. Lewis, J. Iiames, R. Colombo, M. Meroni, L. Busetto, W. Cohen, D. Turner, E. D. Warner, G. W. Petersen, G. Seufert and R. Cook. (2005). "Validation of global moderate resolution LAI Products: a framework proposed within the CEOS Land Product Validation subgroup." LAI Intercomparison Overview Submission – LPV special issue Retrieved 20-August, 2005, from http://cliveg.bu.edu/download/manuscripts/morisette01.pdf.

Mussche, S., R. Samson, L. Nachtergale, A. De Schrijver, R. Lemeur and N. Lust (2001). "A comparison of optical and direct methods for monitoring the seasonal dynamics of leaf area index in deciduous forests." Silva Fennica **35**(4): 373-384.

Myneni, R. B., S. Hoffman, Y. Knyazikhin, J. L. Privette, J. Glassy, Y. Tian, Y. Wang, X. Song, Y. Zhang, G. R. Smith, A. Lotsch, M. Friedl, J. T. Morisette, P. Votava, R. R. Nemani and S. W. Running (2002). "Global products of vegetation leaf area and fraction absorbed PAR from year one of MODIS data." Remote Sensing of Environment **83**(1-2): 214.

Nackaerts, K., P. Coppin, B. Muys and M. Hermy (2000). "Sampling methodology for LAI measurements with LAI-2000 in small forest stands." Agricultural and Forest Meteorology **101**(4): 247.

Nemani, R., L. Pierce, S. Running and L. Band (1993). "Forest ecosystem processes at the watershed scale: sensitivity to remotely-sensed leaf area index estimates." International Journal of Remote Sensing **14**(13): 2519.

Nilson, T. (1971). "A theoretical analysis of the frequency of gaps in plant stands." Agricultural Meteorology **8**: 25.

Norman, J. M. and G. S. Campbell (1989). Canopy structure. Plant Ecology: Field Methods and Instrumentation. R. W. Pearcy, Ehlringer, J., Mooney, H.A., Rundel, P.W. London, Chapman & Hall**:** 301-325.

Peterson, D. L., M. A. Spanner, S. W. Running and K. B. Teuber (1987). "Relationship of thematic mapper simulator data to leaf area index of temperate coniferous forests." Remote Sensing of Environment **22**(3): 323.

Privette, J. L. and M. Mukelabai (2000). SAFARI 2000 Leaf Area Index and Canopy Structure, Kalahari Transect, 1999-2000. SAFARI 2000Southern Africa Validation of EOS (SAVE). Tennesseee, Oak Ridge National Laboratory**:** 7.

Privette, J. L., R. B. Myneni, Y. Knyazikhin, M. Mukelabai, G. Roberts, Y. Tian, Y. Wang and S. G. Leblanc (2002). "Early spatial and temporal validation of MODIS LAI product in the southern Africa Kalahari." Remote Sensing of Environment **83**(1-2): 232.

Pu, R., Q. Yu, P. Gong and G. S. BIGING (2005). "EO-1 Hyperion, ALI and Landsat 7 ETM+ data comparison for estimating forest crown closure and leaf area index." International Journal of Remote Sensing **26**(3): 457-474.

Rich, P. M. (1988). Video image analysis of hemispherical canopy photography. Proceedings of the First Special Workshop on Videography, Terre Haute, IN, American Society for Photogrammetry and Remote Sensing.

Rich, P. M. (1990). "Characterizing plant canopies with hemispherical photographs." Remote Sensing Reviews **5**: 13-29.

Roxburgh, J. R. and D. Kelly (1995). "Uses and limitations of hemispherical photography for estimating forest light environments." New Zealand Journal of Ecology **19**(2): 213-217.

Schaepman, M. E., B. Koetz, G. Schaepman-Strub and K. I. Itten (2005). "Spectrodirectional remote sensing for the improved estimation of biophysical and -chemical variables: two case studies." International Journal of Applied Earth Observation and Geoinformation **6**: 271-282.

Schlerf, M., C. Atzberger and J. Hill (2005). "Remote sensing of forest biophysical variables using HyMap imaging spectrometer data." Remote Sensing of Environment **95**: 177-194.

Schlerf, M., C. Atzberger, M. Vohland, H. Buddenbaum, S. Seeling and J. Hill (2004). Derivation of forest leaf area index from multi-and hyperspectral remote sensing data. EARSeL eProceedings, Trier University, Department of Remote Sensing, D-54286 Trier, Germany.

Scurlock, J. M. O., G. P. Asner and S. T. Gower (2001). Global Leaf Area Index Data from Field Measurements, 1932-2000, Data set available on-line [http://www.daac.ornl.gov] from the Oak Ridge National Laboratory Distributed Active Archive Center, Oak Ridge, Tennessee, USA.

Spanner, M., L. Johnson, J. Miller, R. McCreight, J. Freemantle, J. Runyon and P. Gong (1994). "Remote sensing of seasonal leaf area index across the Oregon transect." Ecological Applications **4**(2): 258.

Spanner, M. A., L. L. Pierce, D. L. Peterson and S. W. Running (1990). "Remote sensing of temperate coniferous forest leaf area index. The influence of canopy closure, understory vegetation and background reflectance." International Journal of Remote Sensing **11**(1): 95.

Stenberg, P., M. Rautiainen, T. Manninen, P. Voipio and H. Smolander (2004). "Reduced simple ratio better than NDVI for estimating LAI in Finnish pine and spruce stands." Silva Fennica **38**(1): 3.

Strub, G., U. Beisl, M. Schaepman, D. Schlaepfer, C. Dickerhof and K. Itten (2002). "Evaluation of diurnal hyperspectral HDRF data acquired with the RSL field goniometer during the DAISEX'99 campaign." Photogrammetry and remote sensing **57**: 184-193.

Sun-Hwa, K. and L. Kyu-Sung (2003). "Local Validation of MODIS Global Leaf Area Index (LAI) Product over Temperate Forest." Korean Journal of Remote Sensing **19**(1): 1-9.

Tian, Y., Y. Wang, Y. Zhang, Y. Knyazikhin, J. Bogaet and R. B. Myneni (2002). "Radiative transfer based scaling of LAI retrievals from reflectance data of different resolutions." REMOTE SENISNINF OF ENVIRONMENT **84**: 143-159.

Turner, D. P., R. E. Kennedy, W. B. Cohen, K. S. Fassnacht and J. M. Briggs (1999). "Relationships between leaf area index and Landsat TM spectral vegetation indices across three temperate zone sites." Remote Sensing of Environment **70**(1): 52.

VITO (2005). Processing and Archiving Facility for Airborne Remote Sensing: Software System Validation Report AHS160 Campaign 2005. J. Biesemans and J. Hooyberghs, Flemish Institute for Technology Research**:** 21.

Wang, Y., C. E. Woodcock, W. Buermann, Y. Tian, J. Hu, Y. Knyazikhin, R. B. Myneni, P. Stenberg, P. Voipio, H. Smolander and T. Häme (2004). "Evaluation of the MODIS LAI algorithm at a coniferous forest site in Finland." Remote Sensing of Environment **91**(1): 114.

Watson, D. J. (1947). "Comparative physiological studies in growth of field crops. I. Variation in net assimilation rate and leaf area between species and varieties, and within and between years." Annatomy and Botany **11**: 41-76.

Weiss, M. (2004). GROUND DATA PROCESSING & PRODUCTION OF THE LEVEL 1 HIGH RESOLUTION MAPS. VALERI 2003: Concepcion site Level 1 map production, http://www.avignon.inra.fr/valeri/fic_htm/database/main.php.

Weiss, M., F. Baret, G. J. Smith, I. Jonckheere and P. Coppin (2004). "Review of methods for in situ leaf area index (LAI) determination Part II. Estimation of LAI, errors and sampling." Agricultural and Forest Meteorology **121**: 37-53.

Welles, J. M. and S. Cohen (1996). "Canopy Structure Measurement by Gap Fraction Analysis Using Commercial Instrumentation." Journal of Experimental Botany **47**(302): 1335-1342.

Welles, J. M. and J. M. Norman (1991). "Instrument for Indirect Measurement of Canopy Architecture." Agronomy Journal **83**: 818-825.

Welles, M. J. (1990). "Some Indirect Methods of Estimating Canopy Structure." Remote Sensing Reviews **5**(1): 31-43.

White, M. A., G. P. Asner, R. R. Nemani, J. L. Privette and S. W. Running (2000). "Measuring fractional cover and leaf area index in arid ecosystems: Digital camera, radiation transmittance, and laser altimetry methods." Remote Sensing of Environment **74**(1): 45.

Zhang, Y., J. M. Chen and J. R. Miller (2005). "Determining digital hemispherical photograph exposure for leaf area index estimation." Agricultural and Forest Meteorology **133**(1-4): 166.

Appendix

Appendix 1. AHS band positions

AHS band	Center WL µm	FWHM
1	0.455000,	0.027000,
2	0.484000,	0.028000,
3	0.513000,	0.029000,
4	0.542000,	0.028000,
5	0.571000,	0.028000,
6	0.601000,	0.028000,
7	0.630000,	0.028000,
8	0.659000,	0.028000,
9	0.689000,	0.028000,
10	0.718000,	0.028000,
11	0.746000,	0.027000,
12	0.774000,	0.027000,
13	0.804000,	0.028000,
14	0.833000,	0.028000,
15	0.862000,	0.028000,
16	0.891000,	0.027000,
17	0.918000,	0.028000,
18	0.948000,	0.028000,
19	0.975000,	0.028000,
20	1.004000,	0.030000,
21	1.622000,	0.159000,
22	2.031000,	0.013300,
23	2.042900,	0.013300,
24	2.055500,	0.013200,
25	2.068000,	0.013200,
26	2.079900,	0.013200,
27	2.092400,	0.013100,
28	2.103900,	0.013000,
29	2.116400,	0.013000,
30	2.128300,	0.012900,
31	2.139900,	0.013000,
32	2.151700,	0.013000,
33	2.163400,	0.013100,
34	2.175300,	0.013200,
35	2.185900,	0.013000,
36	2.198500,	0.013100,
37	2.209900,	0.013000,
38	2.221200,	0.013000,
39	2.232500,	0.013000,
40	2.244100,	0.013000,

AHS band	Center WL µm	FWHM
41	2.255500,	0.013100,
42	2.266300,	0.013000,
43	2.283400,	0.013200,
44	2.294500,	0.013100,
45	2.305700,	0.013000,
46	2.316100,	0.013200,
47	2.326700,	0.013100,
48	2.337000,	0.013100,
49	2.348100,	0.013100,
50	2.359100,	0.013100,
51	2.369600,	0.013000,
52	2.380400,	0.012900,
53	2.390700,	0.012800,
54	2.400800,	0.012900,
55	2.410900,	0.012900,
56	2.421000,	0.012900,
57	2.432300,	0.013000,
58	2.441800,	0.012300,
59	2.452400,	0.012800,
60	2.462100,	0.012700,
61	2.471700,	0.012700,
62	2.482500,	0.012400,
63	2.491600,	0.012500,
64	3.180000,	0.360000,
65	3.500000,	0.340000,
66	3.900000,	0.340000,
67	4.170000,	0.420000,
68	4.600000,	0.370000,
69	4.970000,	0.350000,
70	5.310000,	0.260000,
71	8.190000,	0.470000,
72	8.660000,	0.400000,
73	9.170000,	0.410000,
74	9.600000,	0.430000,
75	10.080000,	0.420000,
76	10.560000,	0.560000,
77	11.160000,	0.550000,
78	11.720000,	0.550000,
79	12.320000,	0.480000,
80	12.890000	0.520000

Appendix 2. AHS QuickLooks. June 19, 2005, Millingerwaard (http://campaigns.vgt.vito.be/images/QL2005/050619_Millingerwaard_27.jpg)

(A). AHS Quicklook 'Millingerwaard', 19. June 2005, Scene 1

(B). AHS Quicklook 'Millingerwaard, 19. June 2005, Scene 2

(C). AHS Quicklook ‘Millingerwaard’, 19. June 2005, Scene 3

(D). AHS Quicklook ‘Millingerwaard, 19. June 2005, Scene 4

Appendix 3. Species abundance per plot

Species name	**Plot code**								
	GH 1	GH 2	GH 3	GH 4	GH 5	GH 6	SH 7	SH 8	SH 9
Alopecurus pratensis	20	0	0	50	1	0	0	0	0
Arctium lappa	1	0	0	1	2	0	0	1	1
Artemisia vulgaris	1	0	0	0	0	0	0	1	0
Brassica nigra	2	0	0	1	1	0	0	0	1
Cirsium arvense	45	0	1	20	1	0	1	5	20
Dipsacus fullonum	5	0	0	0	0	0	0	0	0
Galeopsis tetrahit	1	0	0	0	0	0	0	0	0
Galium aparine	20	0	0	2	20	0	2	0	1
Glechoma hederacea	1	0	1	5	1	0	1	20	0
Poa trivialis	5	0	0	1	1	0	5	50	5
Urtica dioica	35	1	0	2	0	1	30	5	30
Elytrigia repens	1	0	0	0	0	0	0	0	0
Persicaria maculosa	1	0	0	1	0	1	0	0	0
Arrhenatherum elatius	0	5	10	0	0	30	5	0	0
Bromopsis inermis	0	2	0	0	0	0	0	0	0
Equisetum arvense	0	50	0	0	0	0	0	0	0
Eryngium campestre	0	20	30	0	0	30	1	0	0
Galium mollugo	0	1	2	0	2	0	10	0	0
Plantago lanceolata	0	1	1	0	0	0	0	0	0
Potentilla reptans	0	3	2	0	0	5	1	5	2
Rumex acetosa	0	5	1	1	0	20	1	0	0
Saponaria officinalis	0	1	10	0	1	1	1	0	0
Sedum acre	0	1	0	0	0	1	0	0	0
Tanacetum vulgare	0	15	2	0	5	0	5	0	0
Trifolium repens	0	5	2	0	0	2	1	3	0
Erigeron annuus	0	1	1	0	0	0	0	0	0
Senecio inaequidens	0	1	1	0	0	1	0	0	0
Senecio jacobaea	0	5	15	0	0	2	0	1	0
Cichorium intybus	0	0	1	0	0	0	0	0	0
Dactylis glomerata	0	0	1	2	1	0	1	0	0
Euphorbia cyparissias	0	0	1	0	0	0	0	0	0
Festuca rubra	0	0	40	0	0	10	1	0	0
Geranium molle	0	0	1	0	0	1	0	0	0
Hypericum perforatum	0	0	1	0	0	0	0	0	0
Pastinaca sativa	0	0	1	0	0	0	0	0	0
Rubus caesius	0	0	5	30	60	0	50	20	40
Sedum album	0	0	1	0	0	0	0	0	0
Trifolium campestre	0	0	1	0	0	3	0	0	0
Bromopsis inermis	0	0	15	0	5	10	0	0	0
Chaerophyllum temulum	0	0	0	2	0	0	0	0	0
Festuca arundinacea	0	0	0	3	0	0	0	0	0
Lamium album	0	0	0	1	0	0	0	0	0

Lolium perenne	0	0	0	1	1	0	0	15	0
Potentilla anserina	0	0	0	1	0	0	0	0	0
Scrophularia nodosa	0	0	0	1	1	0	1	0	0
Symphytum officinale	0	0	0	1	0	0	0	0	0
Achillea millefolium	0	0	0	0	1	1	1	0	0
Carduus crispus	0	0	0	0	0	1	0	0	0
Carex hirta	0	0	0	0	0	5	3	10	5
Convolvulus arvensis	0	0	0	0	0	1	0	0	0
Galium verum	0	0	0	0	0	1	2	0	0
Herniaria glabra	0	0	0	0	0	1	0	0	0
Oenothera biennis	0	0	0	0	0	1	0	0	0
Ononis repens	0	0	0	0	0	1	0	0	0
Calamagrostis epigejos	0	0	0	0	0	0	10	10	5
Cornus sanguinea	0	0	0	0	0	0	1	1	0
Crataegus monogyna	0	0	0	0	0	0	10	35	20
Thalictrum flavum	0	0	0	0	0	0	2	0	0
Valeriana officinalis	0	0	0	0	0	0	1	0	0
Cerastium fontanum	0	0	0	0	0	0	1	0	0
Rosa species	0	0	0	0	0	0	2	10	0
Agrostis stolonifera	0	0	0	0	0	0	0	10	1
Juncus compressus	0	0	0	0	0	0	0	2	0
Lathyrus tuberosus	0	0	0	0	0	0	0	1	0
Lysimachia vulgaris	0	0	0	0	0	0	0	1	0
Epilobium hirsutum	0	0	0	0	0	0	0	0	10
Vicia cracca	0	0	0	0	0	0	0	0	1
Conyza canadensis	0	0	0	0	0	0	0	0	5
Fraxinus excelsior	0	0	0	0	0	0	0	0	0
Sambucus nigra	0	0	0	0	0	0	0	0	0
Euphorbia esula	0	0	0	0	0	0	0	0	0
Carduus nutans	0	0	0	0	0	0	0	0	0
Carex arenaria	0	0	0	0	0	0	0	0	0
Trifolium pratense	0	0	0	0	0	0	0	0	0
Iris pseudacorus	0	0	0	0	0	0	0	0	0
Holcus lanatus	0	0	0	0	0	0	0	0	0
Trifolium dubium	0	0	0	0	0	0	0	0	0
Plantago major	0	0	0	0	0	0	0	0	0
Phleum pratense	0	0	0	0	0	0	0	0	0
Bromus hordeaceus s. hordeaceus	0	0	0	0	0	0	0	0	0
Taraxacum species	0	0	0	0	0	0	0	0	0
Calystegia sepium	0	0	0	0	0	0	0	0	0
Salix alba	0	0	0	0	0	0	0	0	0
Impatiens glandulifera	0	0	0	0	0	0	0	0	0
Lysimachia nummularia	0	0	0	0	0	0	0	0	0

Alopecurus pratensis	0	0	0	0	0	0	0	0	0
Arctium lappa	1	0	1	1	5	20	1	10	0
Artemisia vulgaris	0	1	1	0	0	0	0	0	0
Brassica nigra	0	0	0	0	0	0	0	0	0
Cirsium arvense	5	5	0	0	1	0	0	0	0
Dipsacus fullonum	0	0	0	0	0	0	0	0	0
Galeopsis tetrahit	0	1	0	0	0	0	0	0	0
Galium aparine	5	10	0	5	0	60	40	80	50
Glechoma hederacea	0	1	0	0	0	2	0	0	0
Poa trivialis	5	5	0	5	5	0	0	0	0
Urtica dioica	40	50	0	60	0	10	60	1	0
Elytrigia repens	0	0	0	0	0	0	0	0	0
Persicaria maculosa	0	0	0	0	1	0	0	0	0
Arrhenatherum elatius	0	1	0	1	0	0	0	0	0
Bromopsis inermis	0	0	0	0	0	0	0	0	0
Equisetum arvense	0	0	0	0	0	0	0	0	0
Eryngium campestre	0	0	0	0	0	0	0	0	0
Galium mollugo	0	0	1	0	0	0	0	0	0
Plantago lanceolata	0	0	0	0	15	0	0	0	0
Potentilla reptans	0	0	1	0	0	0	0	0	0
Rumex acetosa	0	1	1	0	5	0	0	0	0
Saponaria officinalis	0	0	1	0	0	0	0	0	0
Sedum acre	0	0	1	0	0	0	0	0	0
Tanacetum vulgare	0	0	5	0	0	0	0	0	0
Trifolium repens	0	0	10	0	26	0	0	0	0
Erigeron annuus	0	0	0	0	0	0	0	0	0
Senecio inaequidens	0	0	1	0	0	0	0	0	0
Senecio jacobaea	0	0	10	0	1	0	0	0	0
Cichorium intybus	0	0	0	0	0	0	0	0	0
Dactylis glomerata	0	2	0	0	10	1	1	0	0
Euphorbia cyparissias	0	0	0	0	0	0	0	0	0
Festuca rubra	0	0	50	0	0	0	0	0	0
Geranium molle	0	0	0	0	0	0	0	0	0
Hypericum perforatum	0	0	0	0	0	0	0	0	0
Pastinaca sativa	0	0	0	0	0	0	0	0	0
Rubus caesius	30	50	0	20	0	10	1	1	30
Sedum album	0	0	0	0	0	0	0	0	0
Trifolium campestre	0	0	0	0	0	0	0	0	0
Bromopsis inermis	0	0	0	0	0	0	0	0	0
Chaerophyllum temulum	0	0	0	0	0	0	0	0	0
Festuca arundinacea	0	0	0	0	0	0	0	0	0
Lamium album	0	1	0	0	0	0	0	0	0
Lolium perenne	0	0	0	0	30	0	0	0	0
Potentilla anserina	2	1	0	0	0	0	0	0	0
Scrophularia nodosa	0	0	0	0	0	0	0	0	0

Symphytum officinale	0	0	0	0	0	1	1	1	0
Achillea millefolium	0	0	1	0	0	0	0	0	0
Carduus crispus	0	1	0	1	1	0	0	0	0
Carex hirta	2	0	5	0	0	0	0	0	0
Convolvulus arvensis	0	0	0	0	0	0	0	0	0
Galium verum	0	0	0	0	0	0	0	0	0
Herniaria glabra	0	0	0	0	0	0	0	0	0
Oenothera biennis	0	0	0	0	0	0	0	0	0
Ononis repens	0	0	0	0	0	0	0	0	0
Calamagrostis epigejos	0	1	20	0	0	0	0	0	0
Cornus sanguinea	2	0	0	0	0	0	0	0	0
Crataegus monogyna	50	1	0	5	0	0	0	0	0
Thalictrum flavum	0	5	0	5	0	0	1	0	0
Valeriana officinalis	0	0	0	0	0	0	0	0	0
Cerastium fontanum	0	0	0	0	2	0	0	0	0
Rosa species	5	0	0	0	0	0	0	0	0
Agrostis stolonifera	0	0	0	0	0	0	0	0	0
Juncus compressus	0	0	0	0	0	0	0	0	0
Lathyrus tuberosus	0	0	0	0	0	0	0	0	0
Lysimachia vulgaris	0	0	0	0	0	0	0	0	0
Epilobium hirsutum	5	10	0	1	0	0	0	0	0
Vicia cracca	0	0	0	0	0	0	0	0	0
Conyza canadensis	0	0	0	0	0	0	0	0	0
Fraxinus excelsior	2	0	0	0	0	0	0	0	0
Sambucus nigra	0	30	0	70	0	0	0	0	0
Euphorbia esula	0	1	2	0	0	0	0	0	0
Carduus nutans	0	0	1	0	0	0	0	0	0
Carex arenaria	0	0	1	0	0	0	0	0	0
Trifolium pratense	0	0	1	0	1	0	0	0	0
Iris pseudacorus	0	0	0	1	0	1	1	1	0
Holcus lanatus	0	0	0	0	1	0	0	0	0
Trifolium dubium	0	0	0	0	2	0	0	0	0
Plantago major	0	0	0	0	1	0	0	0	0
Phleum pratense	0	0	0	0	40	0	0	0	0
Bromus hordeaceus s. hordeaceus	0	0	0	0	1	0	0	0	0
Taraxacum species	0	0	0	0	1	0	0	0	0
Calystegia sepium	0	0	0	0	0	1	2	2	2
Salix alba	0	0	0	0	0	40	50	50	0
Impatiens glandulifera	0	0	0	0	0	2	1	1	0
Lysimachia nummularia	0	0	0	0	0	0	1	0	0

Appendix 4. Average leaf area of dominant species calculated from field leaf scans.

Species name	Average leaf area (cm^2)
Cirsium arvense	10.23
Urtica dioica	14.62
Rubus caesius	24.80
Salix alba	3.32
Crataegus monogyna	4.96
Tanacetum vulgare	9.31
Grass spp	7.31

Appendix 5. Summary of LAI-2000 measurements analysis report by the FV2000 software. (*1 In. = one instrument to take reference and within canopy measurements, 2 In. = two instruments used (one for reference and the other for within canopy measurements), and Inter. = Interpolation of the reference measurements used from previous day's records).

Plot code	**Number of annulus rings**									
	2 rings (0.0^o-28.6^o)					**5 rings (0.0^o – 75^o)**				
	Sub-plots (# of sub-plots)	LAIe	Mean LAIe	SD	Method*	Sub-plots (# of points)	LAIe	Mean LAIe	SD	Method
GH 1	A	4.49	4.93	0.76	1 In.	A	3.82	3.91	0.52	1 In.
	B	5.52				B	4.46			
	C	5.97				C	4.32			
	D	4.28				D	3.84			
	E	4.39				E	3.13			
GH 2	(9)	2.46	2.46	0.39	2 In.	(9)	2.01	2.01	0.26	2 In.
GH 3	A	5.11	1.69	1.62	1 In.	A	2.58	1.42	0.98	1 In.
	B	0.09				B	0.26			
	C	1.77				C	1.45			
	D	0.00				D	0.36			
	E	1.63				E	1.60			
	F	0.04				F	0.06			
	G	1.84				G	1.84			
	H	2.09				H	2.07			
	I	2.68				I	2.57			
GH 4	(9)	7.51	7.51	0.63	2 In.	(4)	5.28	5.28	0.54	2 In.
GH 6	(9)	3.35	3.35	0.44	Inter.					
SH 7	(7)	10.99	10.99	0.60	Inter.					
SH 8	A	4.53	6.47	2.63	1 In.	A	3.13	4.34	1.26	1In.
	B	6.95				B	2.89			
	C	8.11				C	5.27			
	D	10.12				D	6.17			

	E	3.08				E	3.16			
	F	5.28				F	4.33			
	G	2.89				G	3.26			
	H	8.19				H	5.6			
	I	9.06				I	5.26			
SH 9	(6)	10.46	10.46	0.74	Inter.					
SH11	A	8.41	9.50	1.32	1 In.	A	5.6	5.87	0.74	1 In.
	B	7.93				B	5.68			
	C	11.16				C	6.67			
	D	10.59				D	6.3			
	E	7.93				E	5.83			
	F	10.26				F	6.44			
	G	8.31				G	4.78			
	H	10.76				H	6.73			
	I	10.11				I	4.78			
GH12	A	9.60	4.90	2.33	1 In.	A	5.84	3.20	1.51	1 In.
	B	5.72				B	4.00			
	C	3.18				C	1.58			
	D	3.94				D	2.89			
	E	4.97				E	3.56			
	F	3.47				F	2.82			
	G	1.52				G	0.87			
	H	6.75				H	4.58			
	I	4.94				I	2.63			
SH13	A	10.69	8.89	1.69	1 In.	A	6.53	5.02	1.16	1 In.
	B	5.13				B	2.88			
	C	9.87				C	5.54			
	D	8.94				D	5.02			
	E	8.08				E	3.49			
	F	9.59				F	5.02			
	G	8.61				G	5.18			
	H	10.65				H	6.03			
	I	8.47				I	5.49			
GH14	(7)	3.30	3.30	0.49	Inter.					

Appendix 6. Summary of TRAC measurements analysis report by TRACwin. (Below* = measurements below understory, Above** = measurements above understory).

Plot code	kme		Ω		Mean solar zenith angle (^{o})		PAIe		LAI		W from data (mm)		Mean element Width used (mm)	
	Below*	Above**	Below	Above	Below	Above	Below	Above	Below	Above	Below	Above	Below	Above
	GRASS/HERBS													
GH 1	2.20		0.906		59.85		2.21		2.44		63..984		25	
GH 2	0.76		0.88		45.68		1.06		1.2		73.88		20	
GH 3	0.45		0.932		43.68		0.65		0.70		11.306		20	
GH 4	1.38		0.817		32.61		2.33		2.85		61.148		25	
GH 5	2.27		0.878		34.22		3.76		4.28		191.613		30	
GH 6	1.10		0.937		53.08		1.32		1.41		75.579		30	
	SHRUB													
SH 8	1.27		0.812		54.49		1.48		1.82		216.803		30	
SH 11	0.83	0.50	0.803	0.932	42.66	41.97	1.22	0.75	1.52	0.80	49.391	12.992	30	30
SH 13	3.53	1.13	0.940	0.838	38.71	38.97	5.51	1.76	5.86	2.10	505.865	109.850	30	30
	FOREST													
FR 15	2.73		0.879		31.81		4.65		5.29		169.785		15	
FR 19	2.63	2.54	0.758	0.734	36.30	37.40	4.23	4.04	5.59	5.50	56.512	66.405	25	15
FR 20	5.41	2.00	0.927	0.748	59.19	58.65	5.54	2.08	5.98	2.78	38.392	215.878	25	15

Appendix 7: Instantaneous photosynthetically active photon flux density (PPFD) measured on VALERI plot transects using TRAC instrument.

GH1

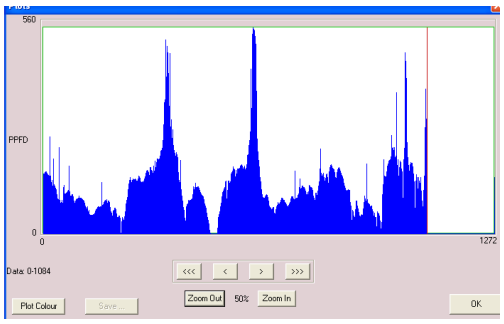

GH 2

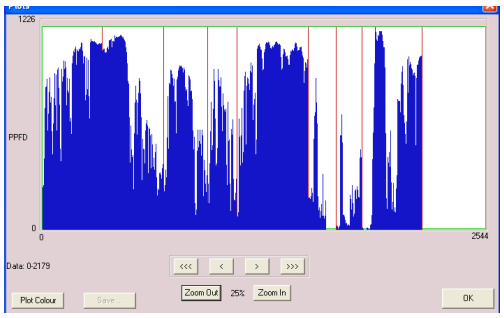

GH 3

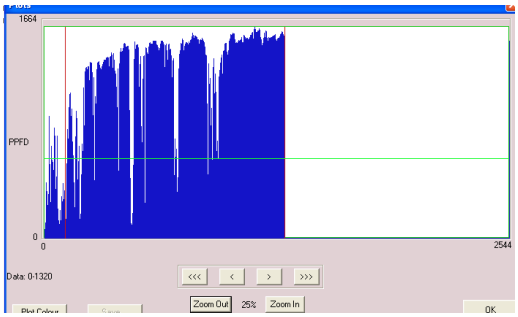

GH 4

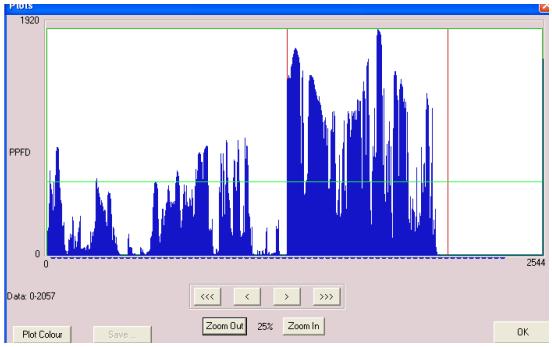

GH 5

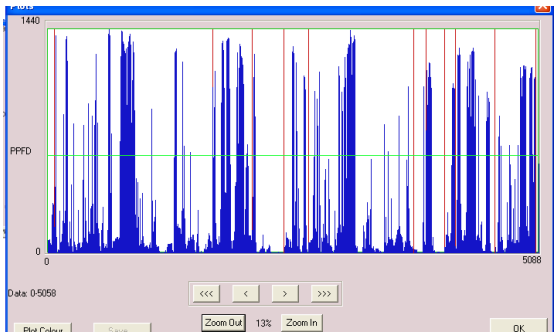

GH 6

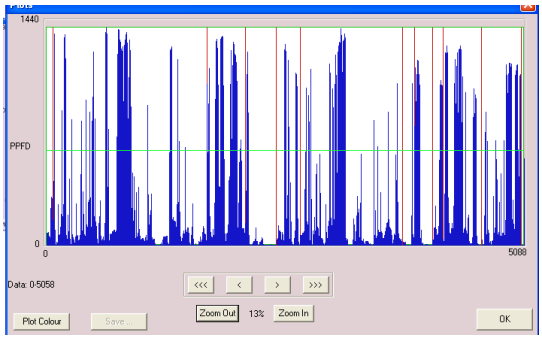

SH 8

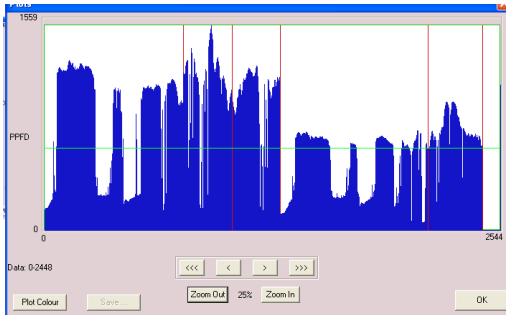

SH11 Above understory

SH 11 Below understory

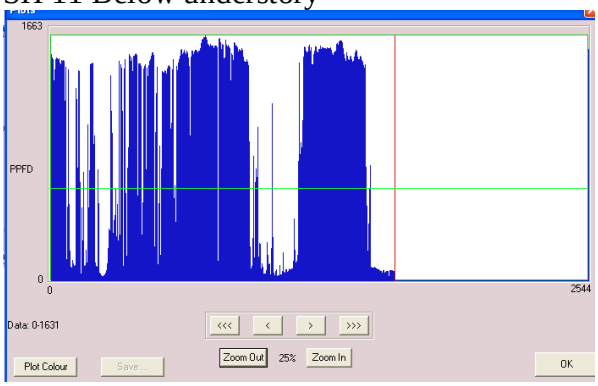

SH 13 Above undersory

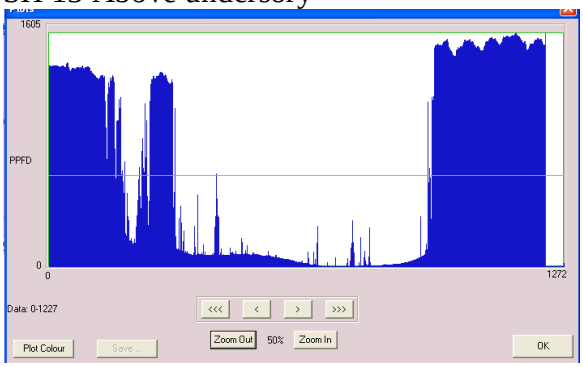

SH 13 Below understory

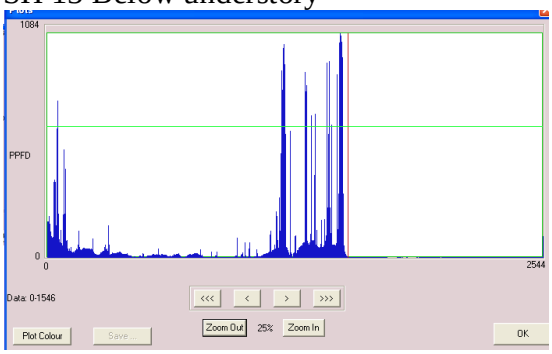

FR 15

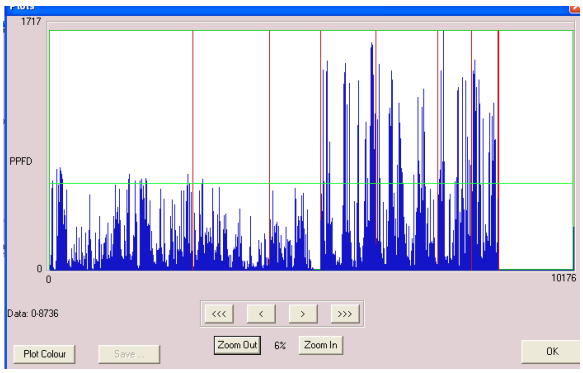

FR 19 Above understory

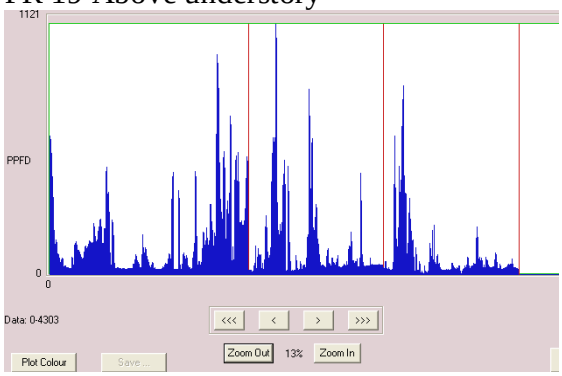

FR 19 Below understory

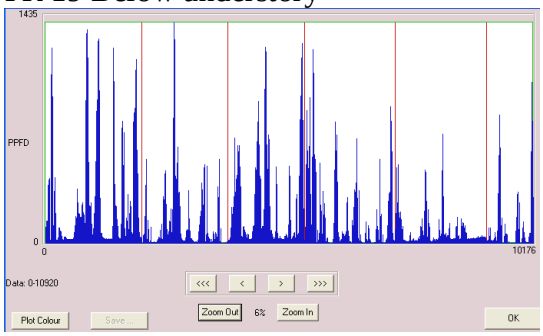

FR 20 Above understory

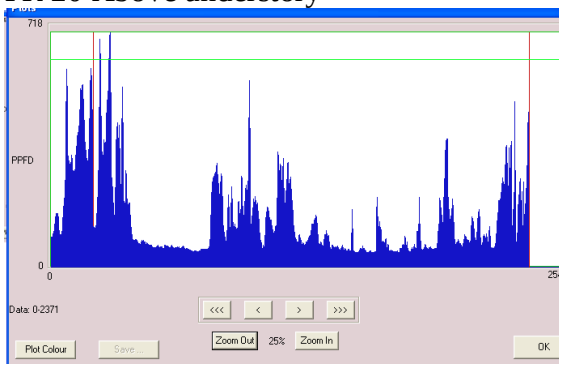

FR 20 Below understory

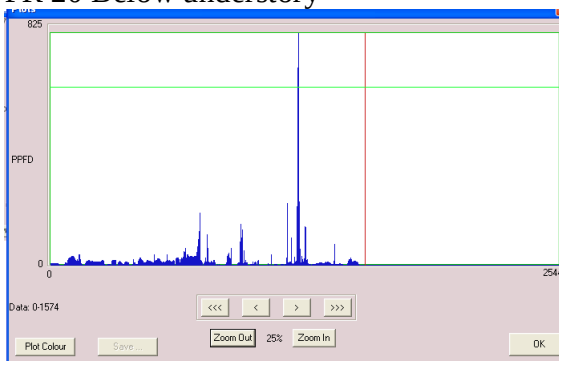

Appendix 8. Summary of upward and downward looking hemispherical photography measurement analysis report by CAN_EYE. (* 4, **5 and ***7 are the number of upward looking hemispherical photographs acquired out of 9 sub sampling points).

Plot code		Soil/Sky(%)	Green veg(%)	fCover	Std(fCover)	LAIe	LAIe(57.5°)	LAIt	ALA°		Clumping factor		
									Effective	True	0°	30°	57.5°
GH 1		0.86	99	0.98	0.981	8.6	5	10	62	64	0.84	0.88	0.65
GH 2		10	90	0.961	0.972	2.7	2.1	5.9	16	10	0.45	0.44	0.43
GH 3		17	83	0.826	0.946	2.3	2	5.1	34	10	0.39	0.34	0.39
GH 4		8.8	91	0.872	0.965	3.2	3	3.8	46	34	0.67	0.75	0.82
GH 5		5.1	95	0.926	0.971	3.7	3.5	5.6	40	10	0.47	0.55	0.61
GH 6		9.9	90	0.92	0.978	2.7	2.5	6.8	24	14	0.38	0.4	0.45
SH 7		3.4	97	0.975	0.981	3.9	3.6	6.5	22	10	0.57	0.57	0.54
SH 8	Down	12	88	0.905	0.953	2.4	2.3	3.7	18	10	0.61	0.61	0.71
	Up*	91	9.3	0	1	0	0.23	0.02	60	80	0.41	0.55	0.43
SH 9	Down	11	89	0.908	0.958	2.4	2.3	4	18	10	0.52	0.54	0.64
	Up*	80	20	0	1	0.1	0.34	0.28	80	80	0.46	0.35	0.35
SH 10	Down	8	92	0.921	0.965	3.2	2.9	5.8	38	10	0.4	0.45	0.49
	Up***	79	21	0.194	0.954	0.3	0.3	1.1	40	42	0.35	0.28	0.29
SH 11	Down	6.6	93	0.878	0.949	3.5	2.9	4.7	42	18	0.52	0.62	0.62
	Up**	47	53	0.556	0.946	0.9	0.81	2.7	24	10	0.31	0.32	0.38
GH 12		5.6	94	0.884	0.948	4.1	3.6	6.9	54	36	0.4	0.5	0.51
SH 13	Down	5.7	94	0.916	0.938	3.7	3.5	5.5	42	10	0.47	0.55	0.57
	Up	35	65	0.625	0.97	1.2	1.2	3.5	22	10	0.32	0.37	0.38
GH 14		5.2	95	0.905	0.979	4.1	3.8	5.3	50	54	0.79	0.83	0.8
FR 15	Down	24	76	0.679	0.927	1.9	1.7	2.8	50	30	0.53	0.59	0.64
	Up	28	72	0.583	0.95	1.9	1.7	3	60	54	0.5	0.56	0.61
FR 17	Down	4.3	96	0.924	0.966	4	3.7	5.8	40	36	0.61	0.71	0.67
	Up	28	72	0.465	0936	2	1.8	4.4	70	74	0.55	0.49	0.48
FR 18	Down	2.3	98	0.965	0.973	4.8	4.4	6.7	40	24	0.65	0.61	0.65

	Up	27	73	0.605	0.928	1.7	1.7	3.8	50	40	0.38	0.41	0.44
FR 19	Down	3.6	96	0.952	0.972	4.3	3.7	7	32	10	0.56	0.53	0.53
	Up	37	63	0.519	0.912	1.5	1.4	3.2	60	38	0.28	0.39	0.48
FR 20	Down	7.7	92	0.854	0.941	3.1	2.5	5.8	3.4	10	0.39	0.47	0.44
	Up	39	61	0.617	0.889	1.2	1.1	3	40	22	0.38	0.35	0.39

Appendix 9. Summary of upward and downward looking hemispherical photography measurement analysis report by CAN_EYE for 0 - 30^{o} view zenith angle. (* 4 and **5 are the number of upward looking hemispherical photographs acquired out of 9 sub sampling points).

Plot code		Soil/Sky(%)	Green veg(%)	fCover	Std(fCover)	LAIe	LAIt	ALA^{o}		Clumping factor	
								Effective	True	0^{o}	57.5^{o}
GH 1		2	98	0.976	0.981	7.5	6.8	60	10	0.49	0.65
GH 2		5.4	95	0.977	0.982	5.1	8.9	46	50	0.66	0.43
GH 3		22	78	0.762	0.956	2.8	6.9	58	66	0.55	0.33
GH 4		7.6	92	0.918	0.971	5	5.7	60	50	0.69	0.74
GH 6		7	93	0.954	0.971	4.8	10	44	66	0.83	0.47
SH 7		3.6	96	0.989	0.987	8.4	10	50	62	0.92	0.55
SH 8	Down	6	94	0.944	0.97	4.4	4.6	46	10	0.63	0.63
	Up*	97	3.2	0	1	0	0.04	60	80	NaN	0.66
SH 11	Down	4.1	96	0.934	0.969	7.2	10	66	70	0.83	0.65
	Up**	47	53	0.557	0.946	1.2	3	44	12	0.29	0.29
GH 12		7.2	93	0.891	0.949	5.7	9.6	64	70	0.8	0.51
SH 13	Down	4.6	95	0.941	0.952	5.2	8.8	52	56	0.65	0.55
	Up	38	62	0.628	0.971	1.5	3.6	42	16	0.28	0.34
GH 14		6.8	93	0.916	0.98	5.2	6.3	60	60	0.82	0.82

Appendix 10. Plant Functional Type map.

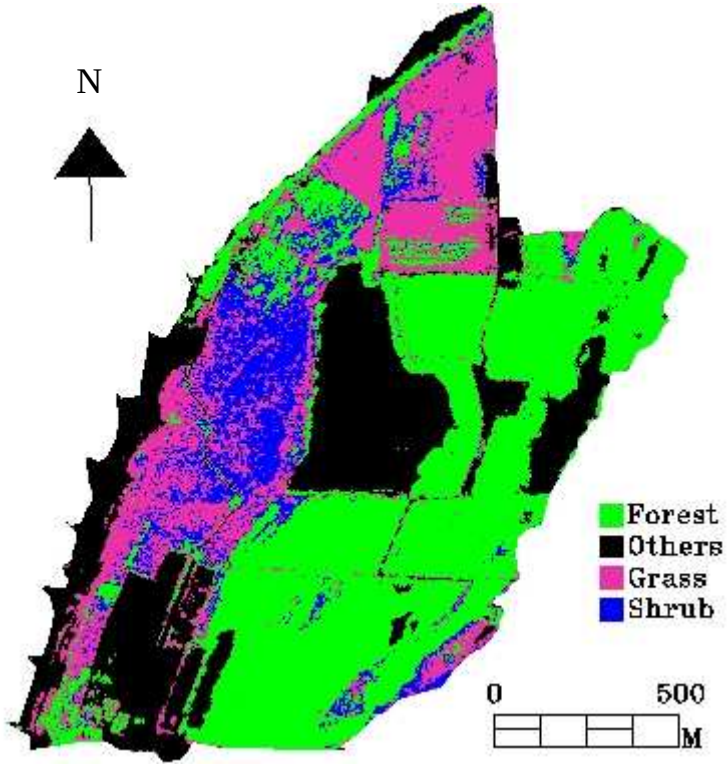

Appendix 11. Validation of leaf scans pre-processing

Scan No.	Known area (cm^2)	Area after pre-processing (cm^2)
1	12.5	12.75
2	25	25.75
3	36	36.64